Laser Processing of Soft Materials: Laser Induced Forward Transfer and 2 photon polymerization-direct writing

Maria Dinescu

National Institute for Lasers, Plasma, and Radiation Physics

http://ppam.inflpr.ro

EUROPE - ROMANIA

Campus Magurele - Bucharest

NATIONAL INSTITUTES

1974

- National Institute for Physics and Nuclear Engineering (800 people)
- **National Institute for Lasers, Plasma and Radiation Physics (aprox. 500 people) - First laser in 1962**
- National Institute for Physics of Materials (300 people)
- National Institute for Earth Sciences (100 people)
- National Institute for Optoelectronics (80 people)

UNIVERSITY OF BUCHAREST

- Faculty of Physics

1949-Institute of Atomic Physics
1953-first Nuclear Reactor, Magurele, Bucharest

Strategy for the development of ultra-intense lasers based facilities in Romania

OUTLINE

- Introduction
- Laser induced forward transfer (LIFT)
  - Solid phase LIFT
  - Liquid phase LIFT and ink printing
  - Applications of LIFT in device fabrication
- Two photon polymerization – fundamentals and applications
- Conclusions

Transfer of Layers with Lateral Resolution: Digital Microfabrication Techniques

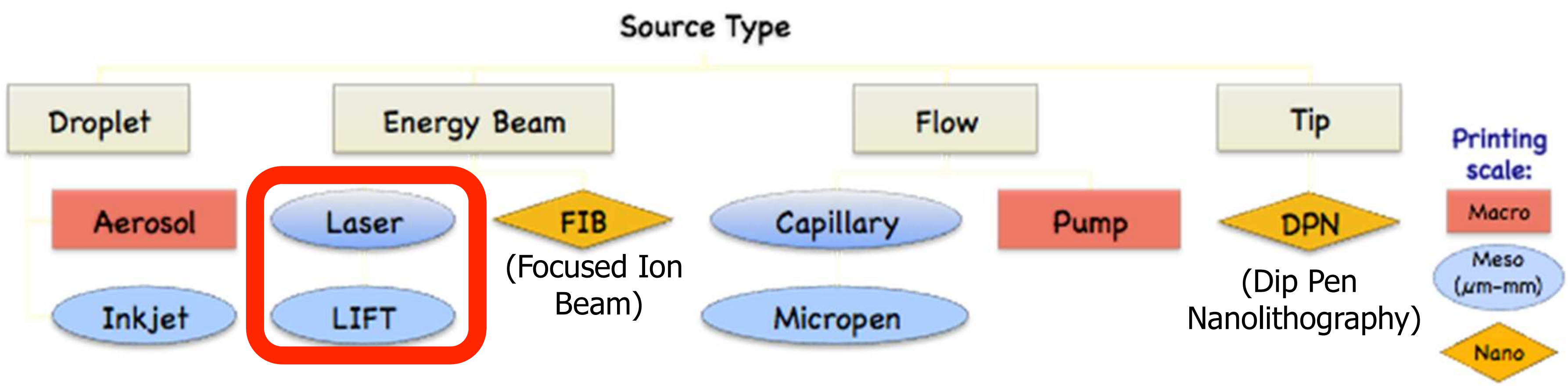

Digital μ-fabrication techniques allow the discrete processing of functional materials for the prototyping, customization and/or repair of microelectronic systems.

- ❑ Classical printing is not flexible as it uses cylinder, masks and screens. Solvents (multilayers) are also an issue.

slide adopted from A.Pique

Transfer of layers with lasers

- First papers: Laser Writing (LR) in 1969 and Material Transfer Recording (MTR) in 1970 (R. S. Braudy in Proceedings of IEEE Oct. 1969, p. 1771, and M. Levene et al. in Appl.Optics 9, 2260 (1970). Then Laser Induced Forward Transfer (LIFT), i.e. transfer of Cu, in 1986. (J. Bohandy et al., J. Appl. Phys. 60, 1538 (1986)).
- Also called laser direct write methods (D. Chrisey & al, Applied Surface Science, 2005)
- Many variations of the original process have been suggested, which are summarized in the following slides.

Laser-induced forward transfer (LIFT)

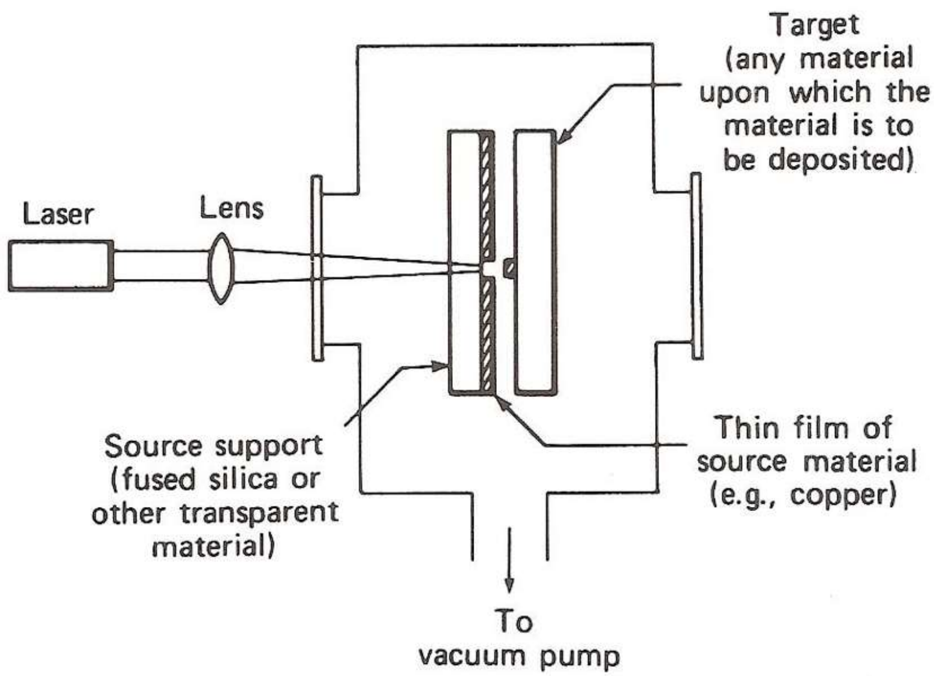

Figure 9.5. A schematic description of the apparatus for metal deposition from a solid-phased precursor. The source material and target are in contact during an actual experiment (from Bohandy *et al.* 1986).

J. Bohandy et al., J. Appl. Phys. 60, 1538 (1986)

- LIFT: mainly UV lasers, direct exposure of film, thermal or UV load. No vacuum is in principle needed.

The processing technique - LIFT

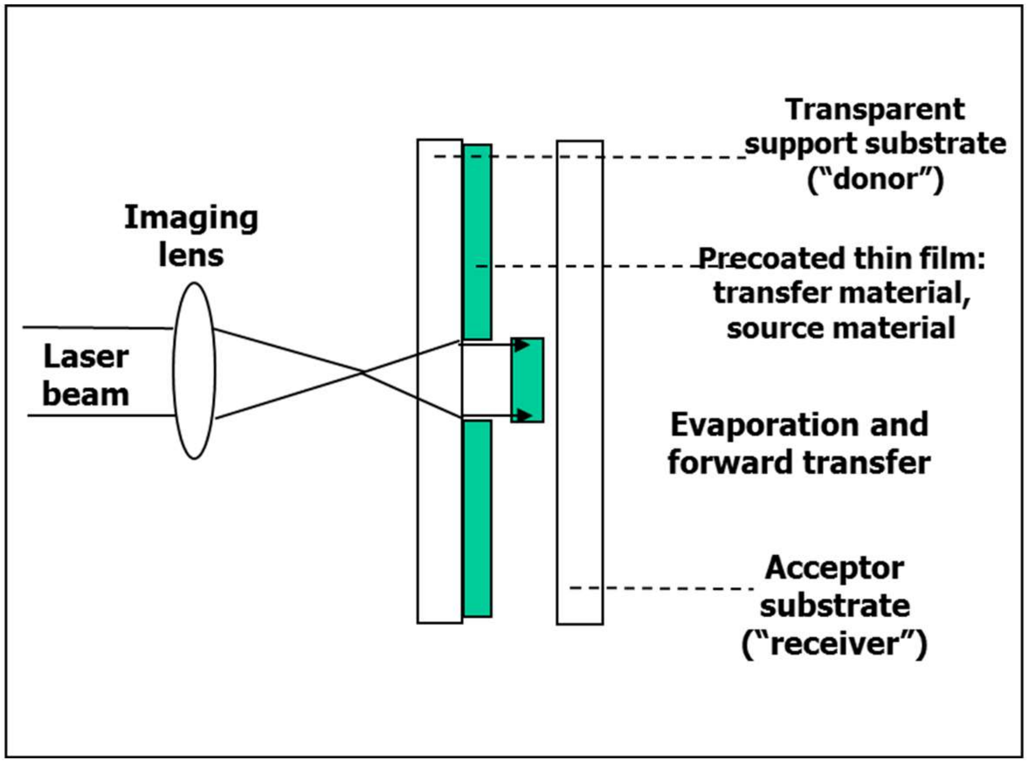

- One step process
- High spatial resolution
- Contact or non-contact
- Flexibility: working distance, size of the transferred patterns, etc.
- Compatible with low fluences
- No nozzles: No clogging
- Printing of organic materials and biological compounds possible, though difficult **however…**

→ **Addition of an intermediate protective layer: metallic, thick polymer, etc. (BA-LIFT, AFA LIFT, etc.)**

Addition of a dynamic releasing layer

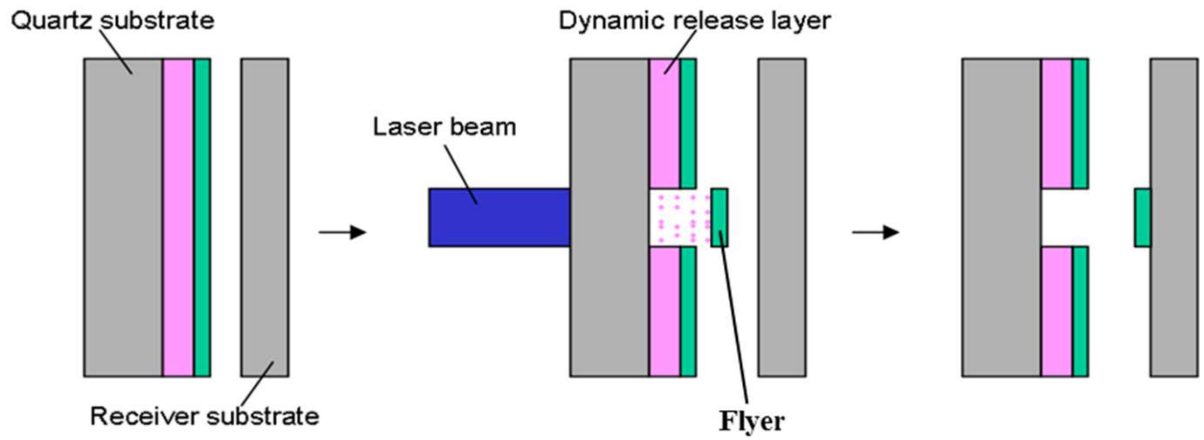

LIFT

- **Addition of DRL**, also named AFA-LIFT (absorbing film assisted-LIFT) and mainly **thin metal layers** (Ag, Ti, Pt, etc. 10-100 nm) are applied. This layer has been added to induce absorption, protect the material, and to lower the required laser energy.
- **Example:** thermoelectric misfit cobaltite thin films.

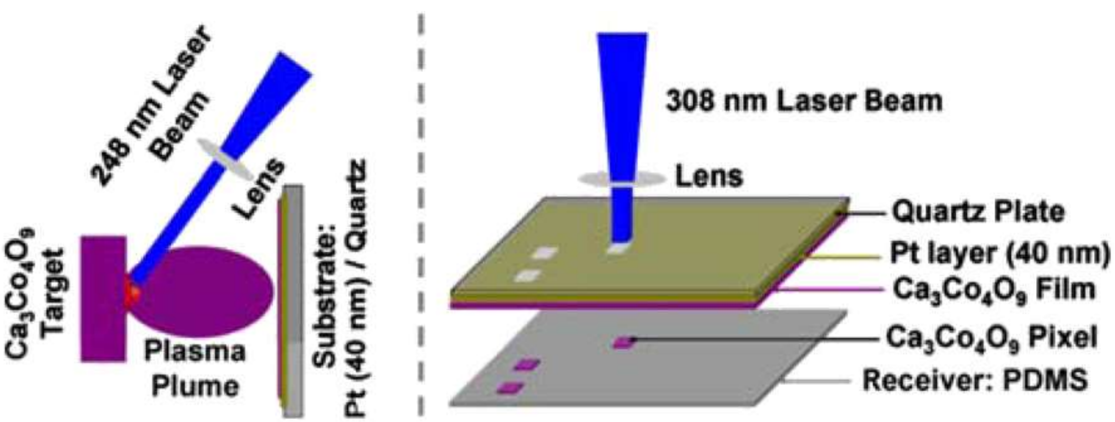

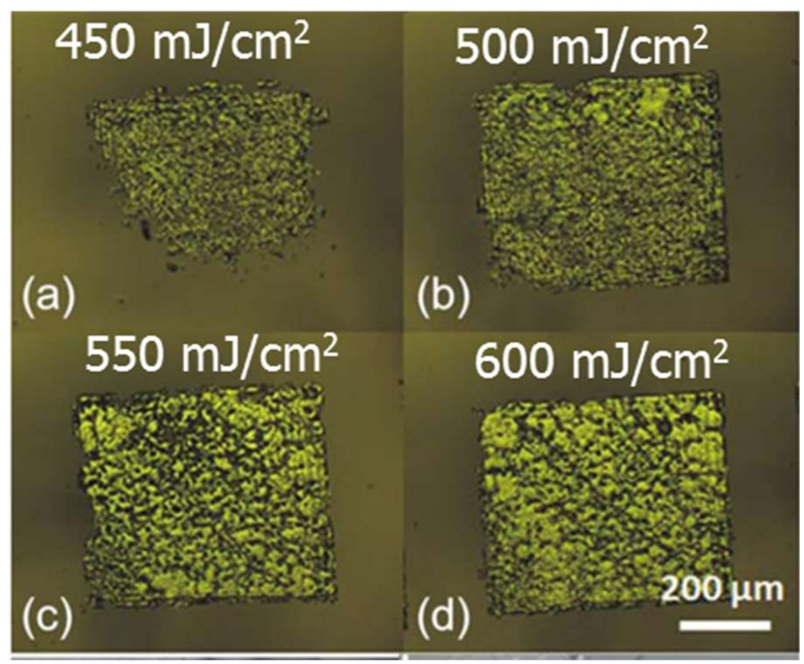

- **RBS (DONOR)** $Ca_{3.0\pm0.15}Co_4O_9$
- **RBS (RECEIVER)** $Ca_{3.2\pm0.3}Co_4O_9$

J. Chen et al. Appl. Phys. Lett. 104, 231907(2014)

Metal DRL – LIFT

Drawbacks

- For organic (liquid phase biomolecules) not a problem, as usually biocompatible metals are used.
- For materials to be used in devices (ex. Polymers) – metal nanoparticles from the DRL may decrease device performance.
- Transfer of semiconductor DS4T with a Au intermediate layer (25 nm) – with EDX observed Au micro and nanoparticles on the surface of the pixel.

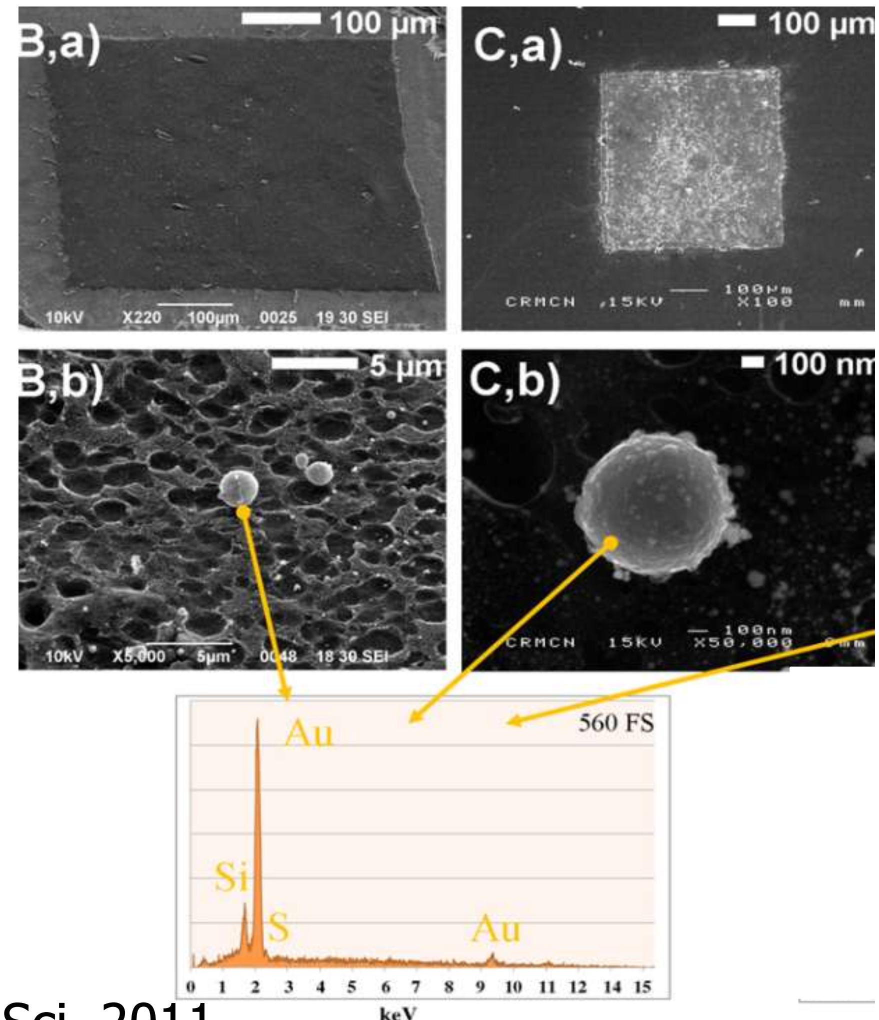

L. Rapp *et al*, Appl. Surf. Sci. 2011

Variation to LIFT: Blister Actuated

Ti and other thin film absorbing layers often fail due to a combination of thermal, optical, contamination, and mechanical effects.

How to isolate the effects:

- **Thermal Effects:** Use thick enough film that the thermal diffusion is not significant over the time of the transfer
- **Optical Effects:** Use a film that is thicker than the laser absorption depth
- **Contamination Effects:** Use a film that remains enclosed and contains any ablation products
- **Mechanical Effects:** Use a film that absorbs mechanical energy through deformation

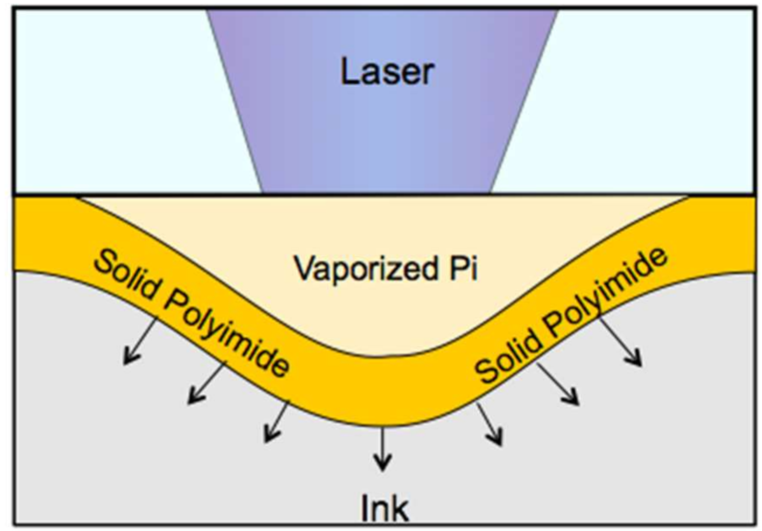

Deformation process is controlled by polymer properties and laser spatial profile

slide adopted from C. Arnold (Princeton University)

Blister actuated LIFT

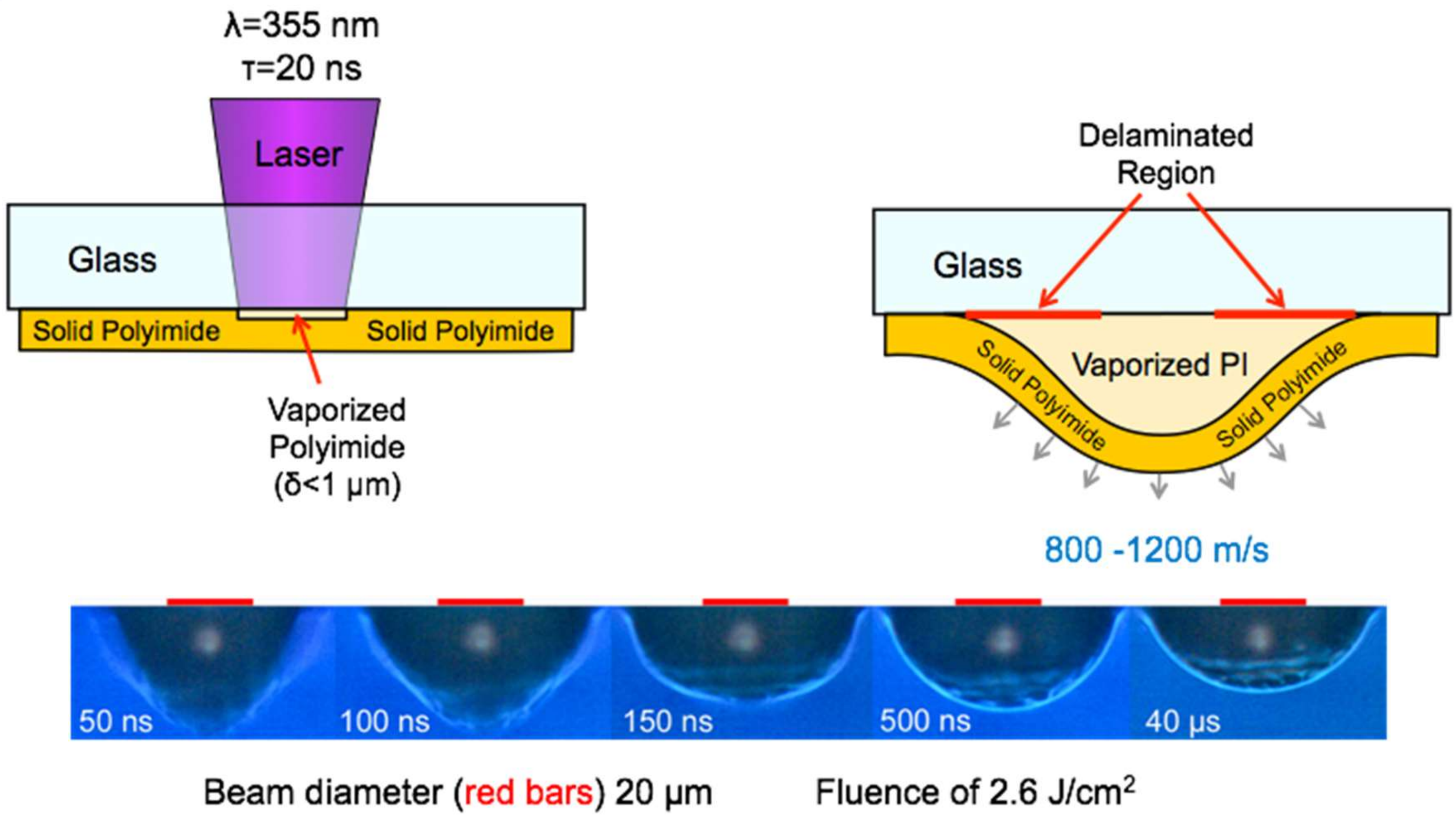

M.S. Brown, N. T. Kattamis, C. B. Arnold, J. Appl. Phys, 107, 083103, (2010)

slide adopted from C. Arnold (Princeton University)

Blister Actuated - LIFT

Surface evolution as a function of laser energy

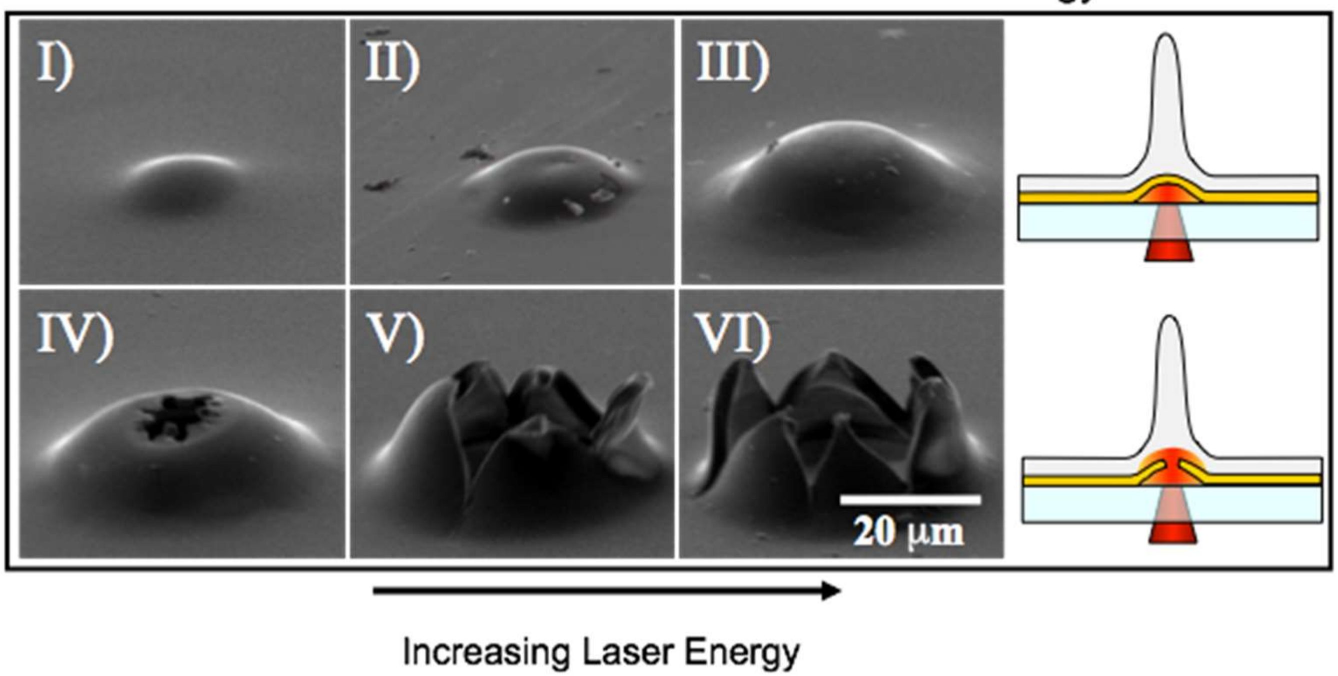

II and III are best
(F ~ 3.6 J cm^{-2})

Used e.g. for printing embryonic stem cells (and Alq_3 and anthracene compounds)

- N. T. Kattamis, P. E. Purnick, R. Weiss, C. B. Arnold, Appl. Phys. Lett. 91, 171120 (2007).
- N. T. Kattamis, N. D. McDaniel, S. Bernhard, C. B. Arnold, Appl. Phys. Lett. 94, 103306 (2009).

slide adopted from C. Arnold (Princeton University)

LIFT using a photodynamic release layer

New approach :

- ❑ Use of a UV-sensitive <u>dynamic release layer,</u> designed for 308 nm

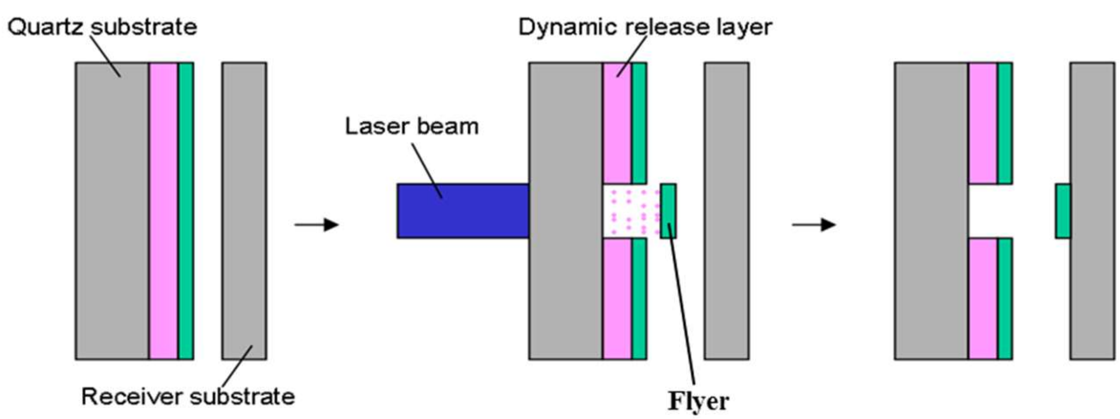

acceptor substrate

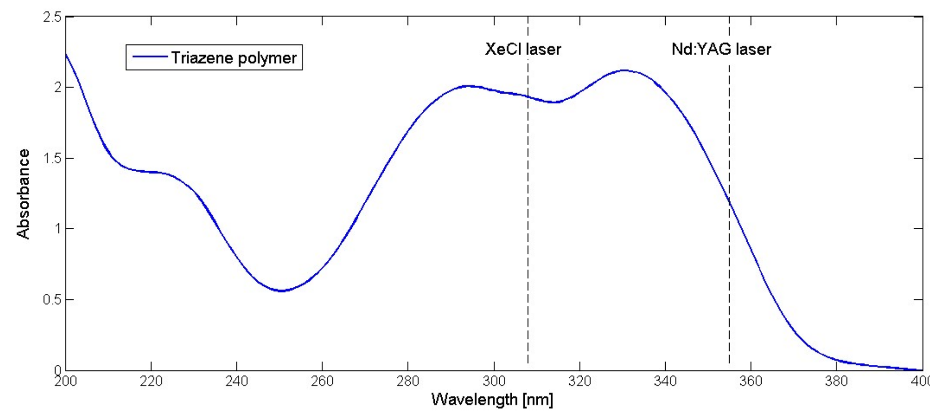

Advantages :

- ❑ Dry transfer technique ➔ not limited by the solvent
- ❑ Three-dimensional structuring allowed
- ❑ Low thermal impact

Triazene polymer (TP) - principle

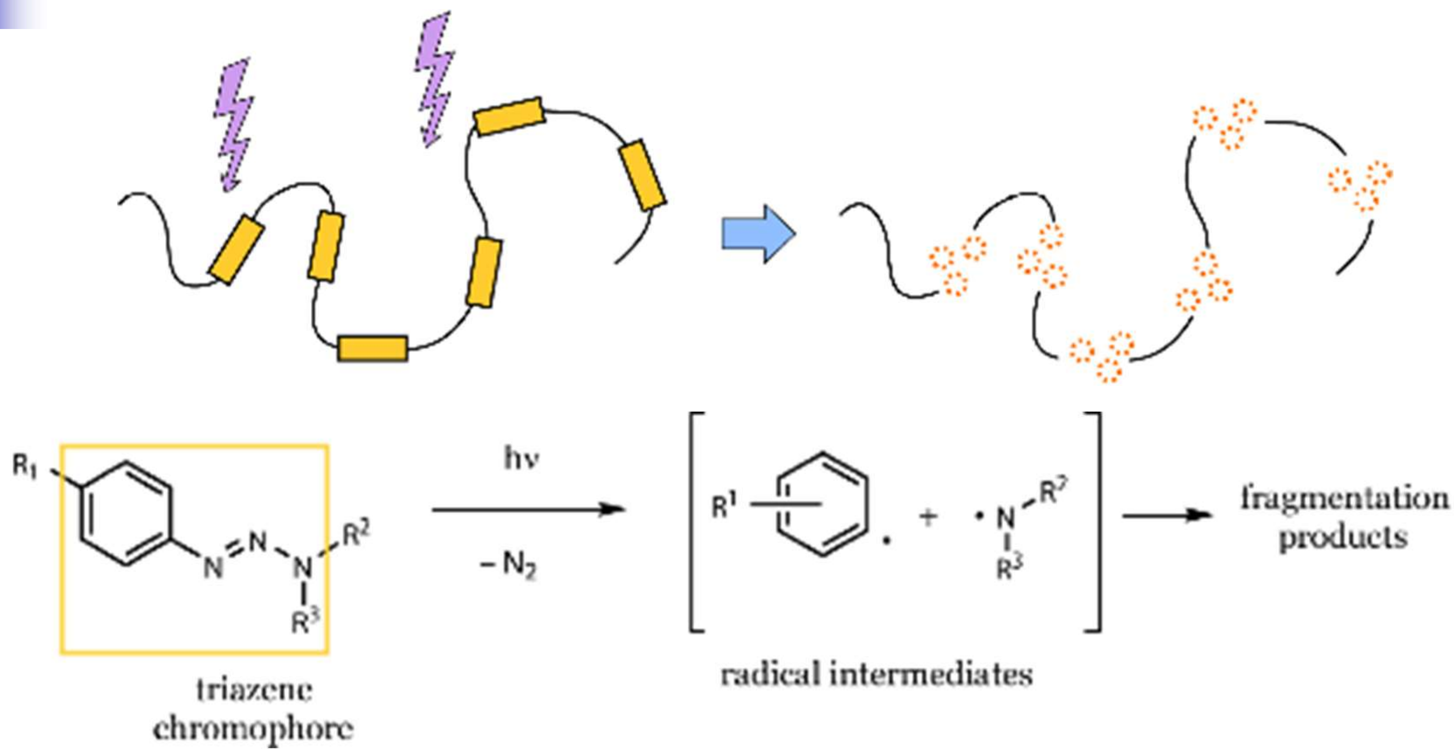

Chromophore in the main chain ➞ decomposition into gas fragments upon UV laser irradiation

Benefits :

- low threshold fluence (~25 mJ/cm^2)
- high ablation rate
- clean ablation, no redeposition
- production of gas ➞ pressure

Examples of materials transferred with TP

- ✓ **1st report on LIFT with TP – transfer of PMMA by T. Mito *et al.* Jpn. J. Appl. Phys. (2001)**
- ✓ **Mammalian cells**, Doraiswamy *et al.*, Appl.Surf. Sci.(2006)
- ✓ **Al**, R. Fardel *et al,* Appl. Surf. Sci. (2007)
- ✓ **Quantum dots**, Xu *et al,* Nanotech (2007)
- ✓ **Functional OLEDs**, R. Fardel *et al,* Appl. Phys. Lett. (2007)
- ✓ **3 color OLED**, J. Shaw-Stewart *et al,* APL (2012)
- ✓ **GdGaO**, Banks *et al.,* (2008)
- ✓ **Polystyrene microbeads**, A. Palla-Papavlu *et al.,* JAP (2010)
- ✓ **Semiconductor DS4T**, L. Rapp *et al,* Appl. Surf. Sci. (2011)
- ✓ **Liposomes**, A. Palla-Papavlu *et al,* Appl. Phys. A (2011)

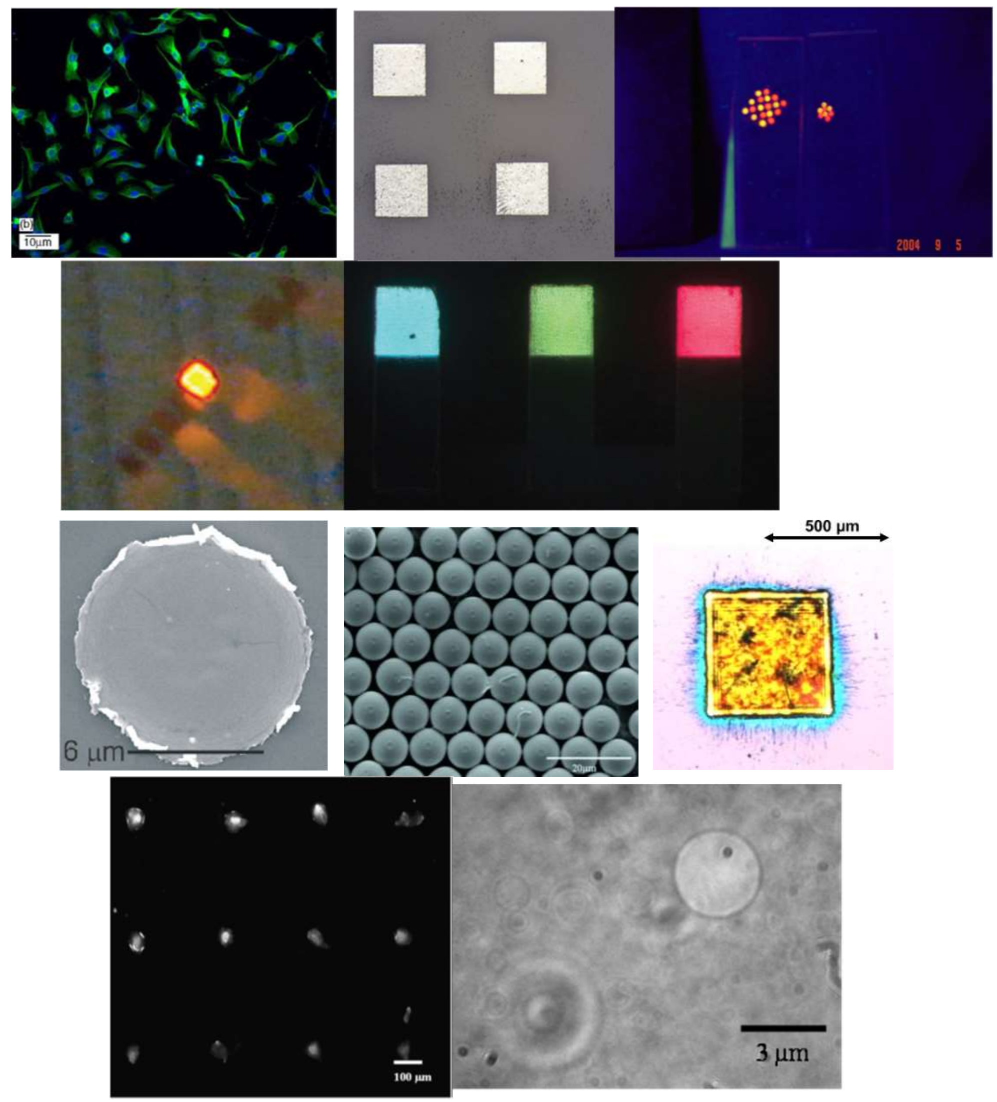

LIFT of polymers: Parameter optimization

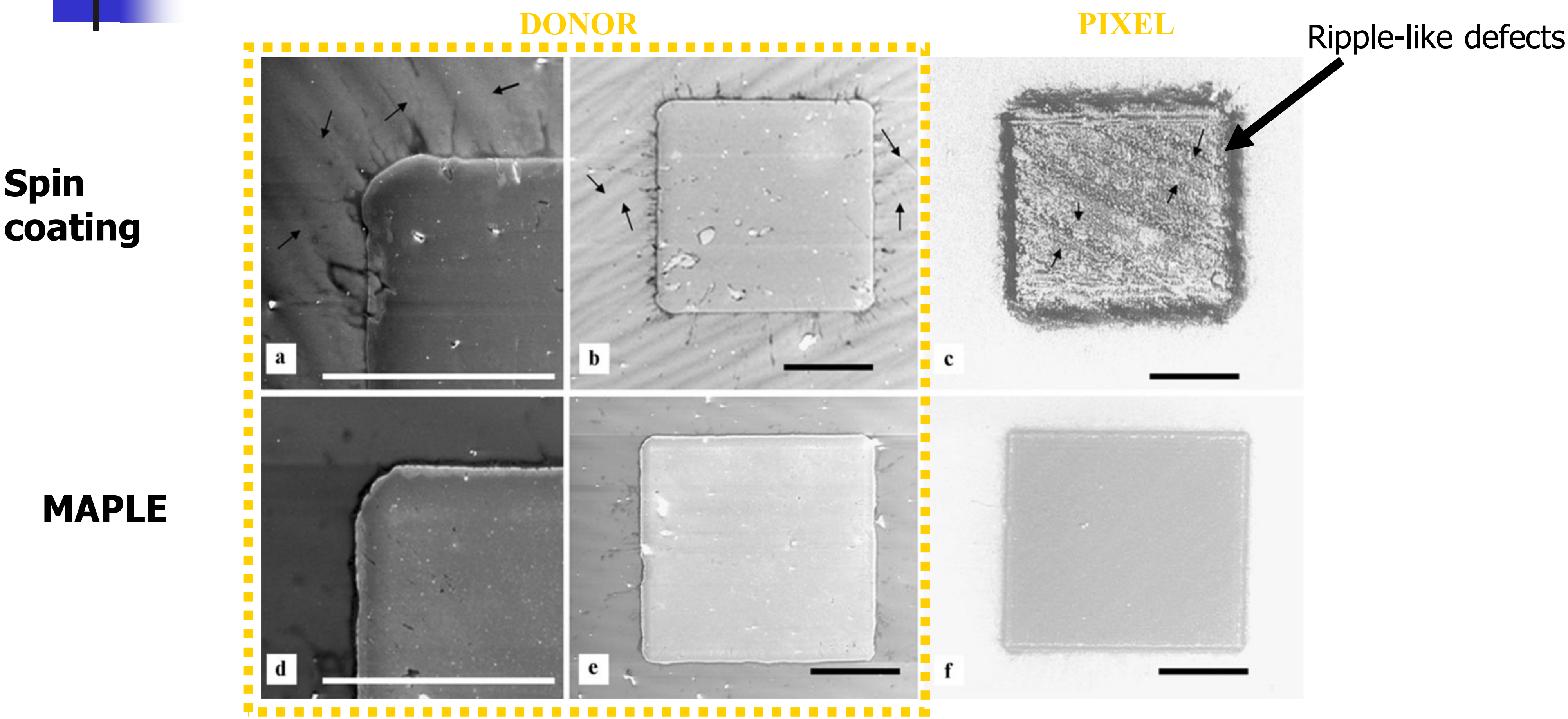

XeCl, 308 nm, 2 Hz, contact, 100 nm TP, 60 nm polymer

- **evaporation driven surface tension forces**

V. Dinca *et al*, Appl. Phys. A (2010)

DRL assisted LIFT

Transfer of single layers **Development of chemical interactive membranes** **Device fabrication**

80 nm Al pixels transferred at 308 nm

R. Fardel et al, Appl Surf Sci (2007)

PEI pixels transferred on BAW sensors

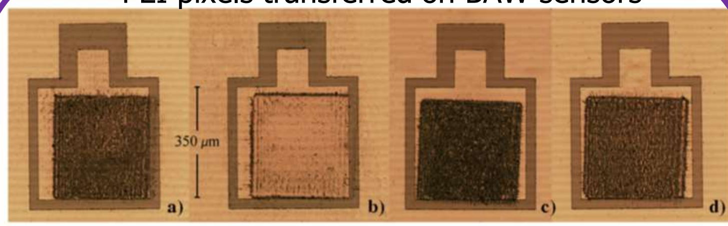

D. Cannatà et al., Sensors and Actuators B (2012)

SnO2 resistive sensors

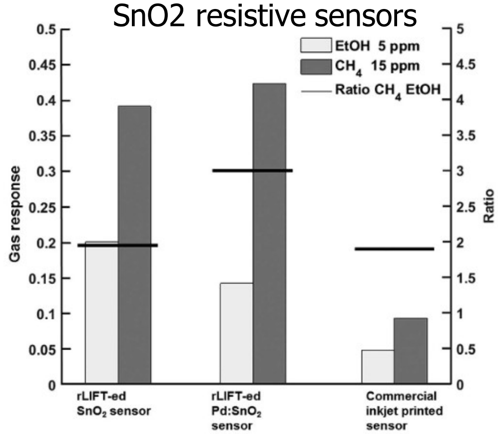

A. Palla-Papavlu et al., Scientific Reports (2016)

Fabricating flexible PEDOT:PSS: GO composite electrochemical sensors for the detection of copper ions

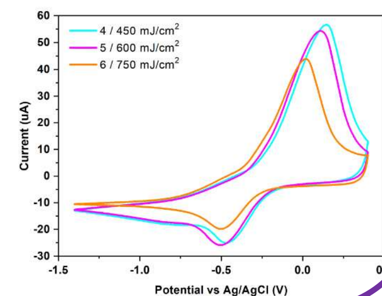

A. Bonciu, F. Andrei, A. Palla-Papavlu, Materials (2023)

SAW sensor fabrication via DRL LIFT

- XeCl, 308 nm, 30 ns pulse duration, 1 Hz, contact, 100 nm TP
- 2port SAW resonators, operating frequency 392 MHz

Sensor responses (vapor/polymer interactions) → solubility interactions and LSER (linear solvation-energy relationship)

(Hydroxypropyl)methyl cellulose (HPMC)	Dipolar and H-bond basic
Polyepichlorohydrin (PECH)	Moderate dipolarity, weak hydrogen bonding
Polyisobutylene (PIB)	Weakly dipolar, weak or no hydrogen bonding
Poly(styrene-co-maleic acid) (PSCMA)	Hydrogen bond acidic
Polyethyleneimine(PEI)	Hydrogen bond basic

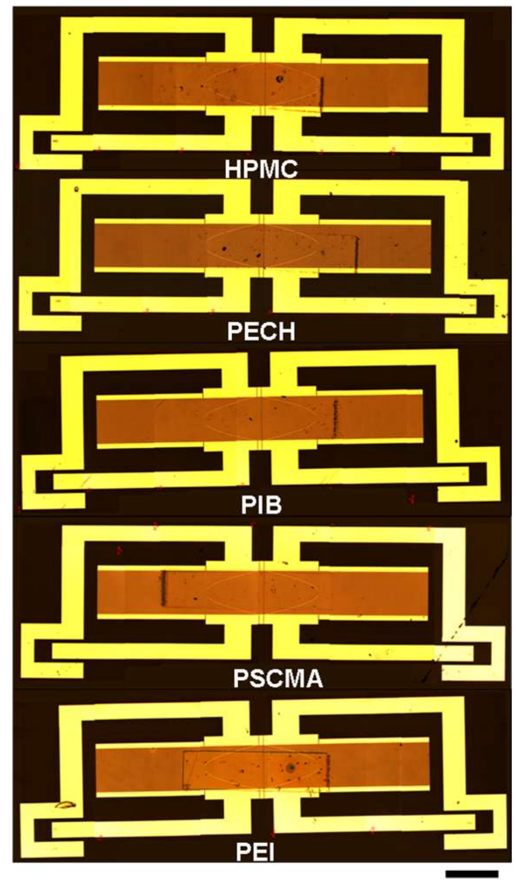

M. Benetti *et al*, Sensors and Actuators B (2019)

SAW sensors for gas detection

Analytes:

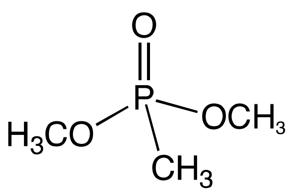

Dimethyl methylphosphonate (**DMMP**)

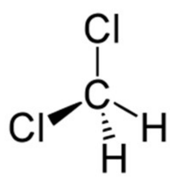

Dichloromethane (**DCM**)

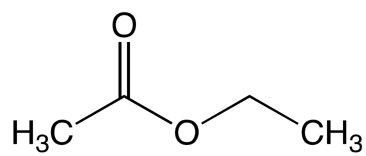

Ethyl acetate (**EA**)

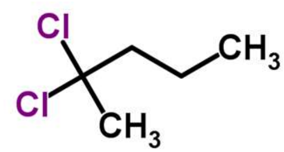

Dichloropenthane (**DCP**)

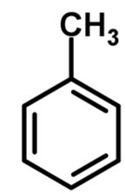

Toluene (**Tol**)

DMMP: simulant for pesticides containing phosphonate ester groups
DCM: an industrially applied toxic compound
EA: a wide spread solvent in medical applications which can be harmful to humans
Tol: common solvent
DCP: solvent, paint and varnish remover, insecticide, and soil fumigant

SAW sensors for gas detection

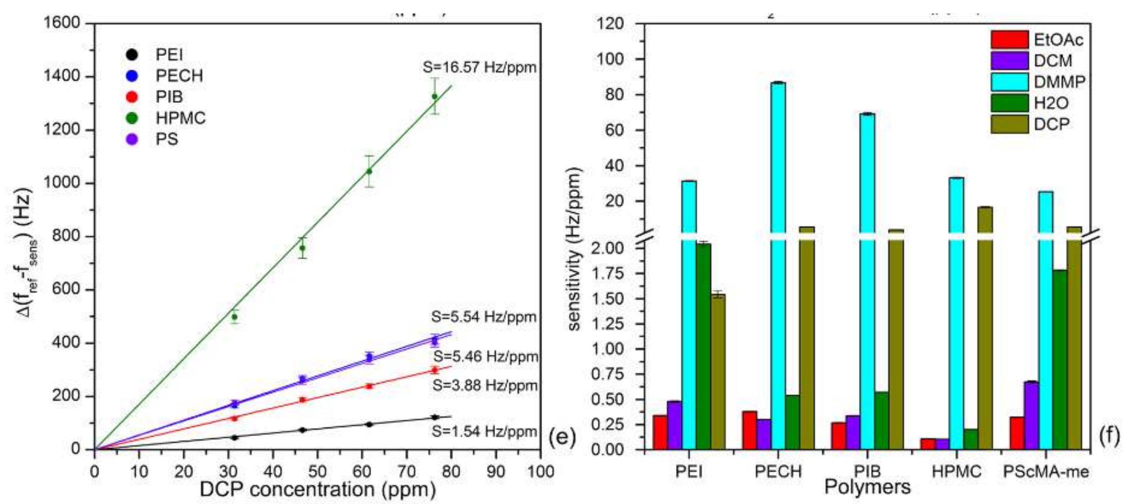

- The SAW sensors showed a fast, remarkable and reversible response. The responses reached approximately 80% of the saturation value within 100 s.
- When the DMMP is removed, the recovery times to return to 80% of the initial baseline values were within 140 s.
- The relative standard deviations between responses obtained in the same conditions were within 5%, demonstrating a good repeatability of the system.

M. Benetti *et al*, Sensors and Actuators B (2019)

SAW sensors for gas detection

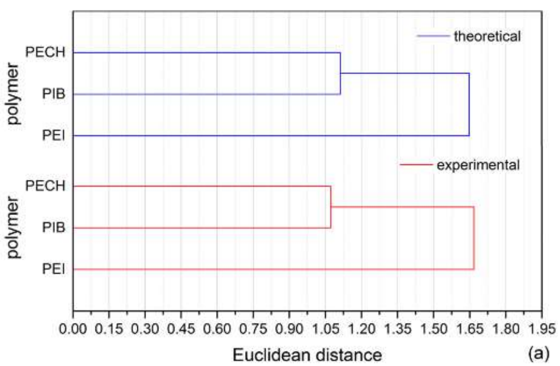

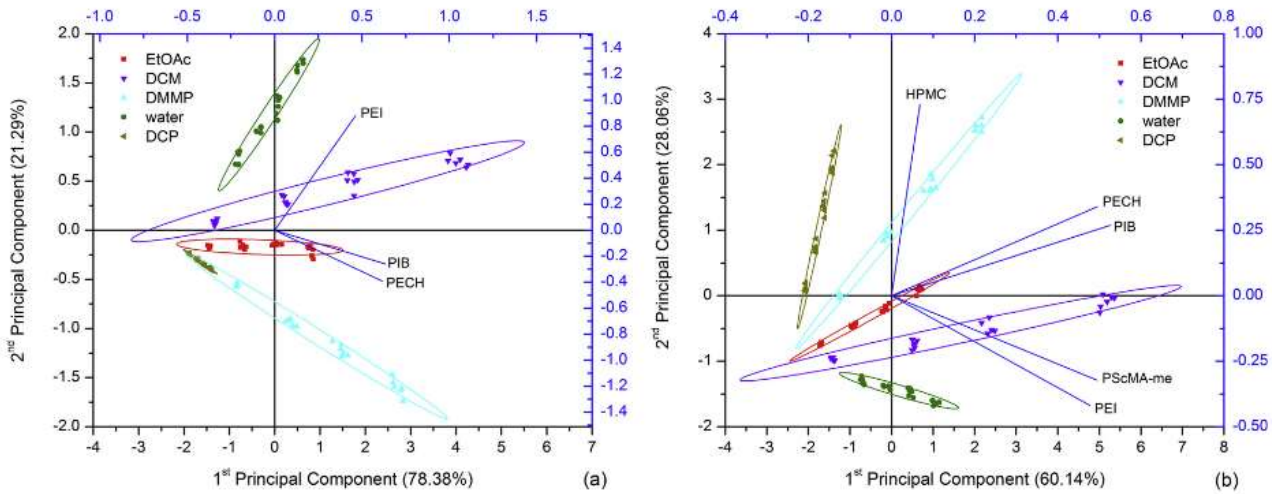

- confirms the feasibility of polymer selection based on the LSER analysis for the preparation of SAW sensors by LIFT

- The 5 sensor array is able to discriminate between the analytes.

M. Benetti *et al*, Sensors and Actuators B (2019)

Sensor fabrication via DRL LIFT

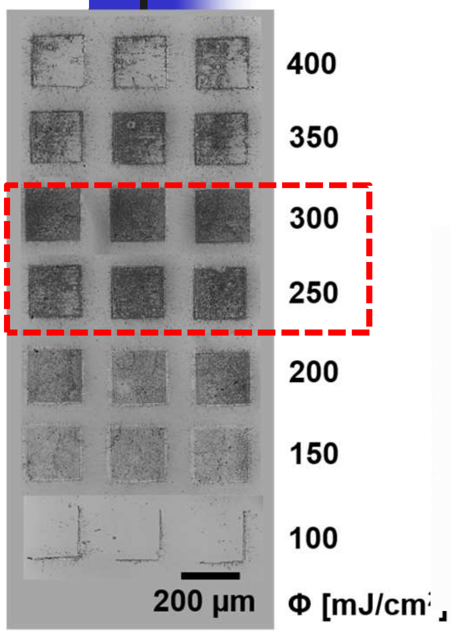

- SWCNT:SnO_2 1:14ratio
- SnO_2 10-14 nm diameter
- TP layer 150 nm thick

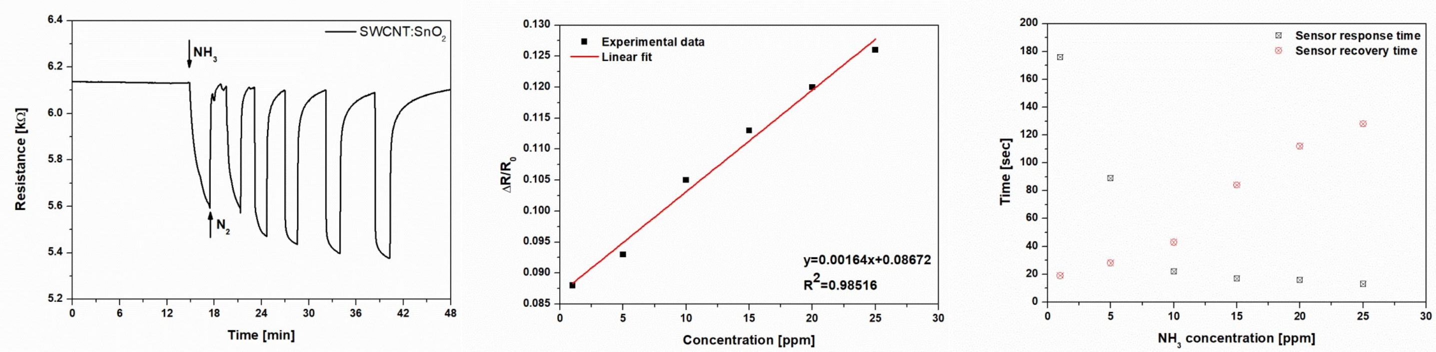

- The sensors are reproducible
- Tested against different concentrations of NH_3 at room temperature
- The SWCNT@SnO_2 sensors exhibit a fast and reversible response over multiple cycles
- They have a theoretical detection limit in the low **ppt range**

A.F. Bonciu, *et al*, Nanomaterials 11, 2604 (2021)

LIFT of CNW

Deposition of CNW thin films

- Radio-frequency plasma beam CVD
- Interconnected network of micron-sized flakes from multi graphene-like structures
- Vertical orientation and chaotic lateral displacement with hundreds of nm mean spacing
- Lamellar morphology with well separated individual flakes of ~ 2 μm in length and sharp edges

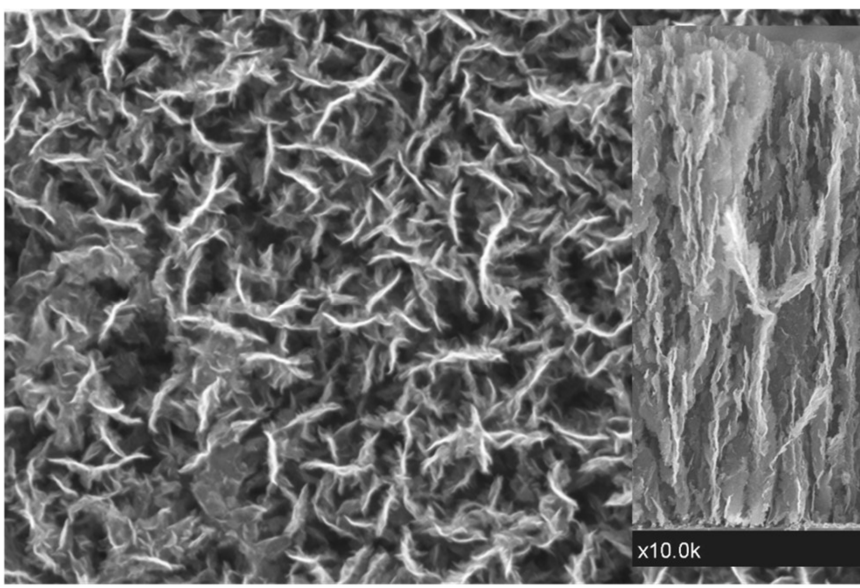

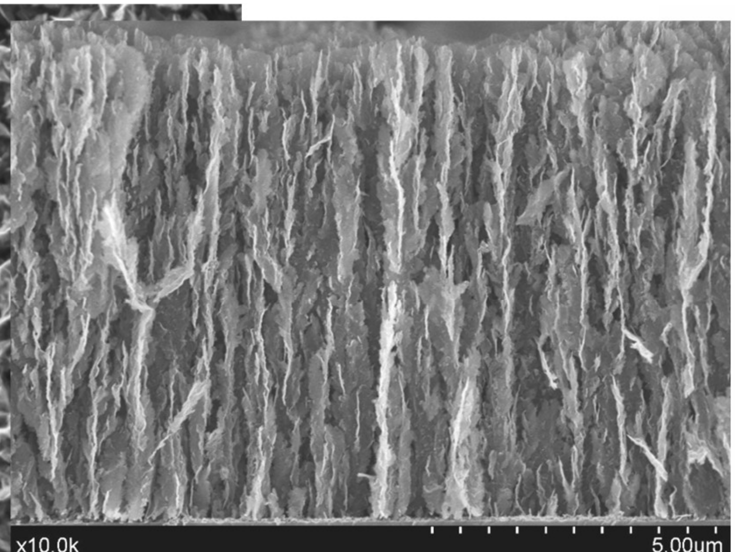

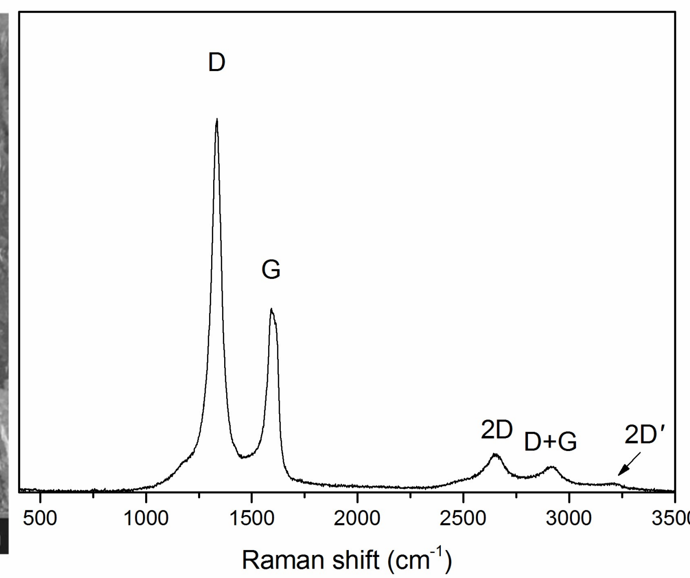

CNW pixel transfer on rigid substrate

- glass substrate, 500-700 mJ/cm^2 laser fluence ⟶ intact pixels
- low adhesion
- pixels are surrounded by debris

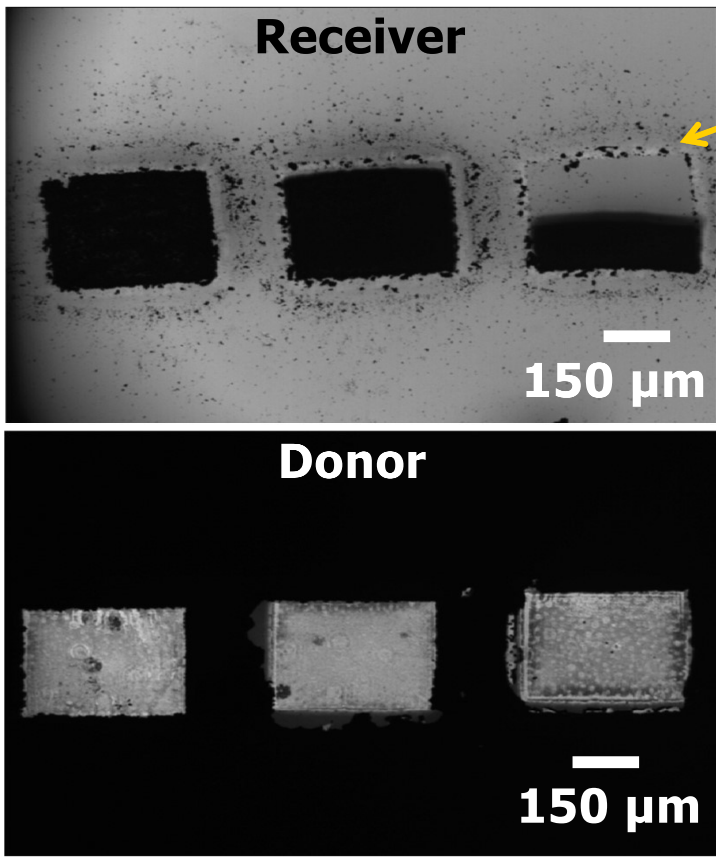

Pixels perpendicular on the substrate

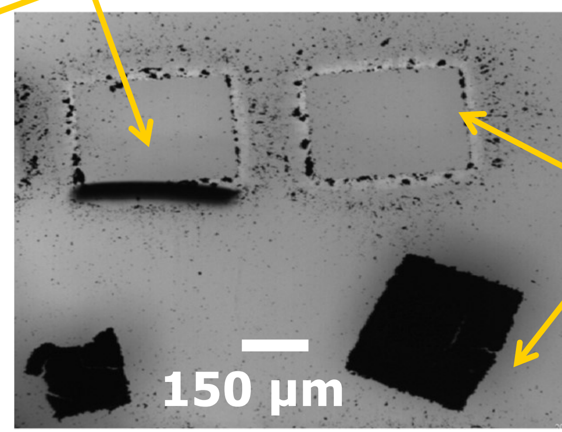

Displaced pixel

Need to reduce stress on pixels during transfer and improve adhesion!

A. Palla Papavlu *et al, Applied Surface Science,* Volume 374, 30 June 2016, Pages 312–317

CNW – flexible substrates

- different flexible substrates, similar roughness below 10 nm for 40x40 μm^2 areas

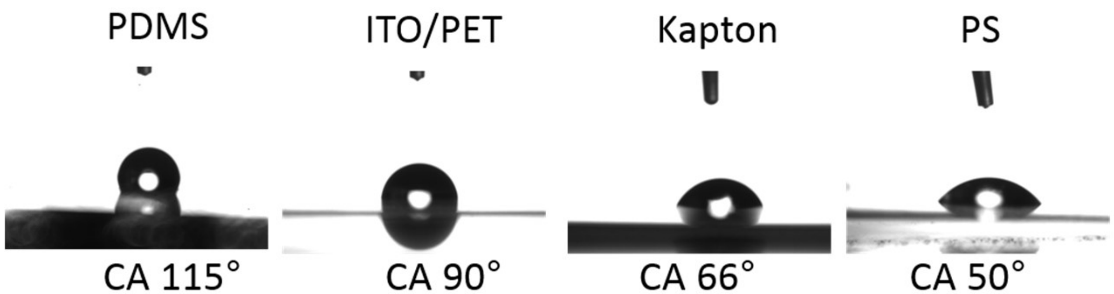

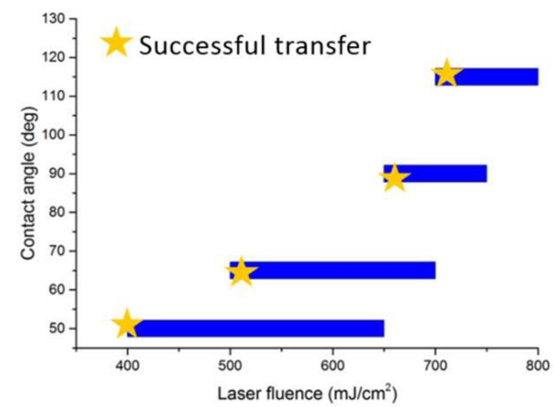

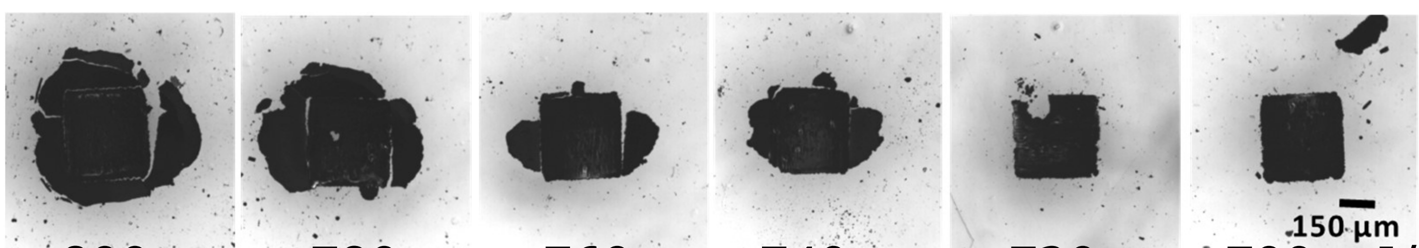

800 780 760 740 720 700 mJ/cm^2

- Adherence evaluation of the pixels - “tape test” method, after eight cycles of Scotch tape tests
- No obvious damage or detachment occurs to the LIFT-ed CNW

Hybrid CNW SnO_2 donor fabrication for sensors membranes printing

- Colloidal solution of SnO_2 (15 %wt)
- SnO_2 NPs with sizes of 5-10 nm
- Preparation of thin films: spin coating onto CNW
- Anneal at 300°C – remove traces of organic material (TritonX)

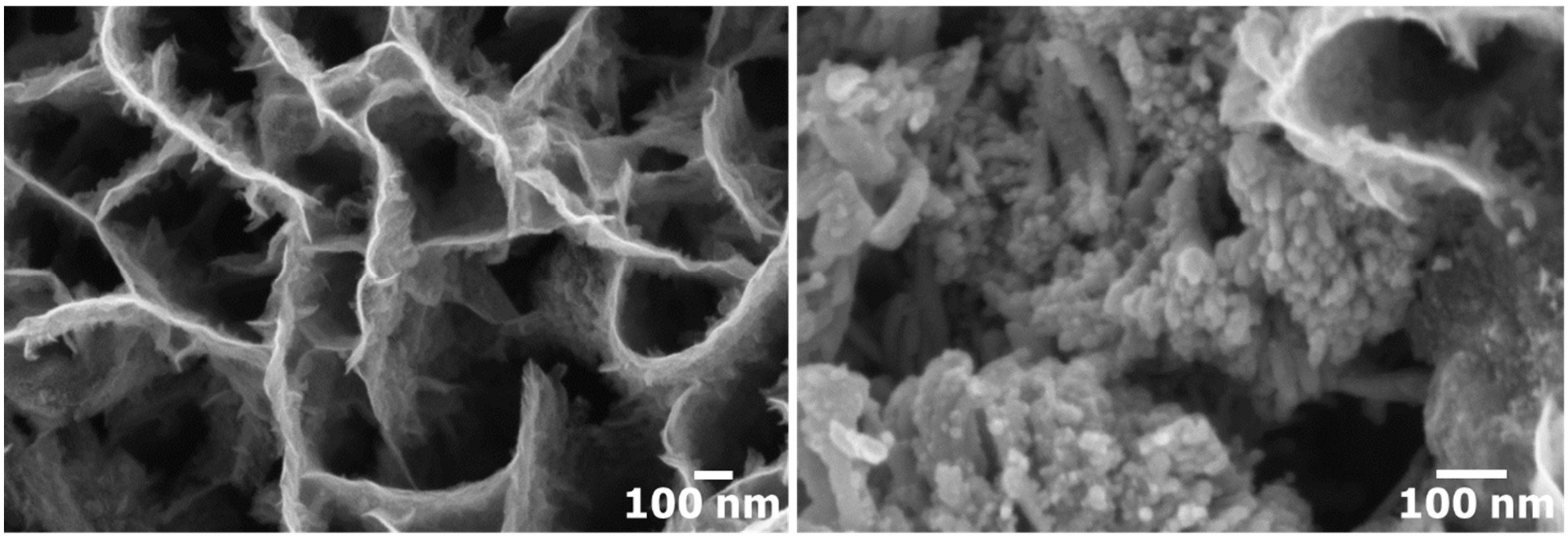

- SnO_2 NPs are homogenously distributed on the CNW
- In some areas, SnO_2 agglomerates are found sparsely distributed on the CNWs
- The SnO_2 NPs are specifically agglomerated at defect points onto the CNWs

A. Palla Papavlu *et al* Appl. Surf. Sci. 2016

LIFT of CNW:SnO_2 on Kapton

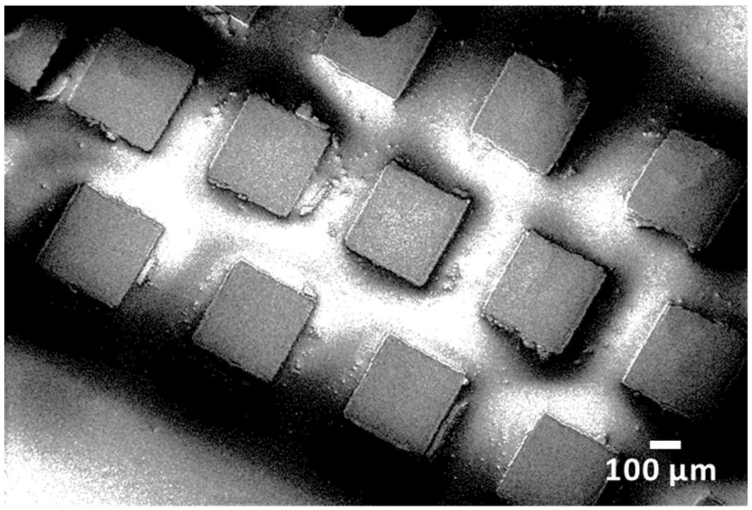

- The CNW:SnO_2 nanocomposite in the pixels maintain their morphology after transfer
- Small cracks in the pixels
- Some tearing induced by shear stress may be seen at the edges

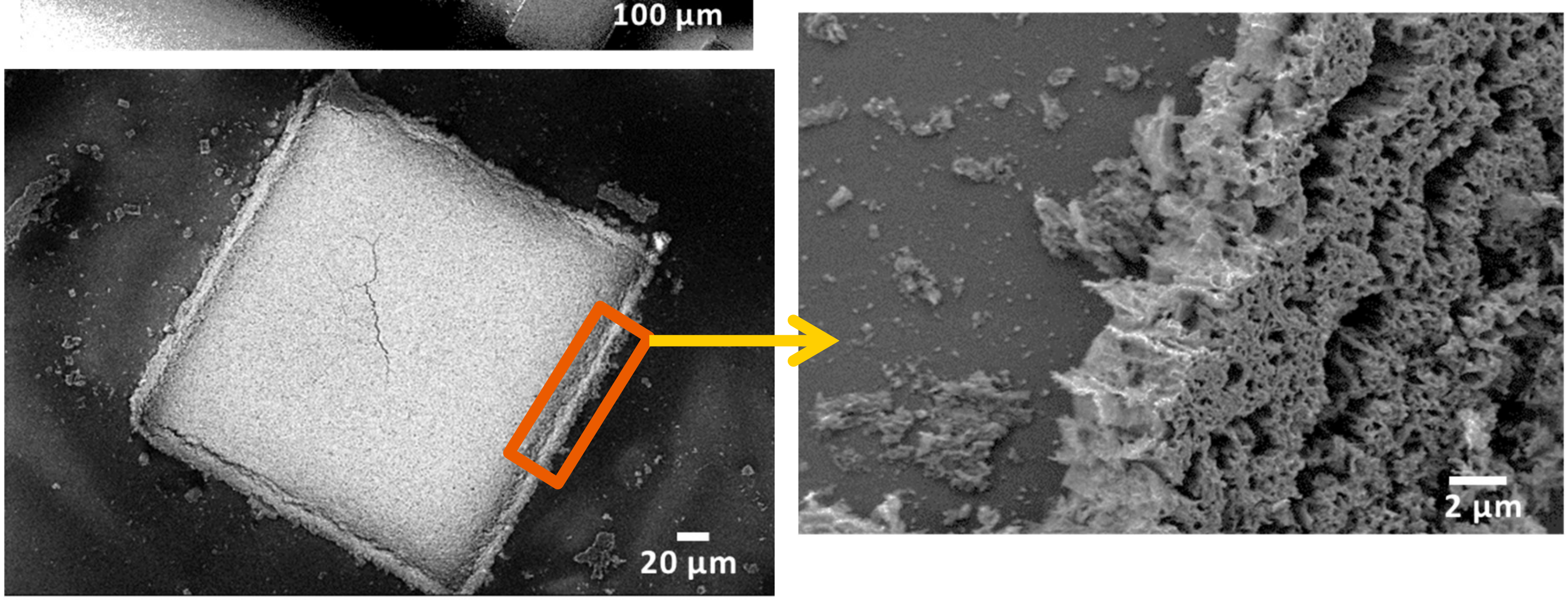

A. Palla Papavlu *et al* Appl. Surf. Sci. 2016

Micro-Raman spectra of CNW (black), SnO_2nanoparticles (blue), and CNW:SnO_2pixels transferred at 600 mJ/cm2 laser fluence (red). Inset: Raman bands observed for the SnO_2nanoparticles in the SnO_2donor and CNW:SnO_2pixels transferred by LIFT

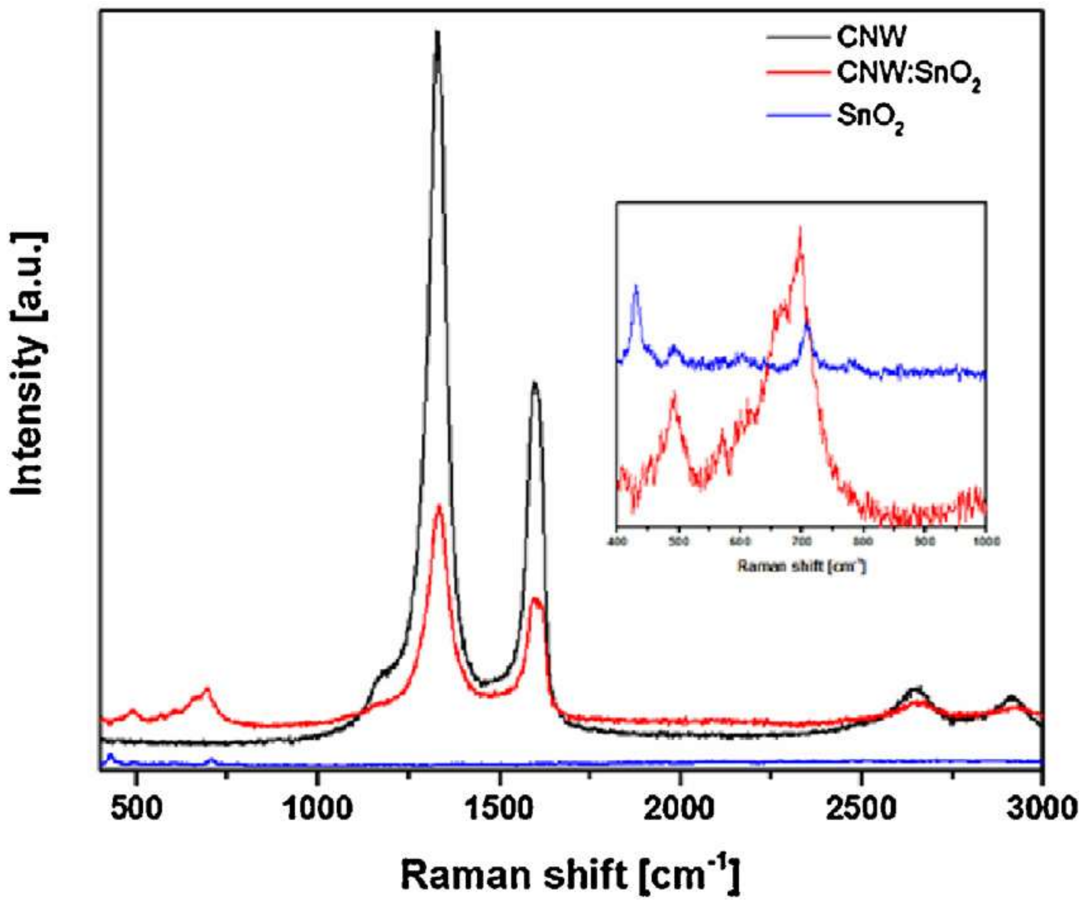

Ammonia sensors with CNW active material

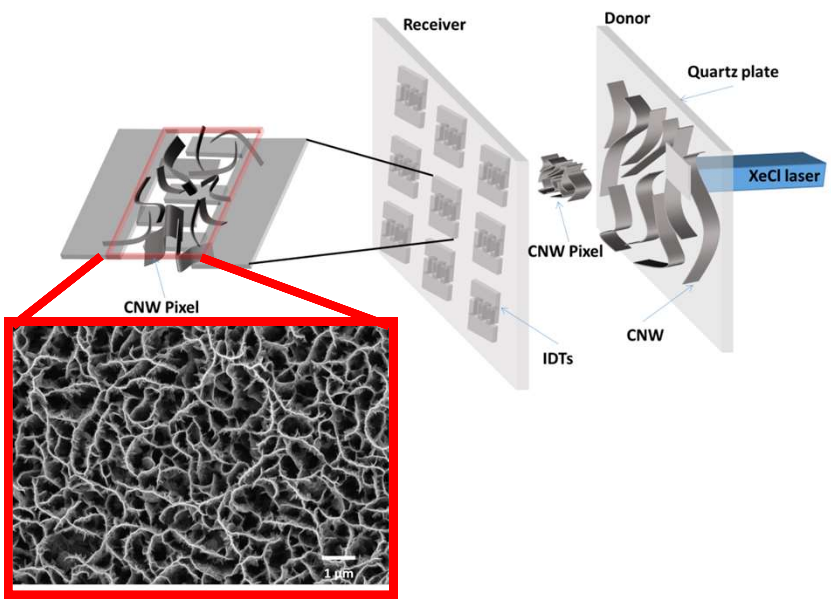

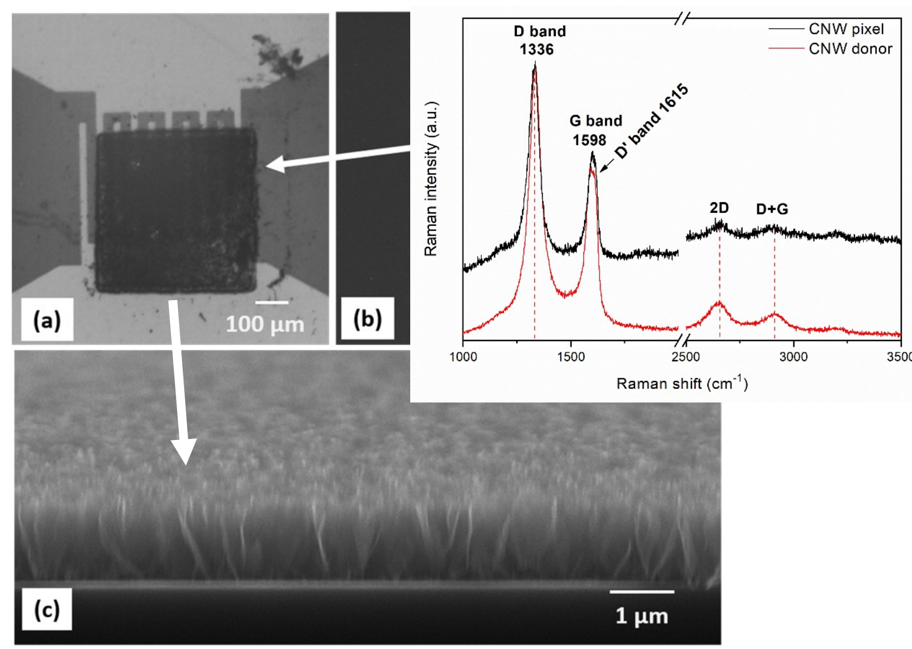

- Synthesis of CNW – RF plasma beam CVD
- Ar plasma jet injected with acetylene and hydrogen at $Ar/H_2/C_2H_2$ 1400/25/1 sccm
- Quartz substrate temperature 700 °C
- Deposition time is 15 minutes, CNW layer thickness is 1 µm

A. Palla-Papavlu et al, Nanomaterials 2022, 12, 2830

Ammonia sensors with CNW active material

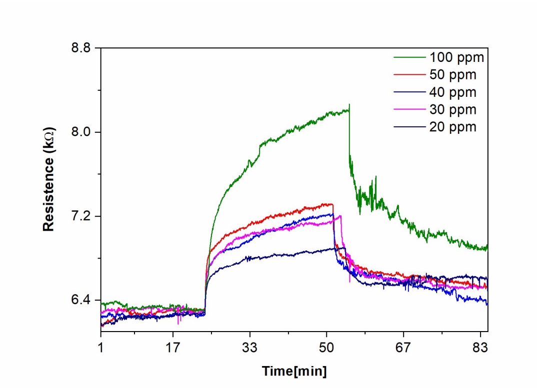

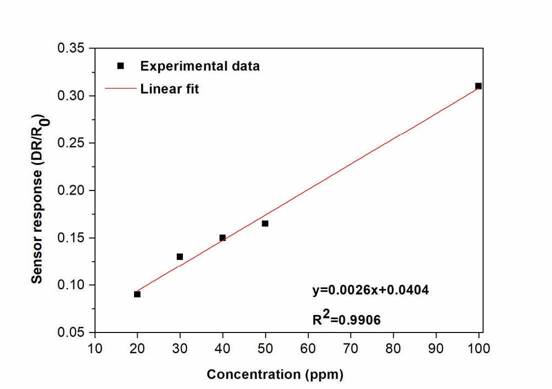

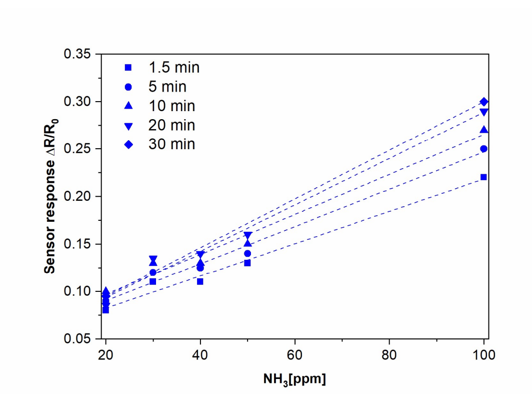

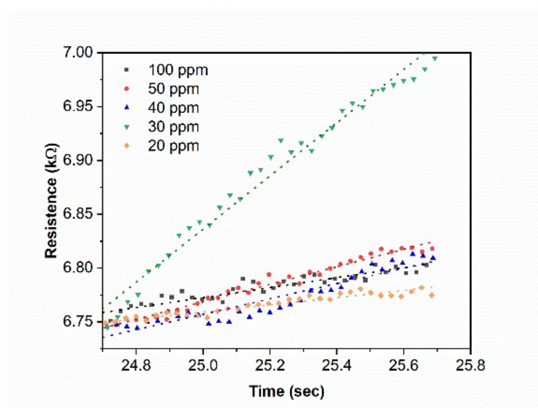

- P-type semiconductor response
- LOD for NH_3 is 89 ppb for 30 min of exposure
- This LOD value is one order of magnitude lower than that of chemiresistive devices based on CNW reported previously
- The CNW are sensitive to NH_3 within 1 minute of exposure
- Full reversibility only for 20 ppm NH3 exposure
- Quasi-dosimetric response

A. Palla-Papavlu et al, Nanomaterials 2022, 12, 2830

Ammonia sensors with CNW active material

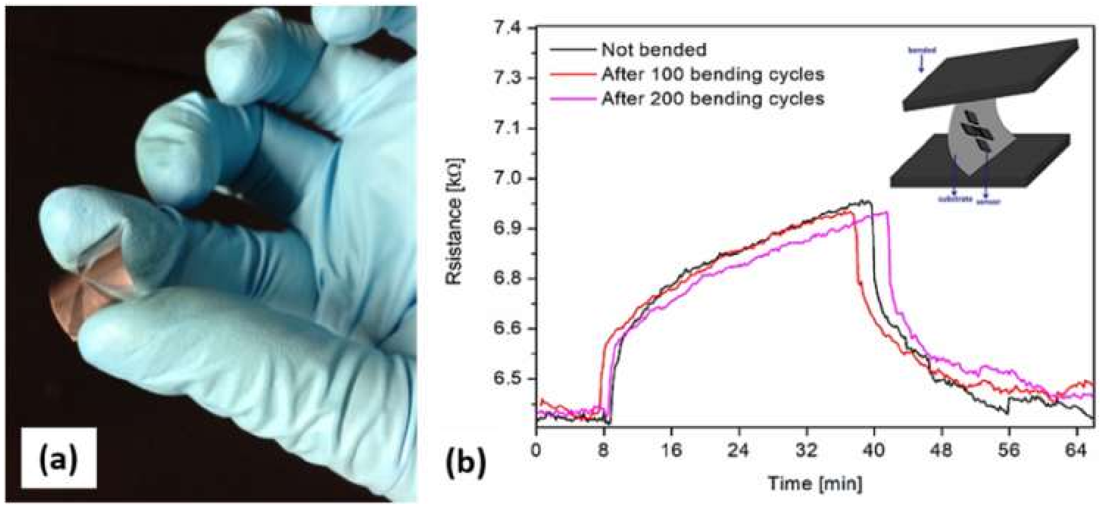

- The sensors exposed to 20 ppm of ammonia after carrying out multiple bending cycles – 100 and 200
- We noticed that without any bending, the initial resistance of the fabricated flexible chemiresistor was measured to be around 6300 Ω at 22 ◦C
- The Ohmic behavior did not change after the applied bending cycles
- The resistance variation of the chemiresistor at a 20 ppm concentration of NH_3 was small (~3%) with increasing bending cycles

A. Palla-Papavlu et al, Nanomaterials 2022, 12, 2830

Liquid phase LIFT
Laser Transfer as Function of Viscosity

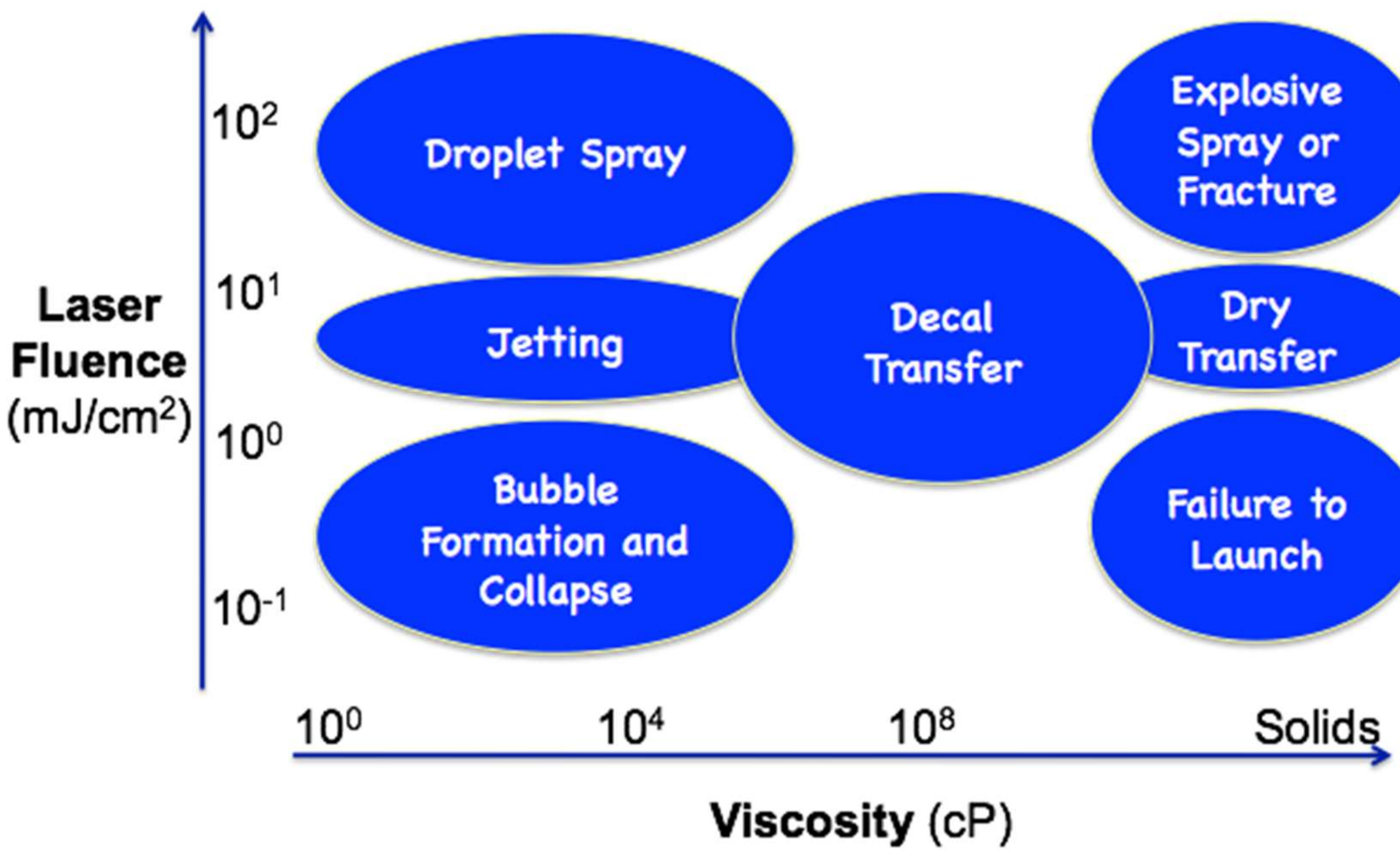

centipoise (1miliPascal second) slide adopted from A.Pique

Liquid phase LIFT

- Microarray fabrication: fs, ps, or ns lasers were used
- Transfer of a water:glycerol solution as model solution for biomolecules

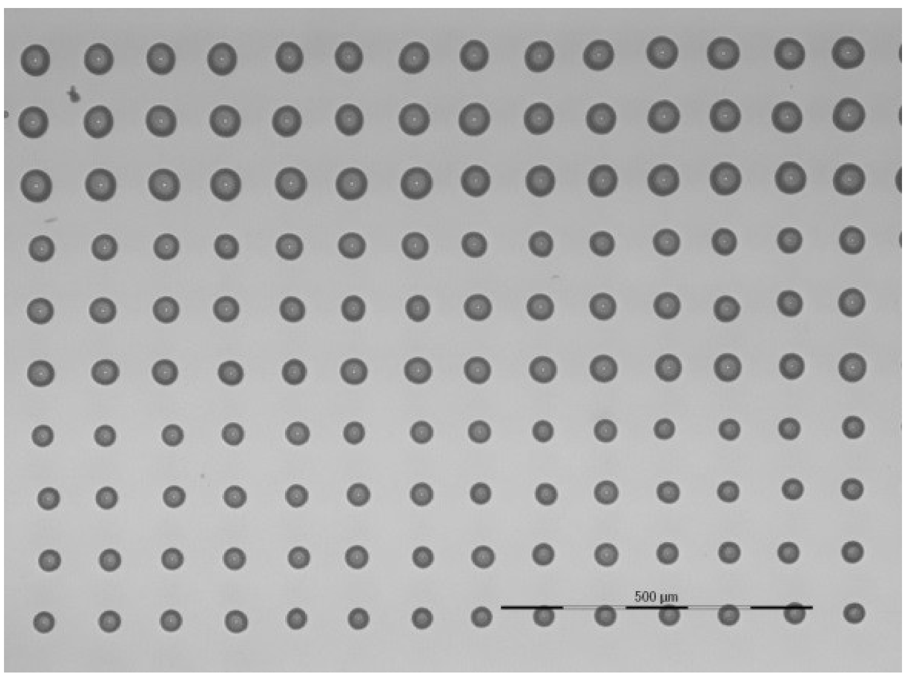

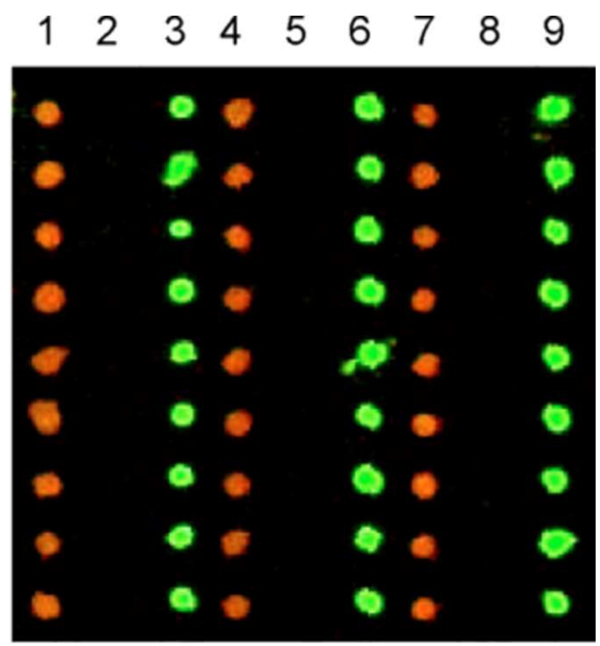

DNA Microarray (using Ti layer)

P. Serra et al. Appl. Phys. Lett (2004)

From droplets to lines (overlapping...)

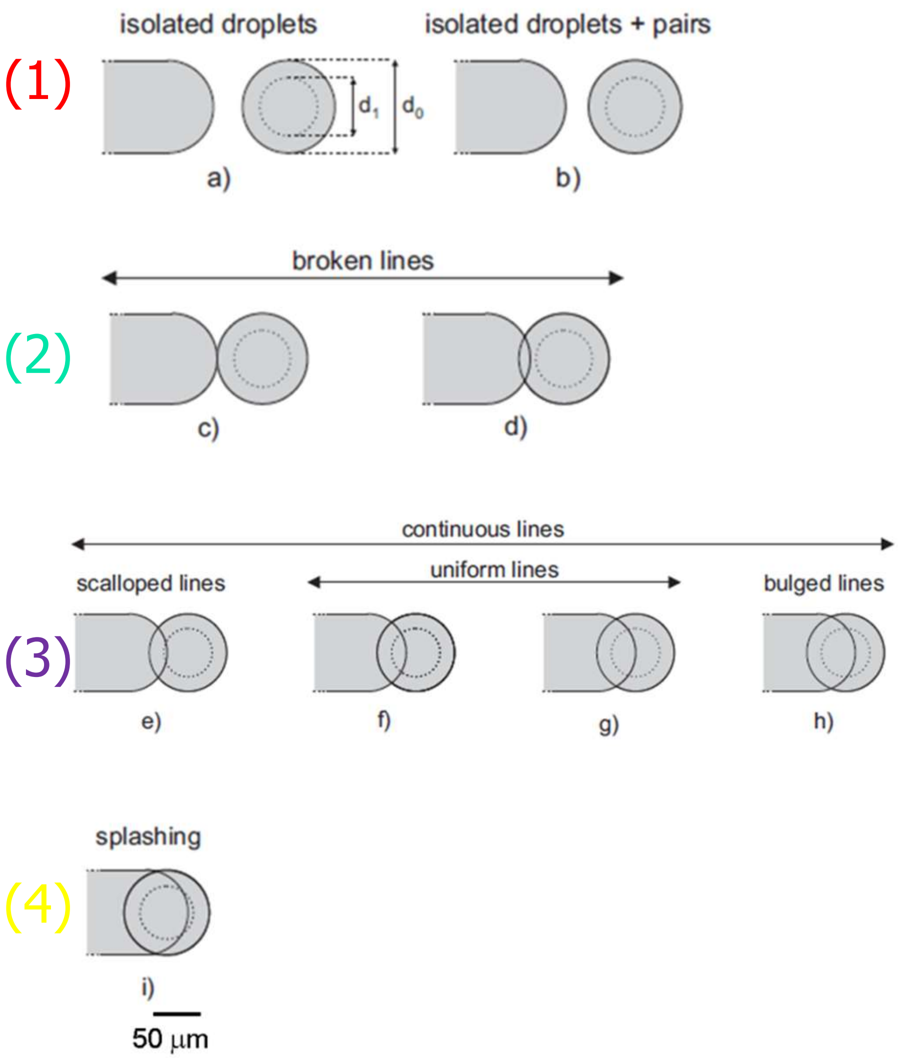

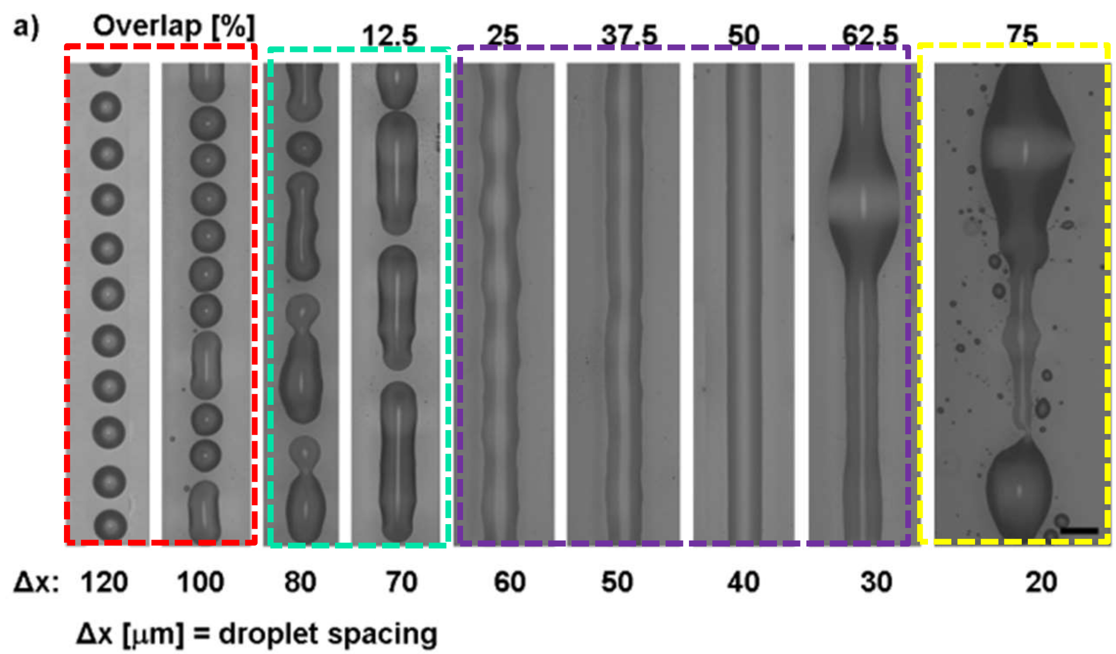

A. Palla-Papavlu *et al.* Appl Phys A (2013)

C. Florian *et al.* Appl Surf Sci (2015)

Liquid phase LIFT - applications

Array composed of 3 sensors: SAW resonators operating at 392 MHz

Proteins: Wild-type bovine odorant-binding protein (wtbOBP)
Mutant bOBP (mutbOBP)
OBP from pig (pOBP)

Odorants: 1-octen-3-ol (octenol), carvone

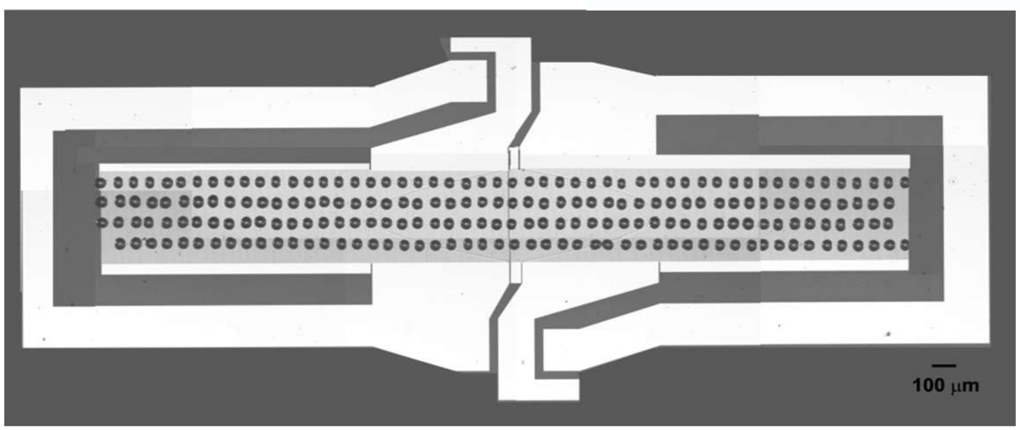

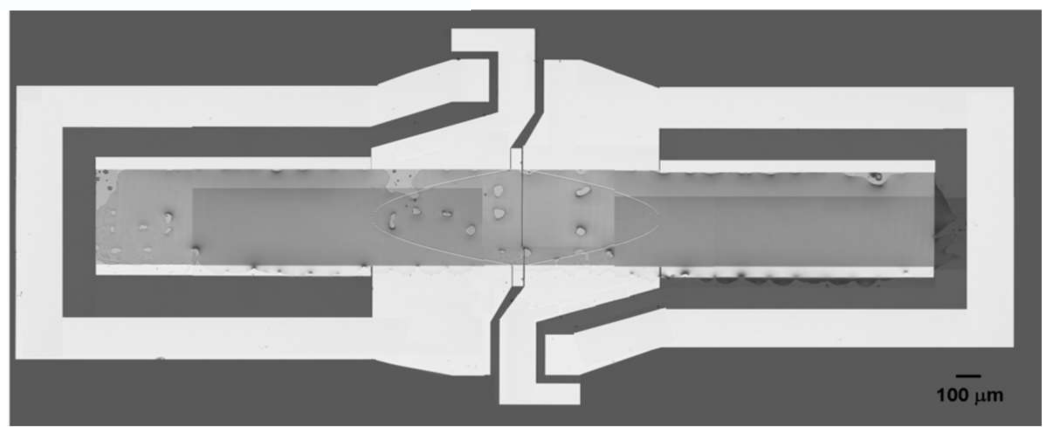

To minimize SAW scattering and diffraction → <u>uniformly</u> covered active area.

A. Palla Papavlu *et al*. Sensors and Actuators B (2013)

Liquid phase LIFT - applications

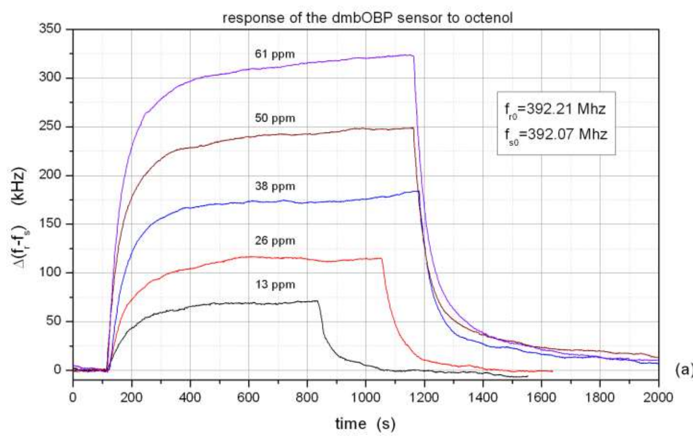

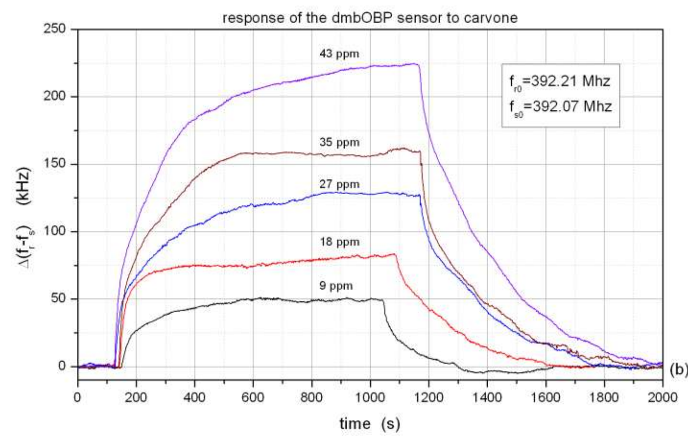

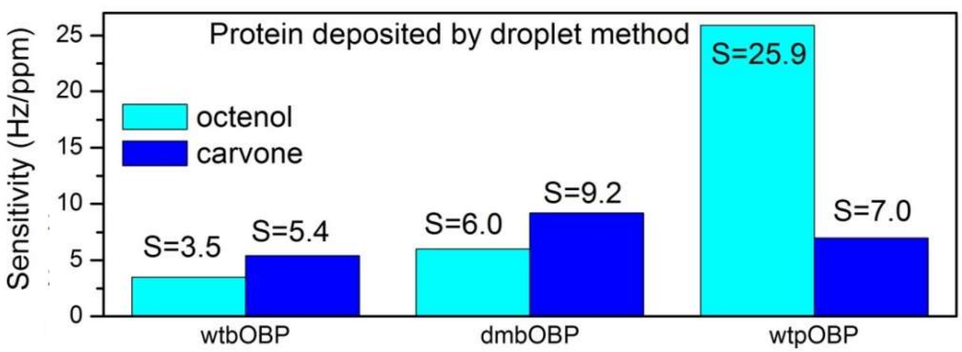

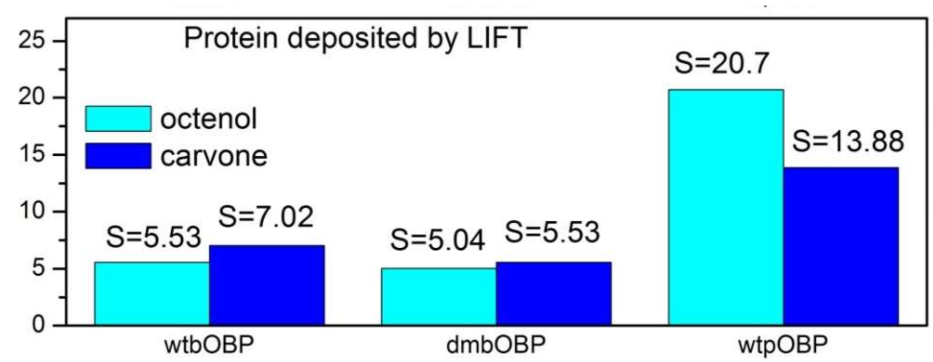

Volume=5 µL

Volume=15 nL

- The obtained sensitivities for odorant detection are comparable with results reported in the literature obtained with SAW sensors and the same proteins, deposited by other methods.

F. Di Pietrantonio *et al* Biosensor and Bioelectronics (2015)

Ink printing at high velocity

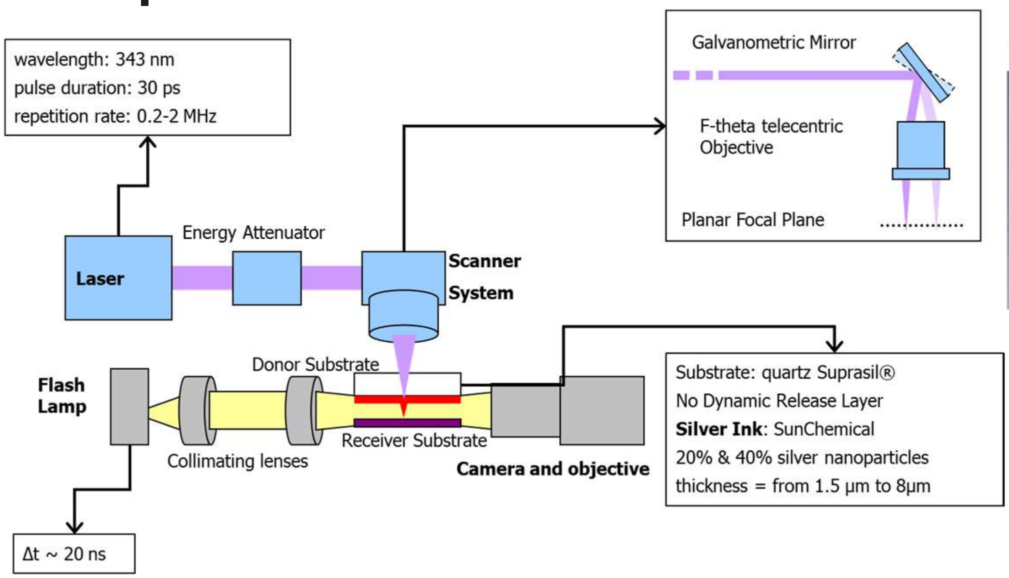

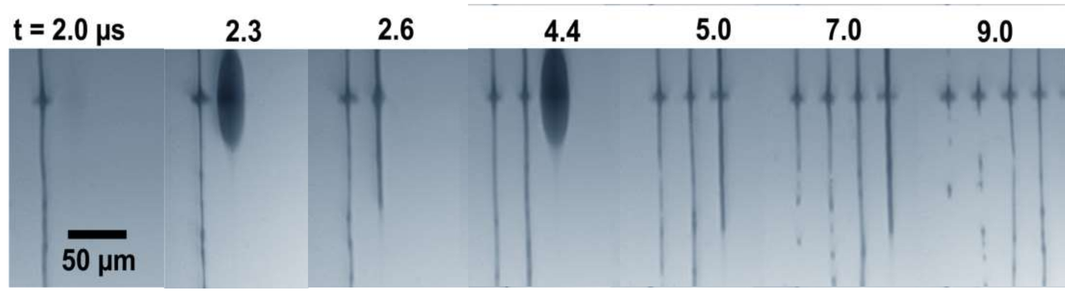

3 passes, 50% overlap

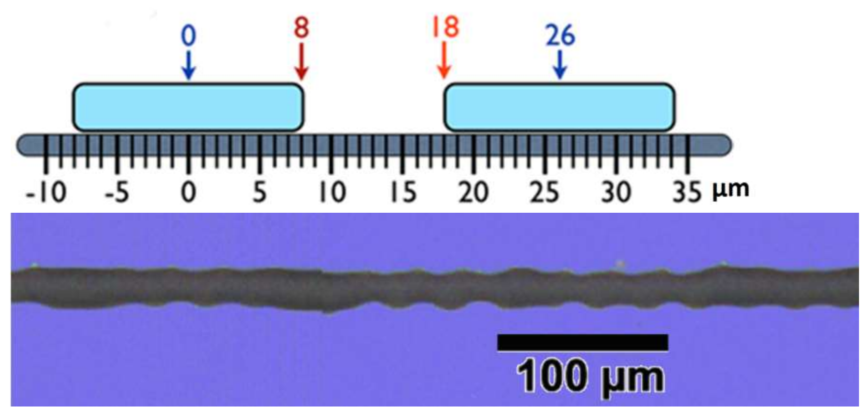

1 pass at 26µm

- **With multi-passes approach, line can be printed at velocities up to 4m/s**

E.Biver *et al.* Applied Surface Science (2014)

L. Rapp *et al.* J. of Laser Micro/ NanoEngineering (2014)

slide adopted from P. Delaporte

Influence of ink metal content

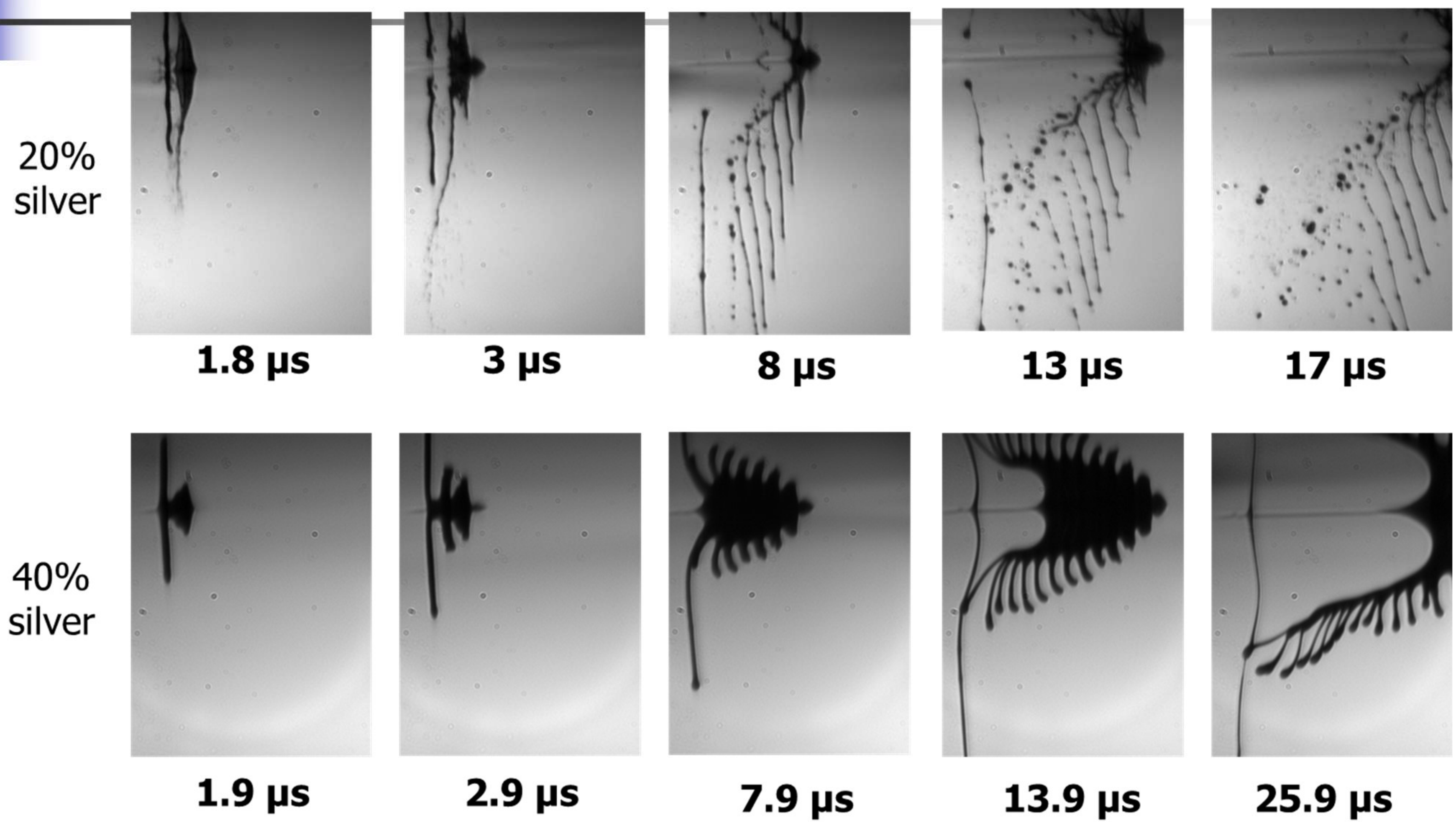

Film thickness 4µm - f = 1MHz - velocity = 17m/s

slide adopted from P. Delaporte

Single step printing of continuous lines

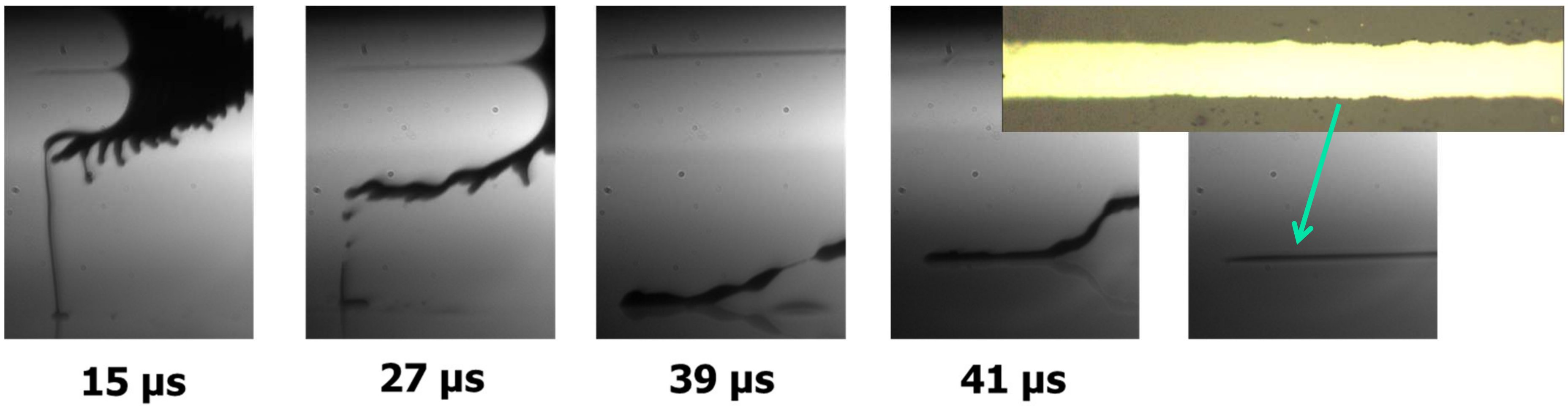

40% Silver ink - 17m/s - with receiver

- Increasing metal content of the ink allows the stabilization of the ejection process (higher surface tension? Viscosity?)
- Tuning the position of the following laser shot (scanning velocity, laser frequency) as a function of the bubble size allows transferring a continuous line instead of multiple jets

slide adopted from P. Delaporte

Applications: Interconnects

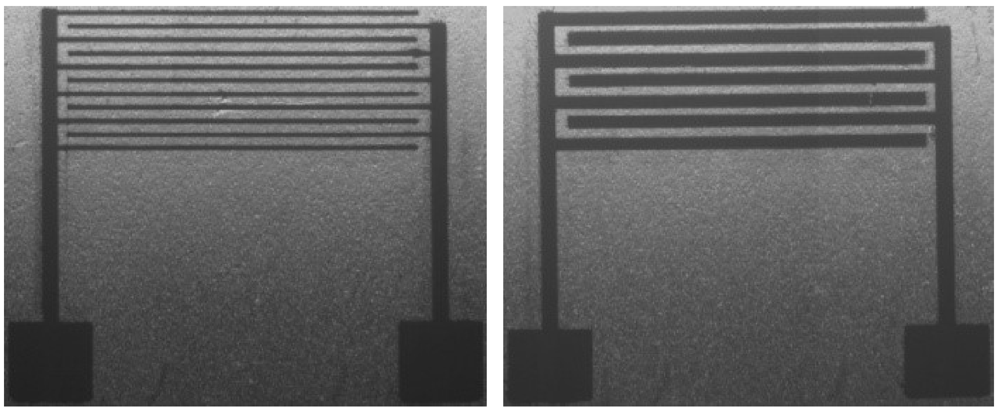

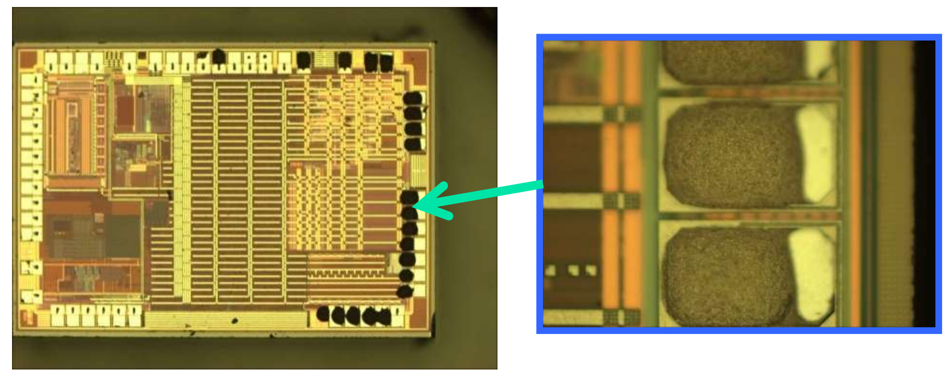

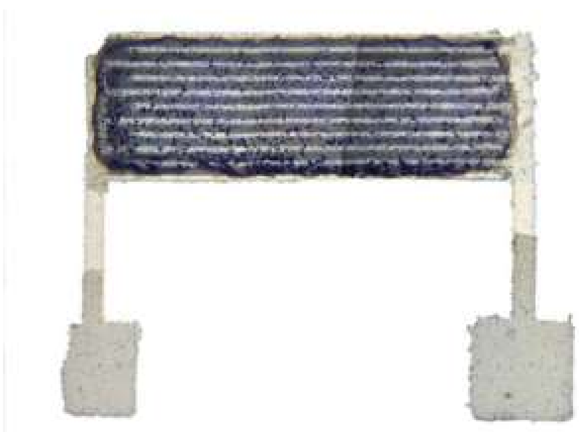

Interdigited electrodes for sensors

High resolution printing on flexible substrates

What is "DECAL"?

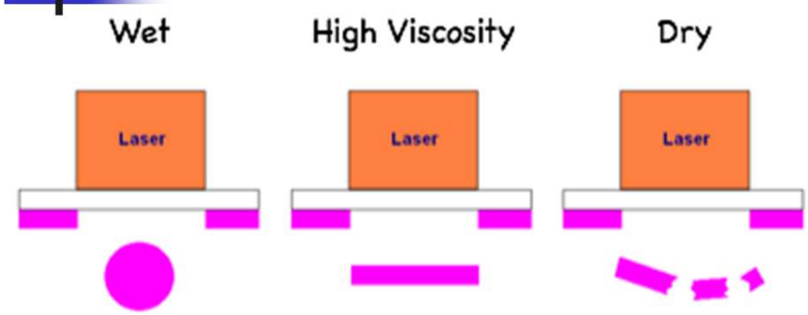

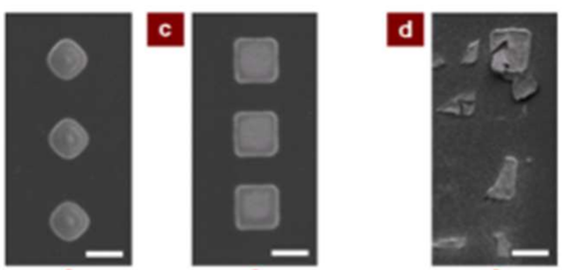

"Decal" transfer

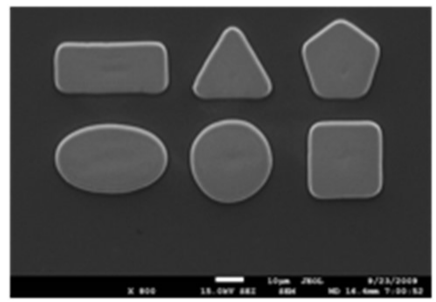

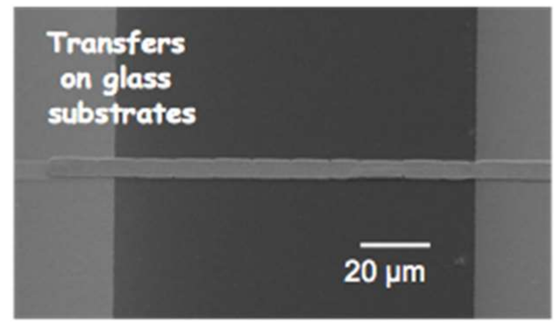

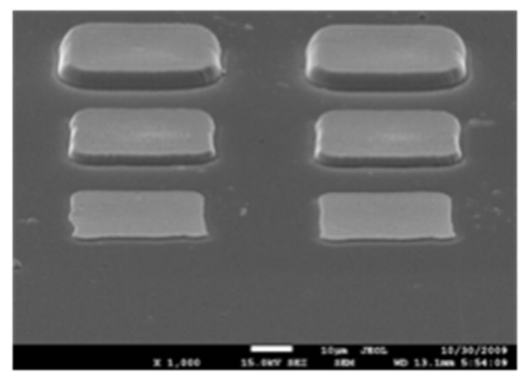

Decal since it maintains the original beam geometry (gap 5-50 µm)

Ag nanoink: 3 – 7nm, η ≈ 10^5 cP, 80 wt% solids loading content

Ag nanoparticles allow for efficient laser to nanoink energy coupling

Auyeung, et al., J. of Laser Micro/Nanoeng. 2, (2007) 21

Piqué, et al. J. Laser Micro/Nanoeng., 3 (2008) 163.

~10-30 mJ cm^{-2} (355 nm, 30 ns)

slide adopted from A.Pique

3D and Free Standing Structures

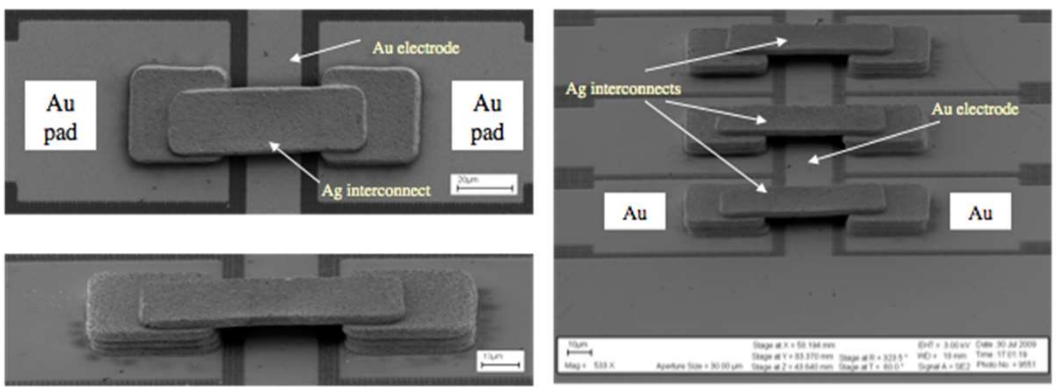

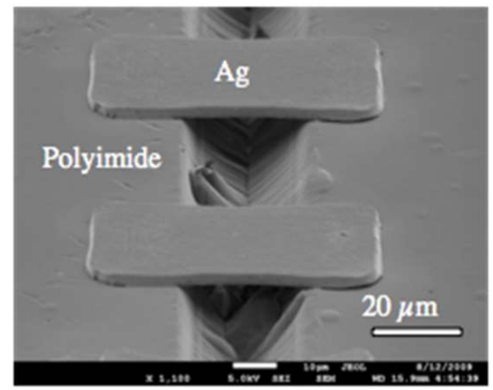

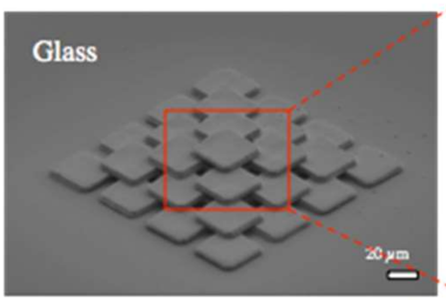

A low aspect ratio micro pyramid

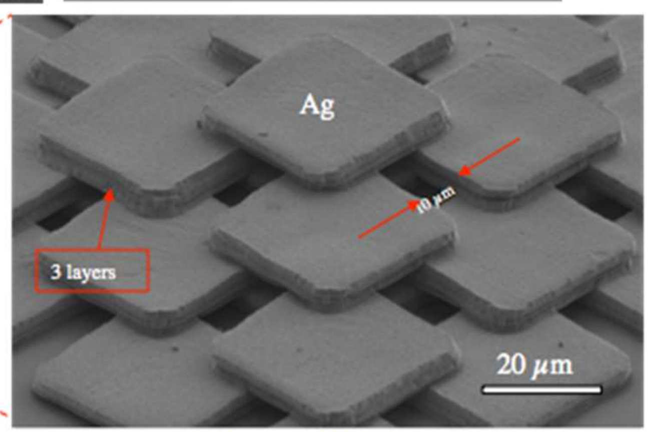

Multilayer scaffold structure

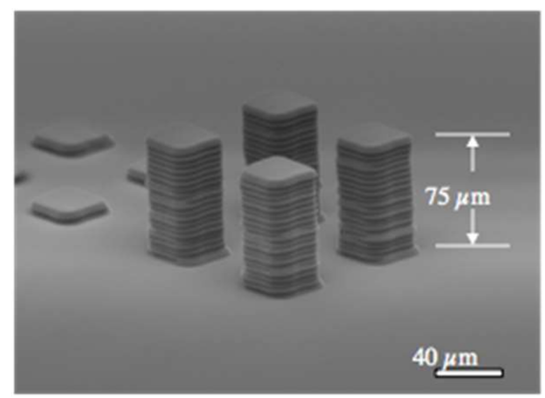

slide adopted from A.Pique

Ag and Cu nanoparticle printing

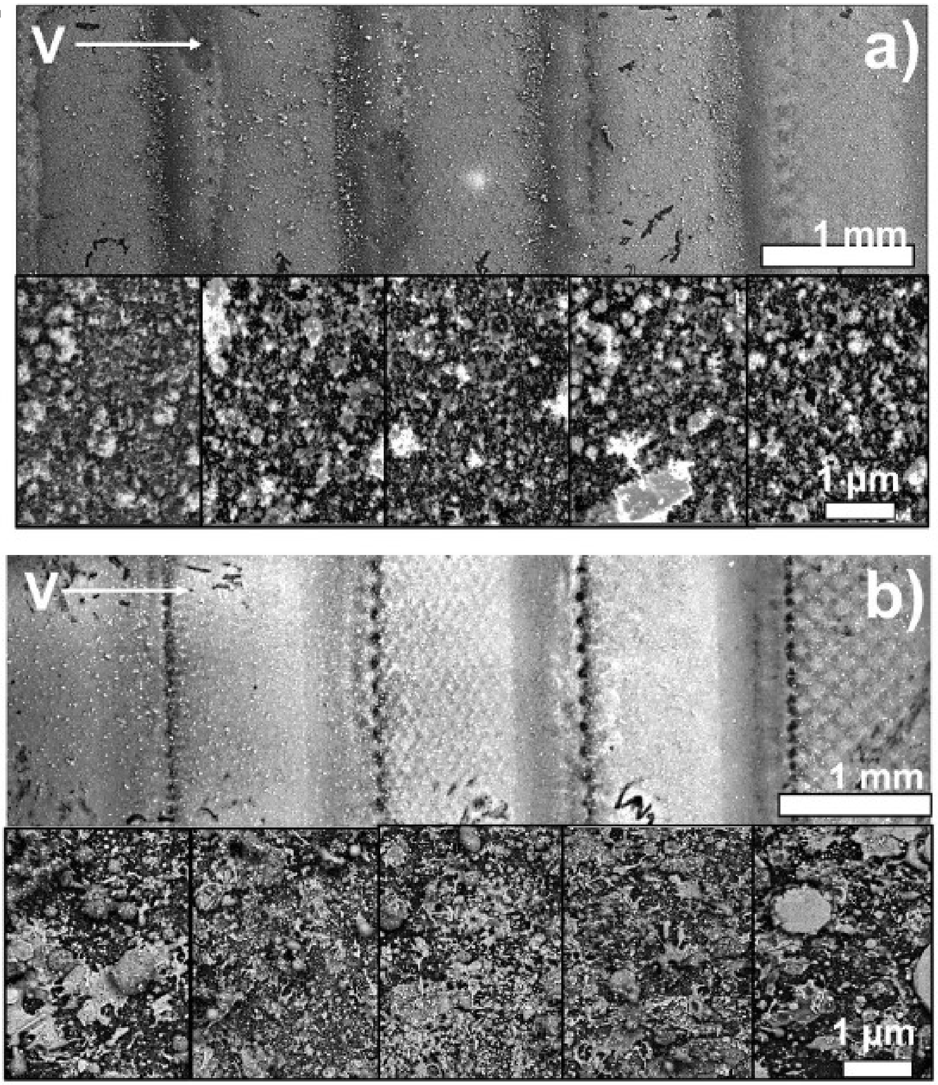

One-step additive LIFT printing of conductive elements
Alena Nastulyavichus et al, Laser Phys. Lett. 21 (2024) 035603

Graphite from inks

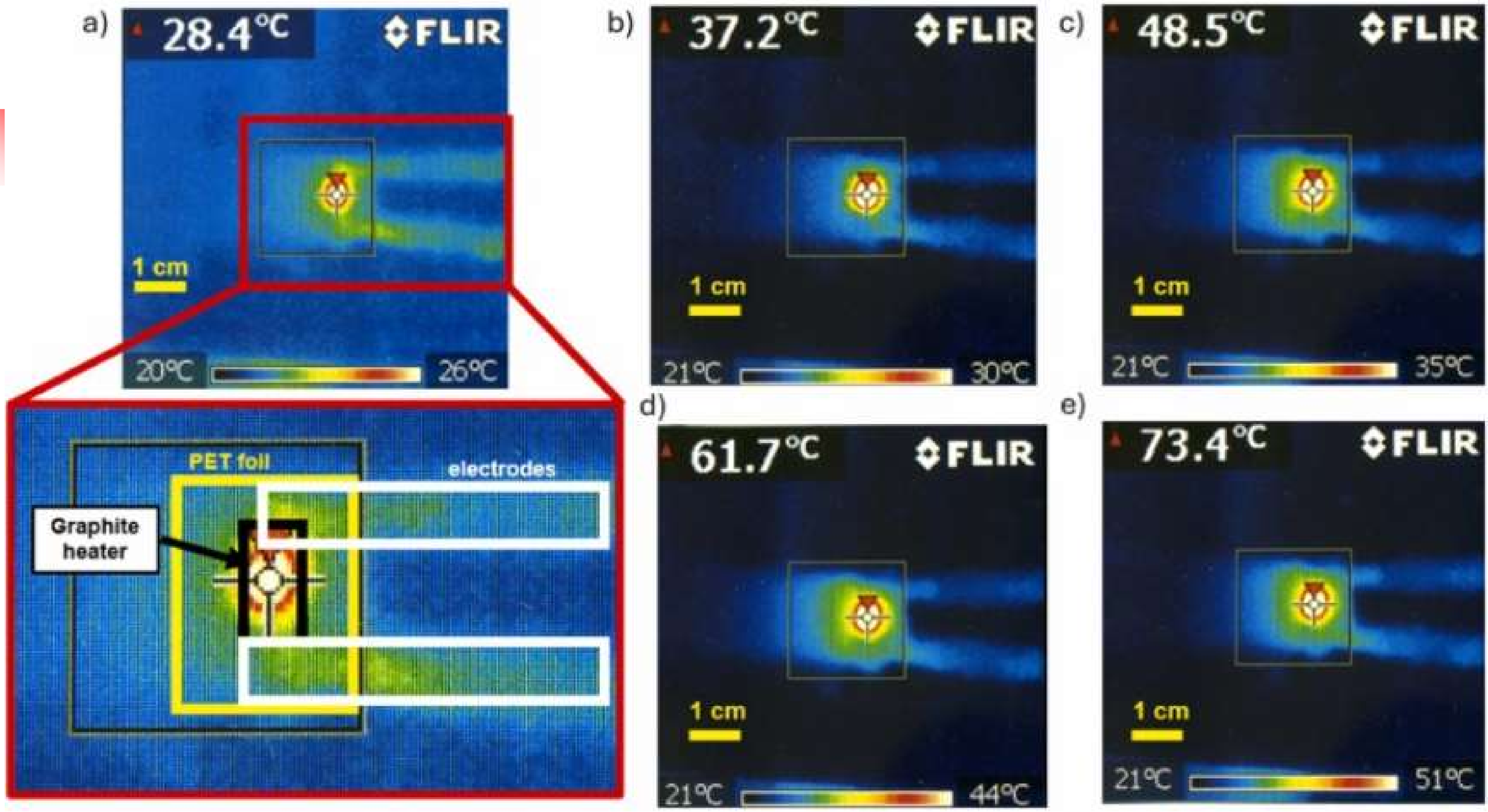

Thermal image of the surface temperature of a 18 mm^2 graphite heater printed on PET foil with a resistance of 48.6 Ω at a) 2 V, b) 3 V, c) 4 V, d) 5 V and e) 6 V. Inset shows an enlarged thermal image marking the size of the heater, substrate, and electrodes. The big square on the images denotes the region of interest and the marker is at the region with maximum temperature Logaheswari Muniraj et al, **Laser-induced forward transfer for manufacture of graphite-based heaters on flexible substrate**, **Sensors and Actuators A: Physical**, Volume 373, 1 August 2024

Commercial applications

A roll to roll LIFT printing machine for graphic applications

DI PROJEKT AG
digitalimaging

Daetwyler
Graphics

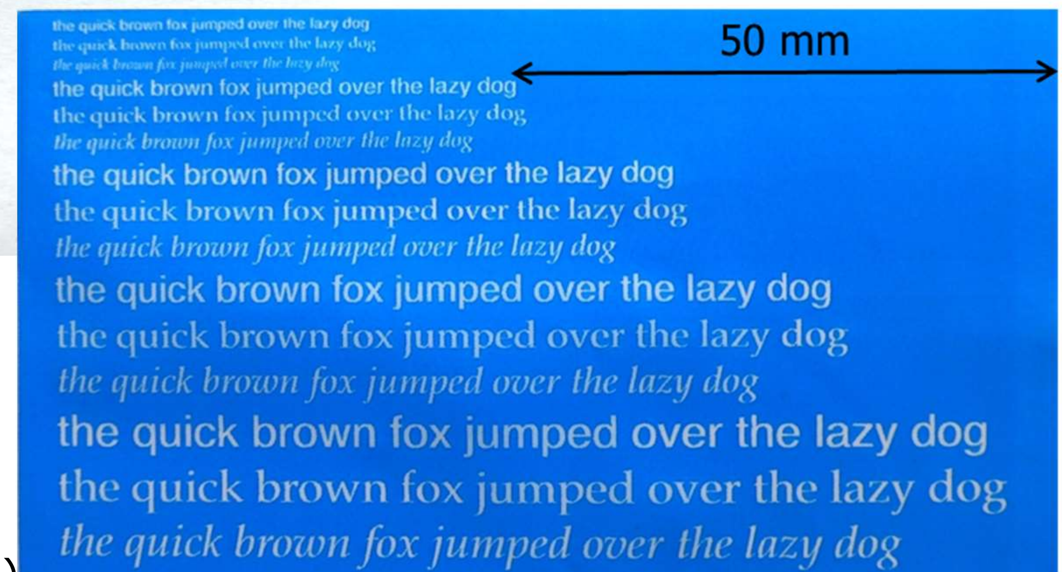

G. Hennig *et al.* J. Laser Micro/Nanoengineering (2012)

Conclusions

- Laser direct write techniques are possible alternatives to printing techniques.
- A wide variety of materials can be transferred.
- Even sensitive materials, e.g. biomaterials or polymers can be transferred.
- The application of a dynamic release layer (absorbing layer) increases the possibilities for laser direct write methods.
- Still many open questions and many parameters to study, e.g. role of pulse length and beam homogeneity.
- Time-resolved methods, such as shadowgraphy help understanding of the process (for solids and liquids).
- It is possible to deposit even functional layers in “devices”.

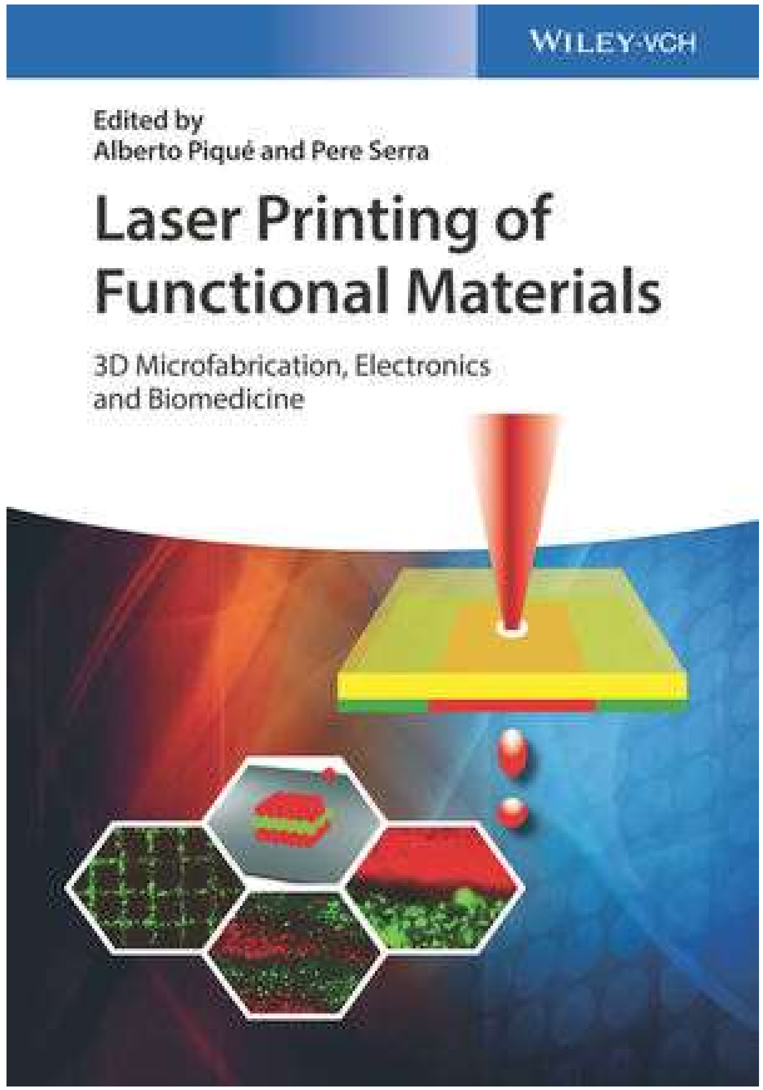
WILEY-VCH
Edited by
Alberto Piqué and Pere Serra
Laser Printing of
Functional Materials
3D Microfabrication, Electronics
and Biomedicine

LDW by 2PP

- Three-dimensional polymeric microstructures
- No topological constrains
- High penetration depth without surface modifications
- Resolution bellow the diffraction limit

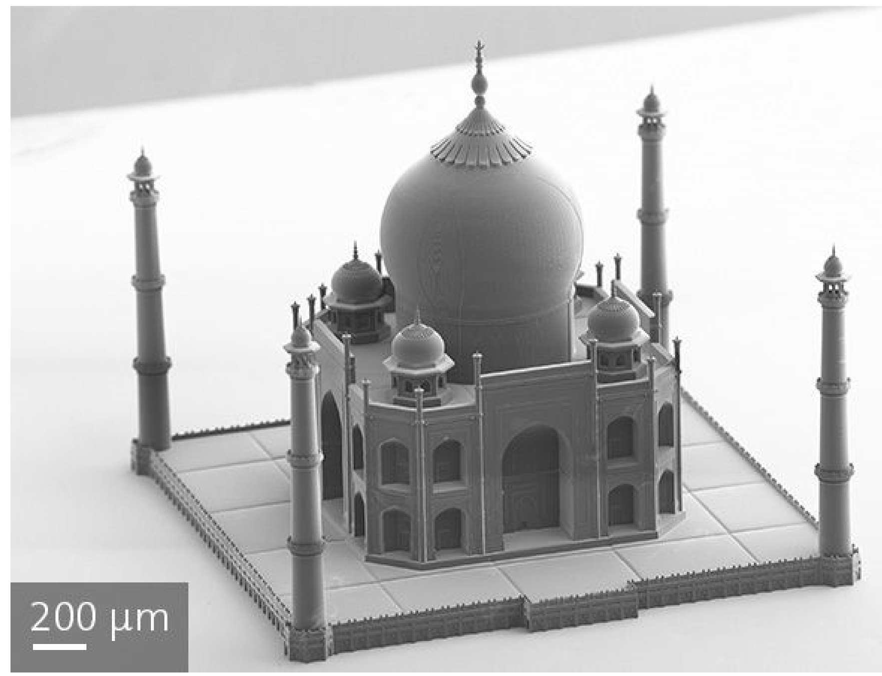

SEM image of the Taj Mahal structure fabricated by TPP
http://www.nanoscribe.de/en/applications/micro-rapid-prototyping/

APPLICATIONS of LDW via 2PP

Photonic Surfaces

√ diffractive optical elements (DOEs) and gratings
√ metamaterials
√ optical security labels
√ optical waveguides

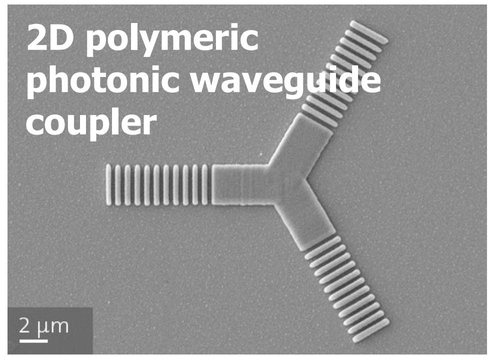

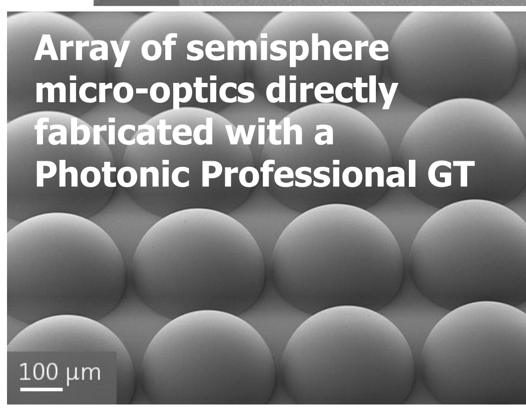

Mechanical Microstructures

√ Mechanical metamaterials
Ultralight materials

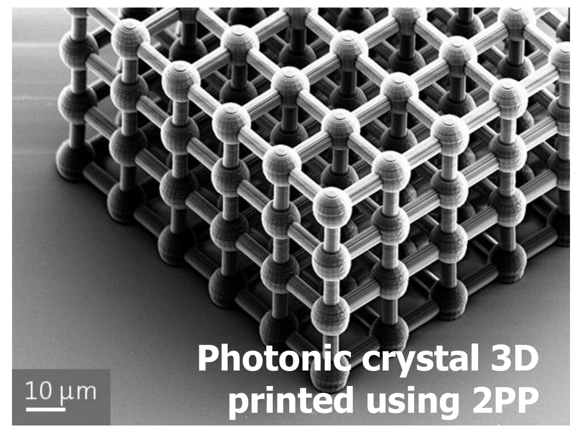

Micro-Optics

√ Complex and replicable 2.5D structures as molds for replication or masters for pattern transfer

Cell Scaffolds and Biomimetics

√ 3D tailored environment acting as an artificial extracellular matrix, i.e., a scaffold for the cells

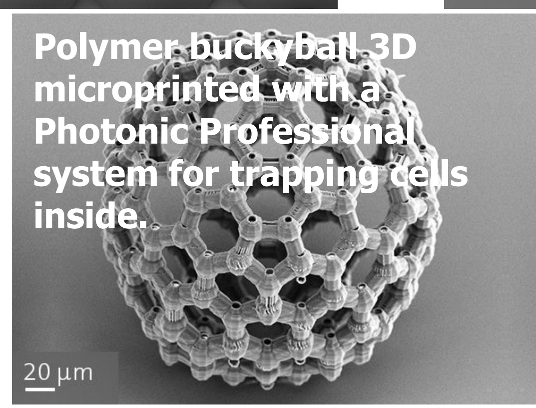

http://www.nanoscribe.de/en/applications/

A little bit into the theoretical background...

LDW by 2PP

- **Photopolymerization:** chemical reaction that turns monomers into macromolecules consisting of repeating units, by using light as reaction trigger
- **Two-photon absorption (2PA) polymerization**: simultaneous absorption of two photons
  - Polymerization occurs only in the vicinity of the focused laser beam
  - Small solidified volume (voxel) around the focal spot
- **Femtosecond laser pulses** promote **two-photon absorption (2PA)** of photosensitive molecule dissolved in the resin.

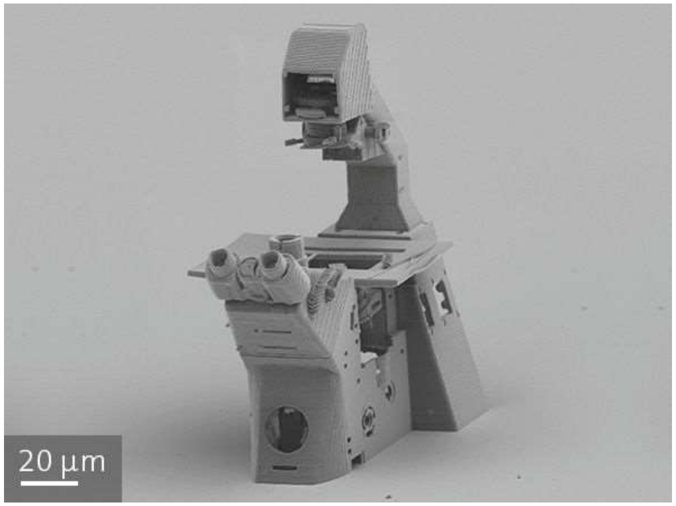

http://www.nanoscribe.de/en/applications/micro-rapid-prototyping/

2PA absorption

- An atom or molecule taken to an excited state by simultaneously absorbing two photons
- Difficult to be attained by using conventional (low intensity) light sources
- Pulsed laser light is employed
- Chemical reaction in a tiny focal volume
  - → Tridimensional polymeric structures with resolution below the diffraction limit

The two-photons can have:

√ same energy *(degenerate process)*

√ different energies

(nondegenerate process)

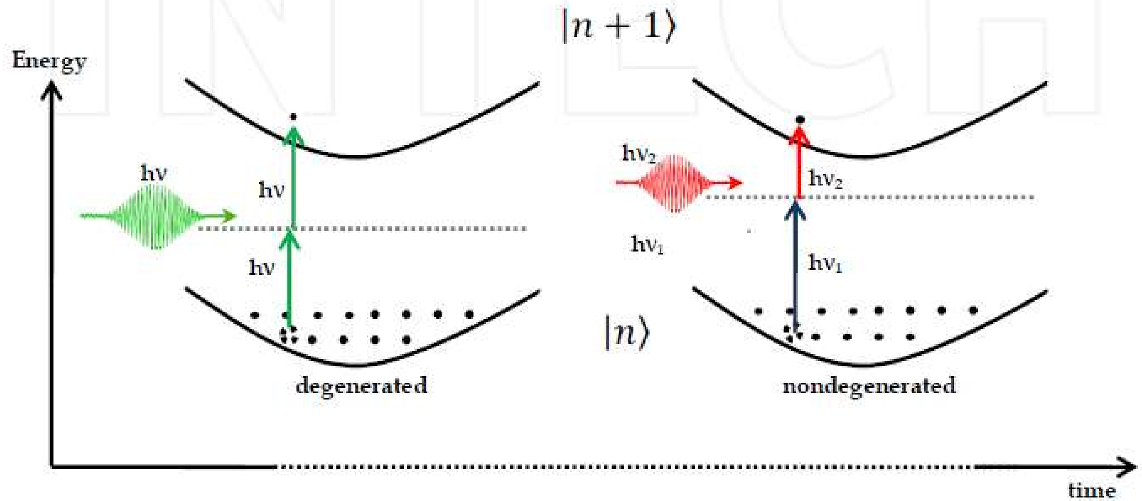

Representation of a degenerated and nondegenarated two-photon transition between $|n\rangle$ and $|n+1\rangle$ electronic states of an atom or molecule. The dotted lines represent a virtual state which intermediate the two-photon absorption process.

D.S. Correa *et al*. Two-Photon Polymerization Fabrication of Doped Microstructures (2012) InTech

2PA absorption

Two-photon absorption occurs in defined spatial regions where the light intensity is high enough

→Polymerization only in a small region

→No other changes in the surrounding regions

Evidence about the spatial confinement of the excitation:

→ two-photon excitation gives **localized** fluorescence

→ one-photon excitation gives **extended** fluorescence along the whole optical path

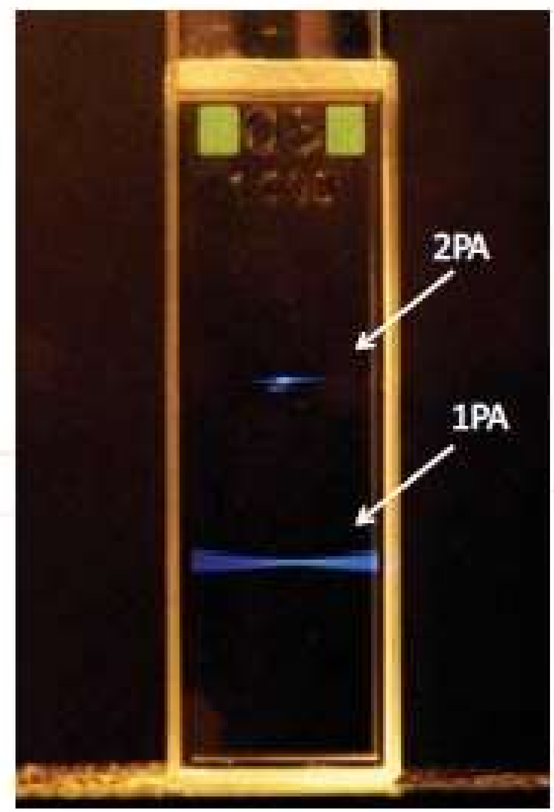

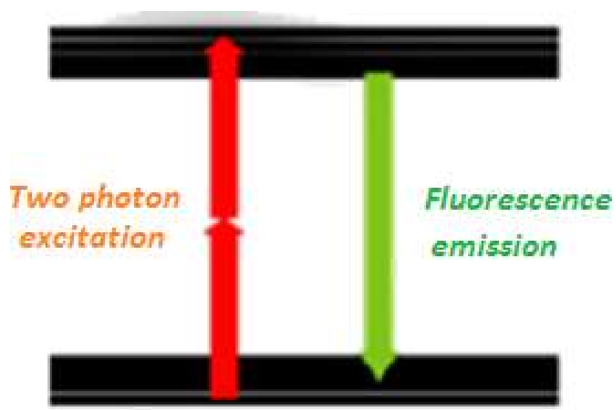

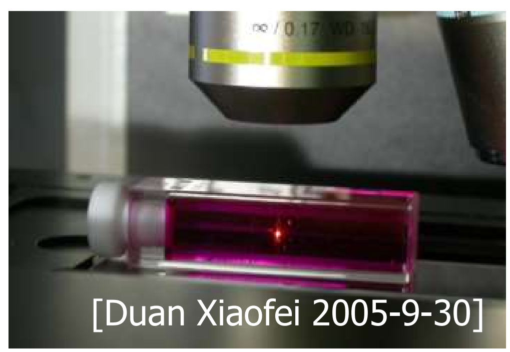

D.S. Correa *et al*. Two-Photon Polymerization Fabrication of Doped Microstructures (2012) InTech

(Marder, et al.,2007).Copyright [2007], Materials Research Society.

2PA absorption

- Polymerization threshold imposes a minimum power (**power thershold**)
- Even though the outer regions of the beam might not have enough power to start the reaction, the central part of the beam can overcome the threshold.

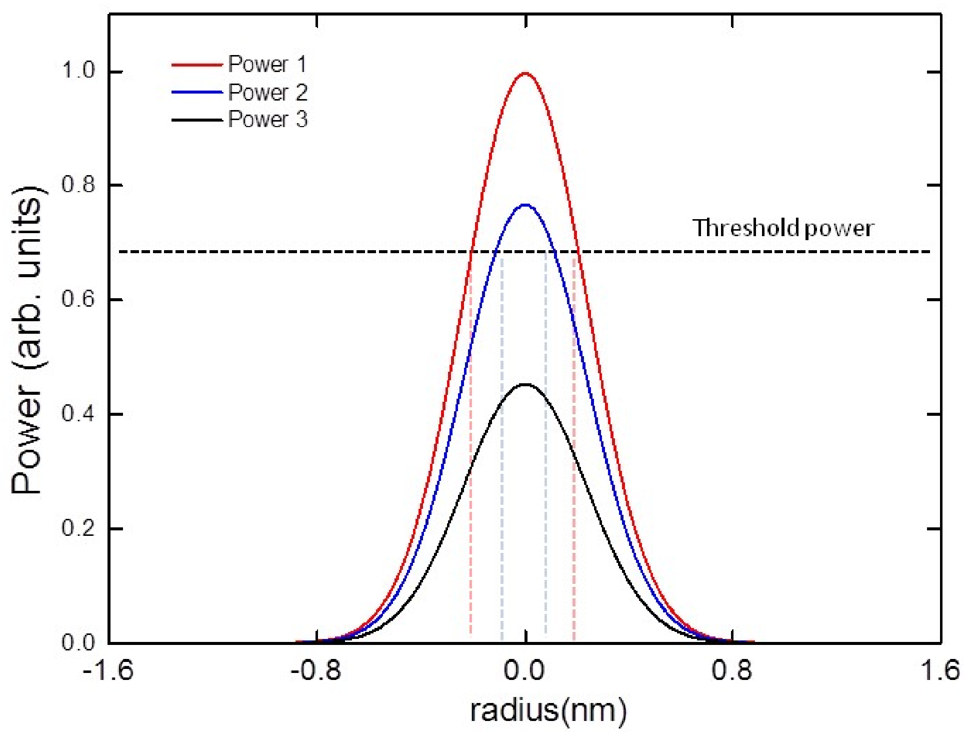

Laser power near the polymerization **threshold** pushes the resolution **below the diffraction limit**

D.S. Correa *et al*. Two-Photon Polymerization Fabrication of Doped Microstructures (2012) InTech

Principle of LDW by TPP

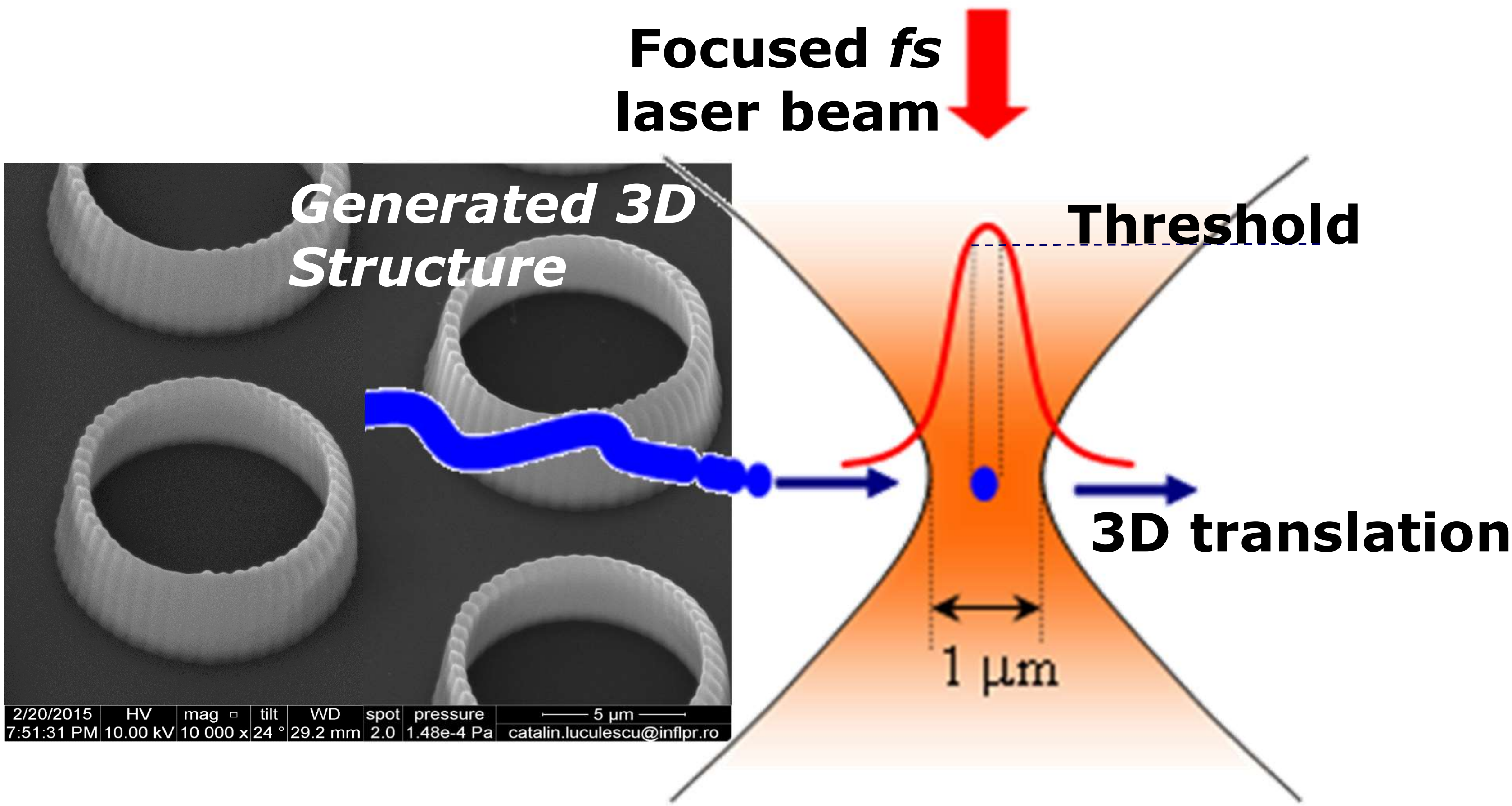

Experimental setup for LDW by TPP

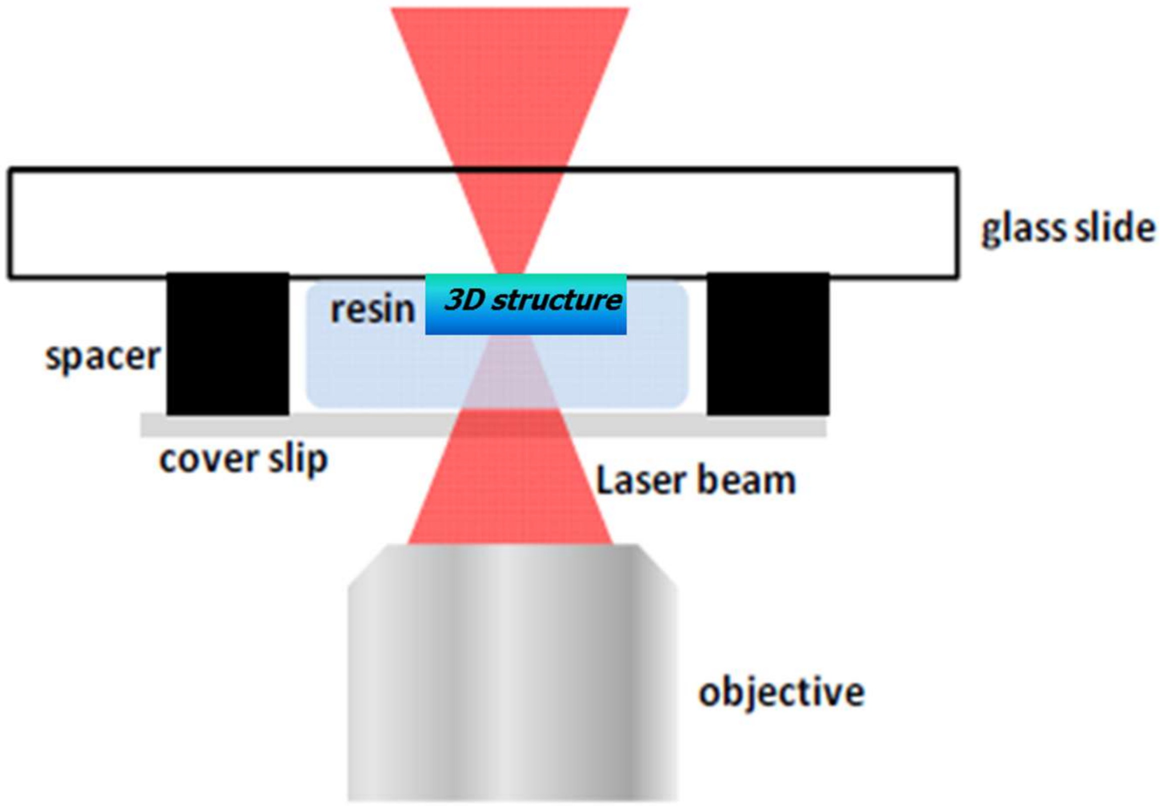

Arbitrary tridimensional microstructures by

→ scanning the laser beam through the resin volume OR

→ moving the sample in X, Y and Z directions

2PA absorption

Voxel, the primitive building block of a 3D structure

Volume where the laser intensity is higher than the polymerization threshold

→The voxel size can be controlled by:

√ changing the exposure time

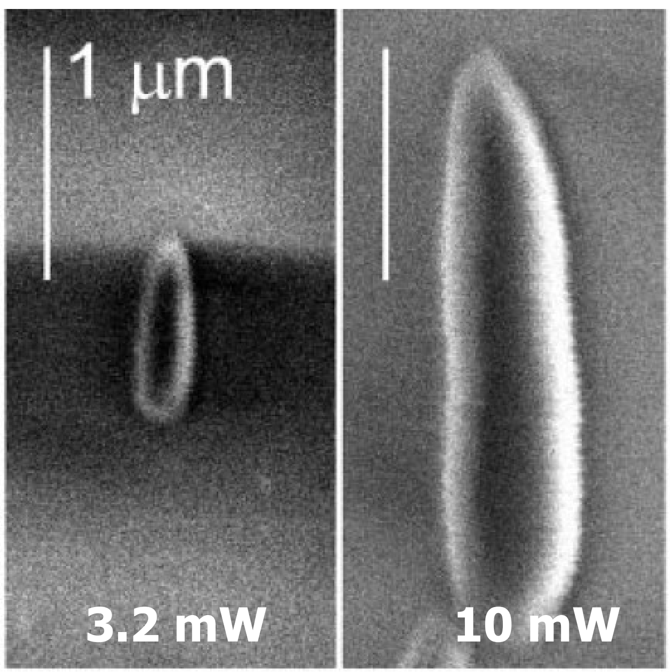

32 ms exposure time

√ adjusting the average irradiation laser power

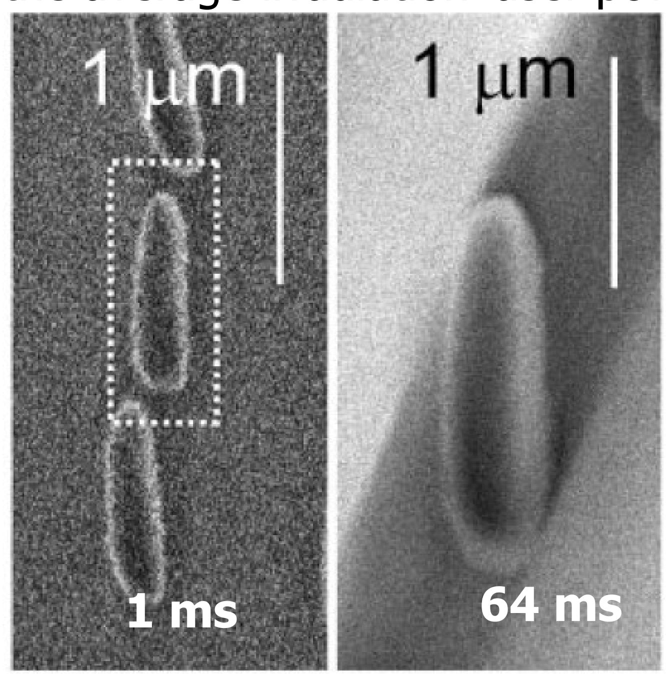

Power 5 mW

Hong-Bo Sun Appl Phys Lett (2003)

Experimental setup for LDW by TPP

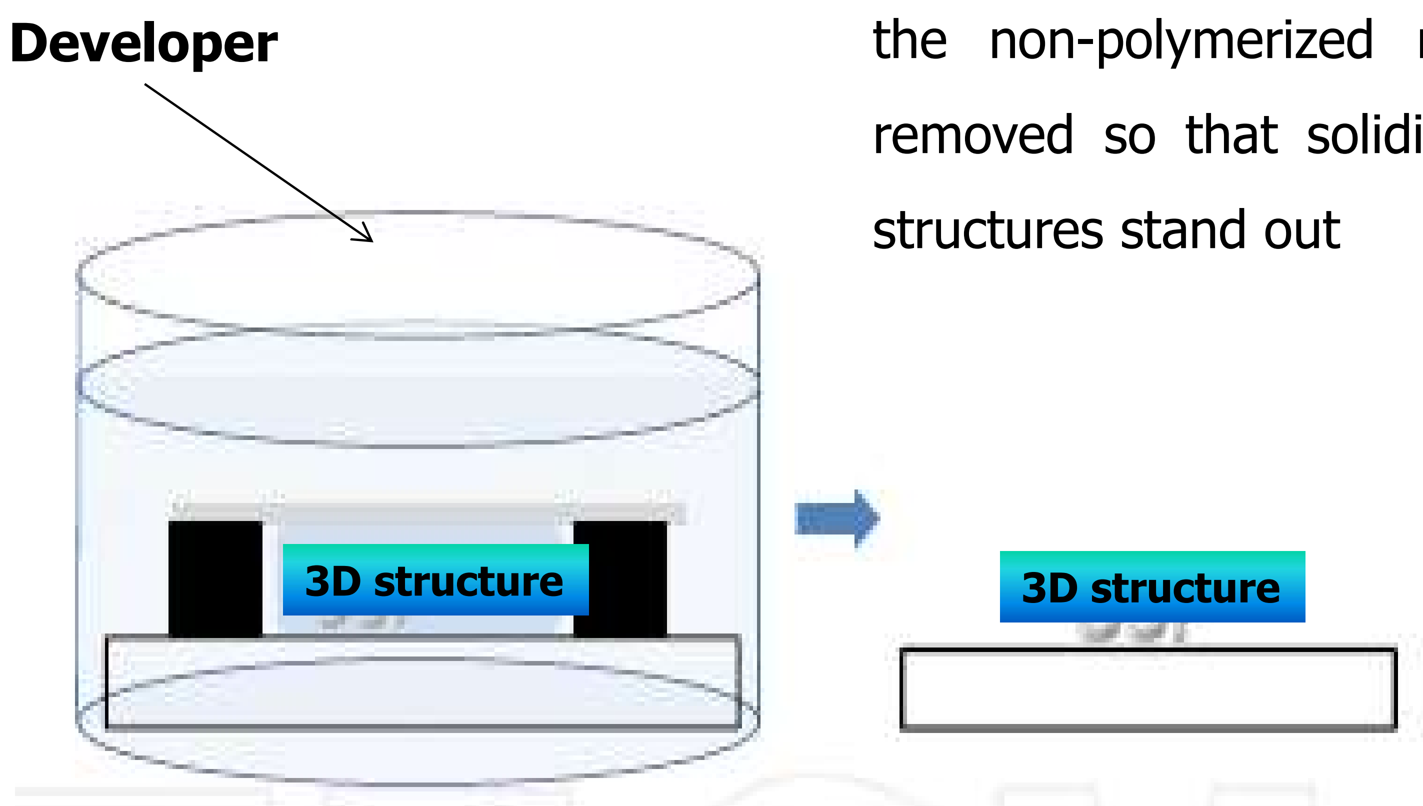

During the developing process, the non-polymerized resin is removed so that solidified 3D structures stand out

D.S. Correa *et al*. Two-Photon Polymerization Fabrication of Doped Microstructures (2012) InTech

2PP-DW by fs laser
1D, 2D, 3D scaffolds for tissue engineering
INFLPR

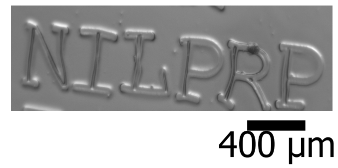

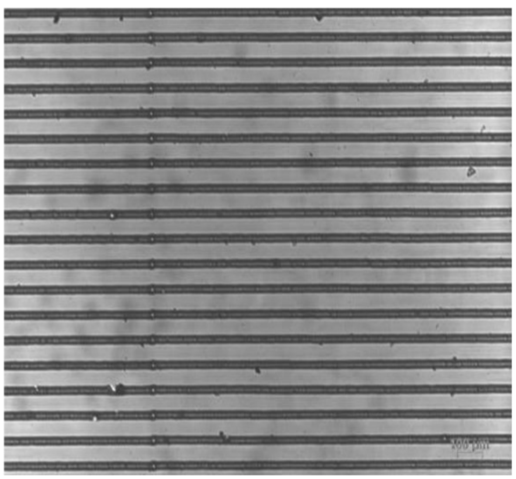

50 lines polymerized SIM 3 sample. Distance between lines: 100 µm

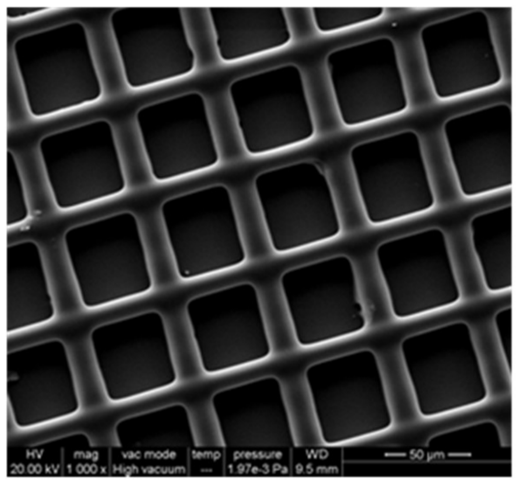

30x30 lines polymerized SIM 3 sample. Distance between lines: 50 µm

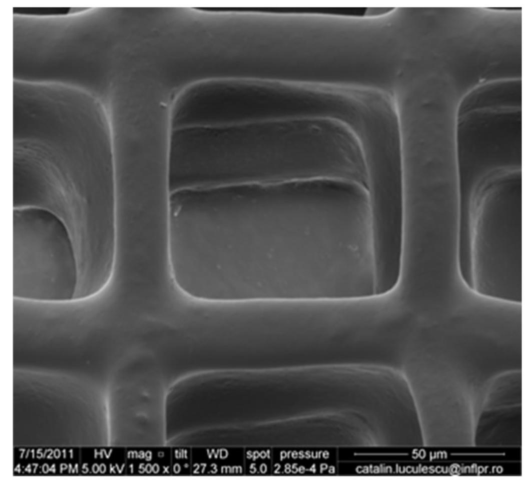

3 layers 30x30 lines polymerized SIM 3 sample. Distance between lines: 100 µm

2PP-DW by fs laser
1D, 2D, 3D scaffolds for tissue engineering

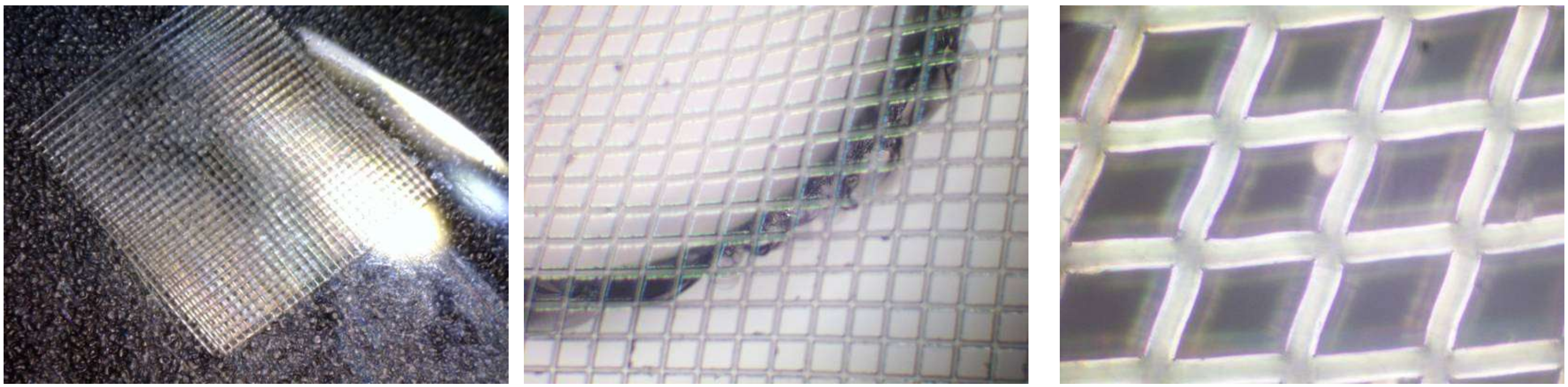

Optical image of a free-standing structure 3x3 mm^2: spacing between lines 100 μm

2PP-DW by fs laser
1D, 2D, 3D scaffolds for tissue engineering

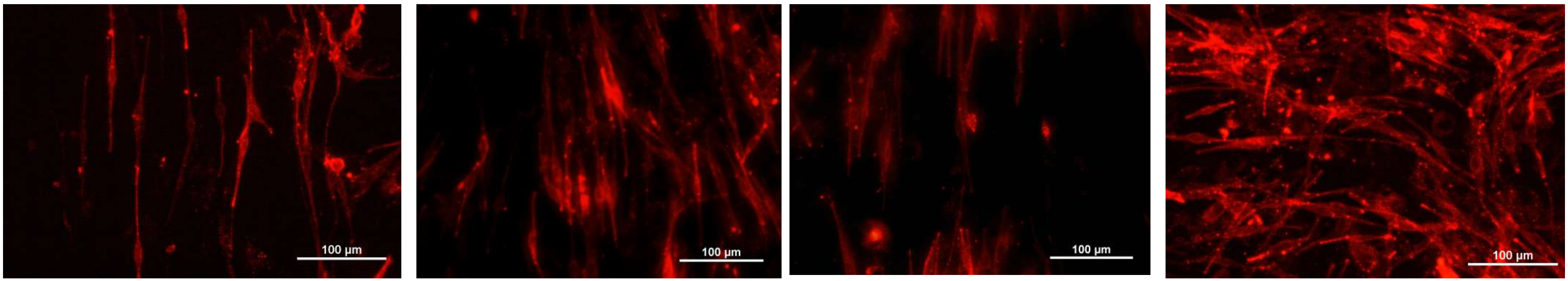

30 µm lines 50 µm lines 100 µm lines glass

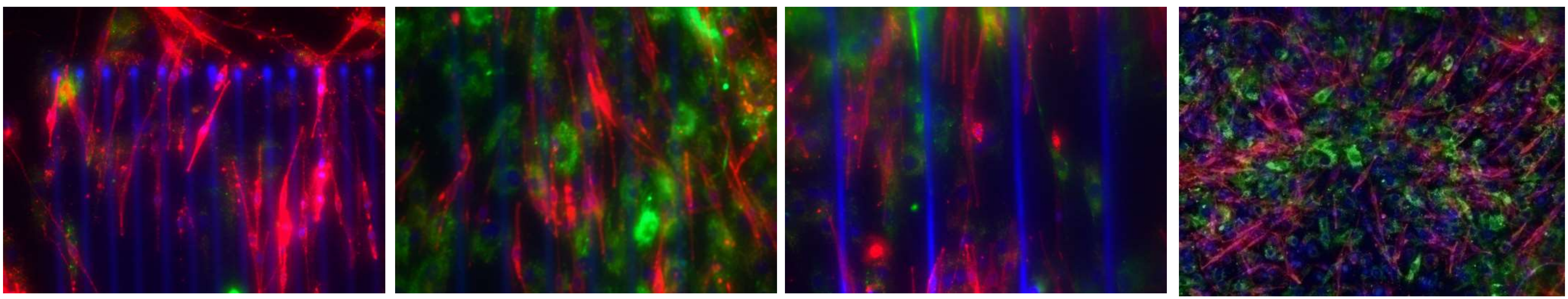

30 µm lines 50 µm lines 100 µm lines glass

L. E. Sima *et al*, Feb 2013 | JOURNAL OF TISSUE ENGINEERING AND REGENERATIVE MEDICINE 7 (2) , pp.129-138

Applications on LDW by TPP

- If one could "mechanically actuate" the micro-reservoires, the process of bone regeneration could be stimulated.

✓ 1st step: fabricate simple vertical microtubes and check if they are favorable for the growth of bone-forming cells (osteoblasts).

Applications on LDW by TPP

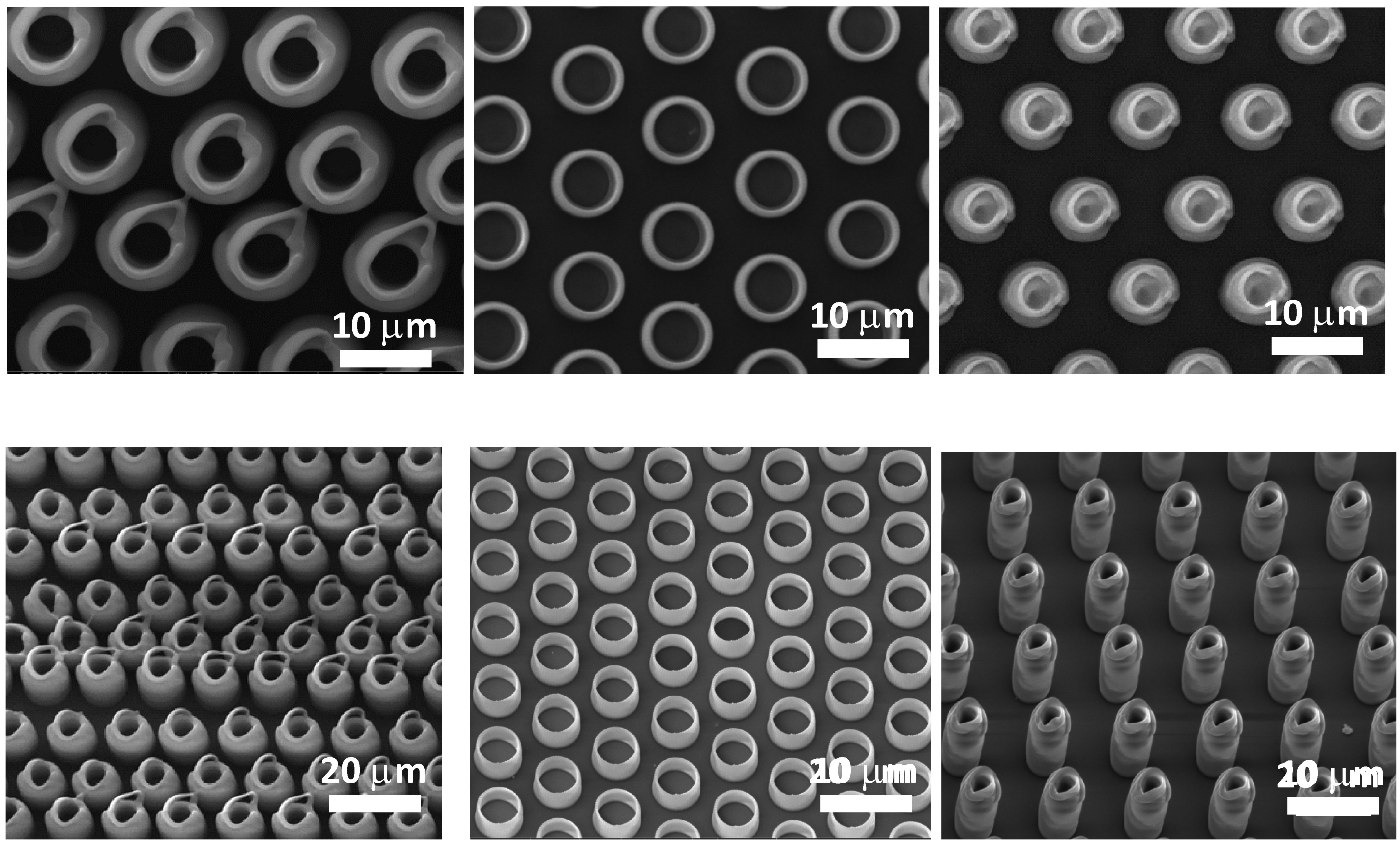

Low laser power (20 mW) "incomplete" shapes, insufficient polymerized material

Medium laser power (34 mW) self-standing microtubes, with clean bottom and sharp walls

High laser power (44 mW) irregular tube walls and residual polymer on the bottom; extensive material polymerization

M. Mihailescu, I. A. Paun, et al. J Mat Sci (2016)

Applications on LDW by TPP

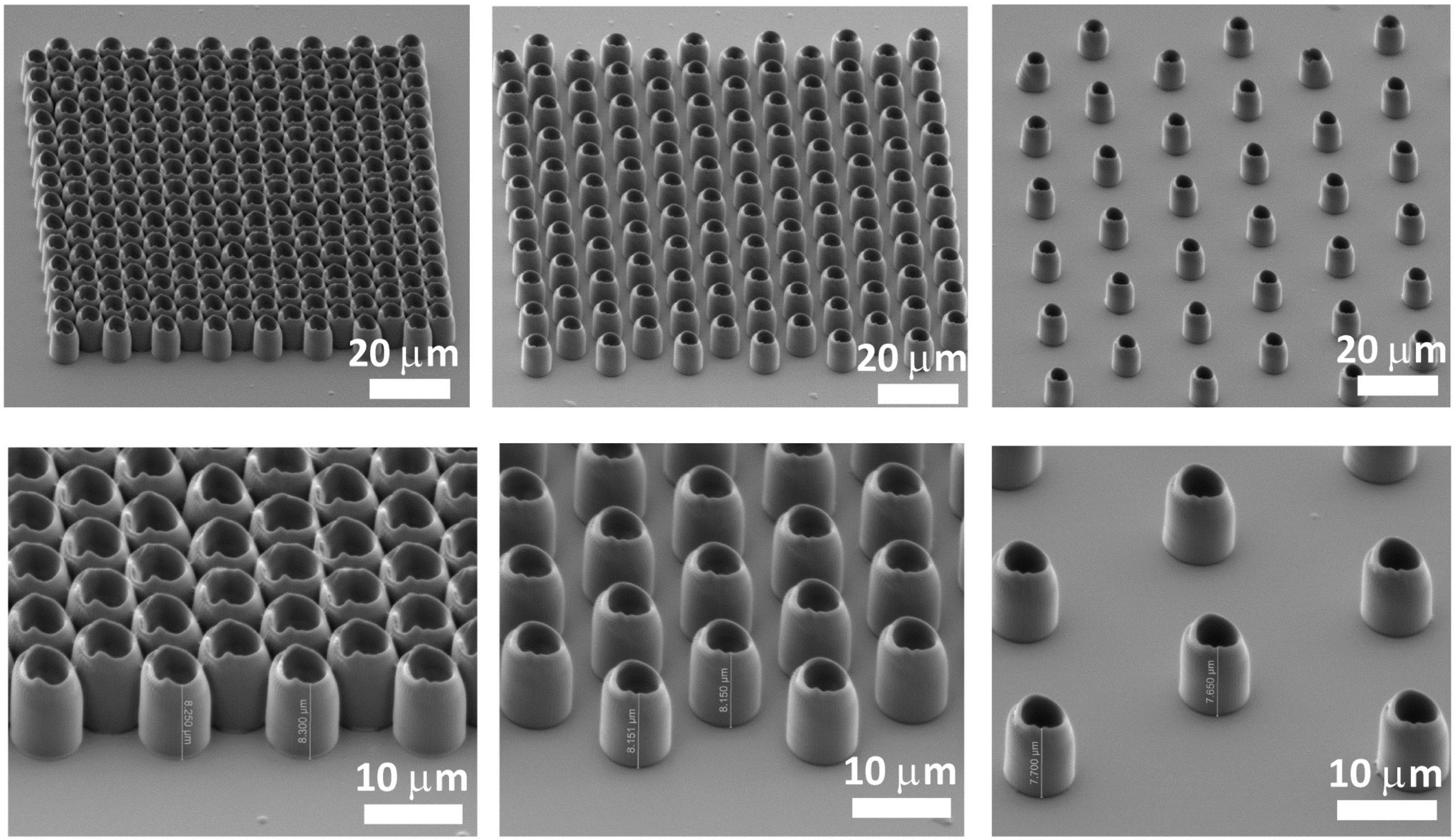

- Experimental conditions: 34 mW laser power; 50 µm/s scan speed; IP-L780 polymer.
- Vertical microtubes arranged in triangular lattices with different constants: 8 µm (tightly packed); 12 µm (medium packed); 24 µm (rarely packed) were produced.

M. Mihailescu, I. A. Paun, et al. J Mat Sci (2016)

Applications on LDW by TPP

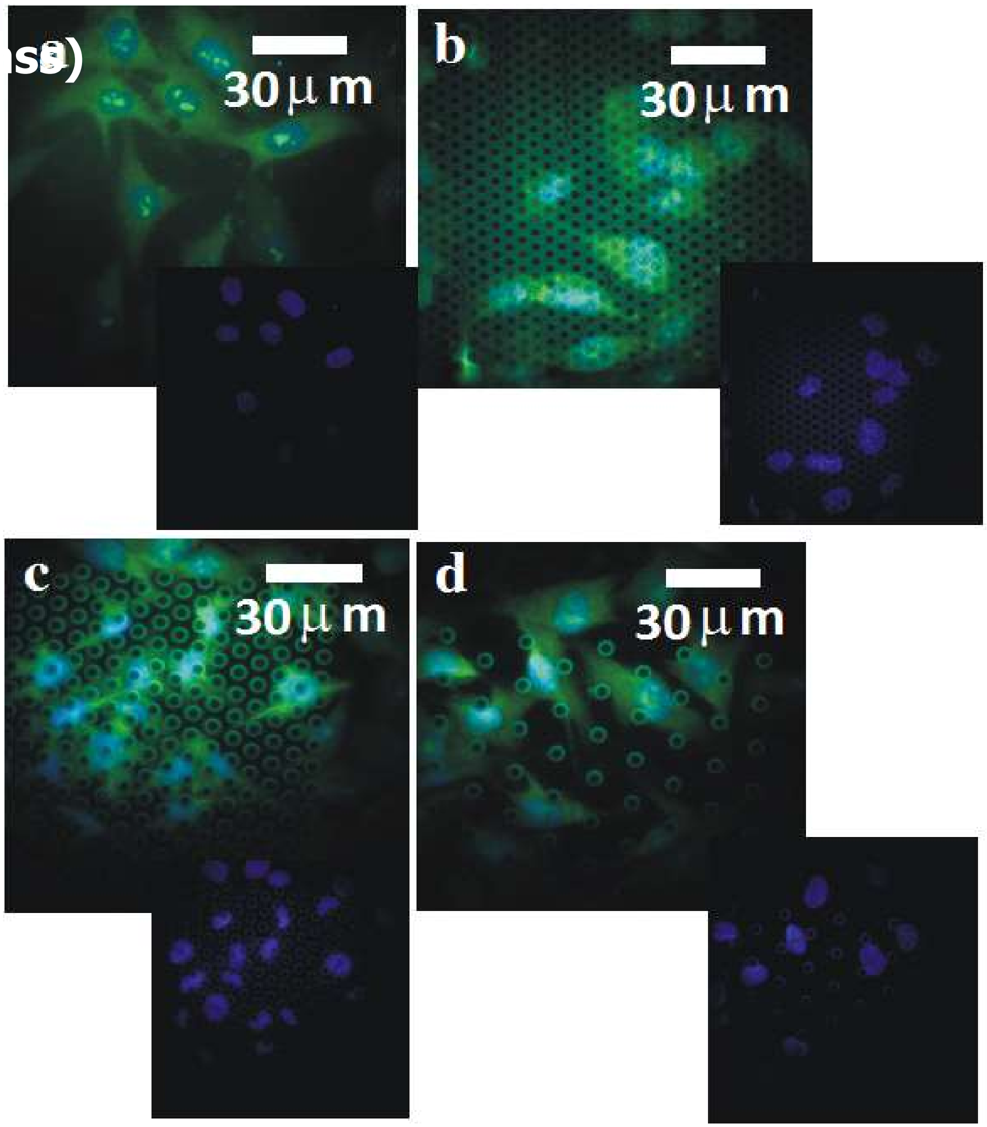

The microtube arrays promote osteoblasts growth

M. Mihailescu, I. A. Paun, et al. J Mat Sci (2016)

Applications on LDW by TPP

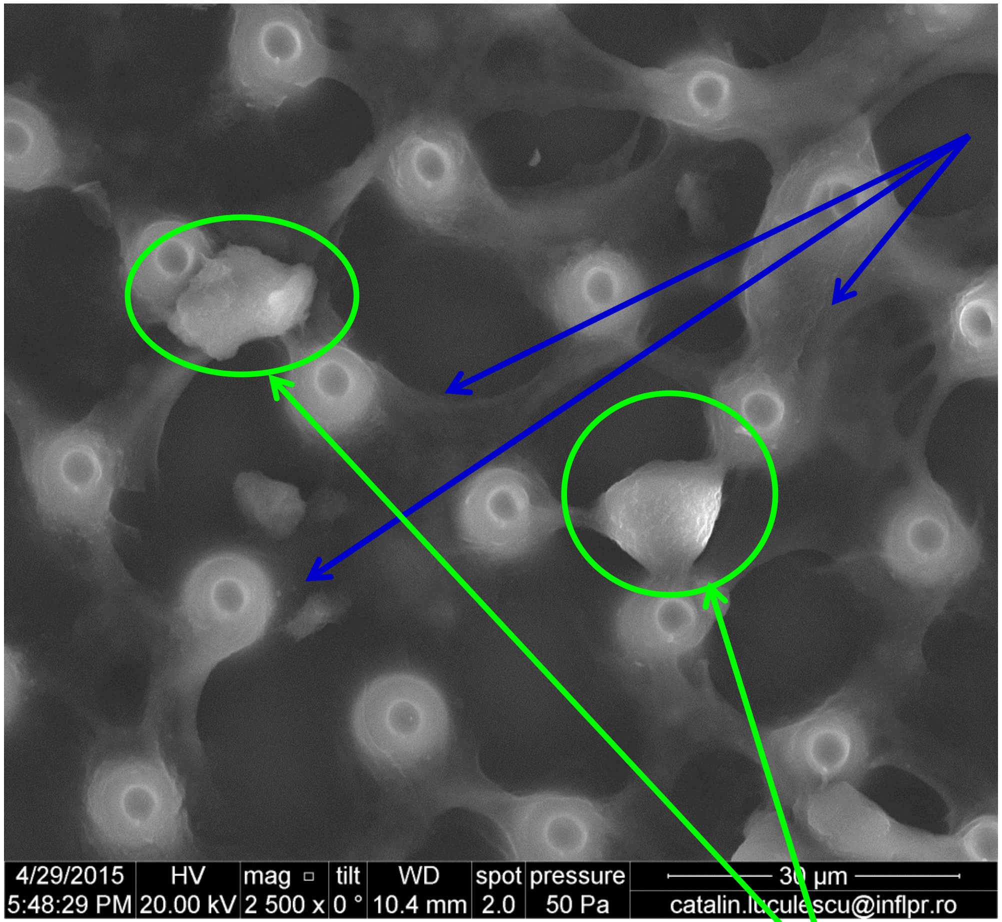

The osteoblasts are spreading across the microtube arrays

The cells produce mineralization nodules (Ca/P):

→ evidence for the starting point of new bone formation

Applications on LDW by TPP

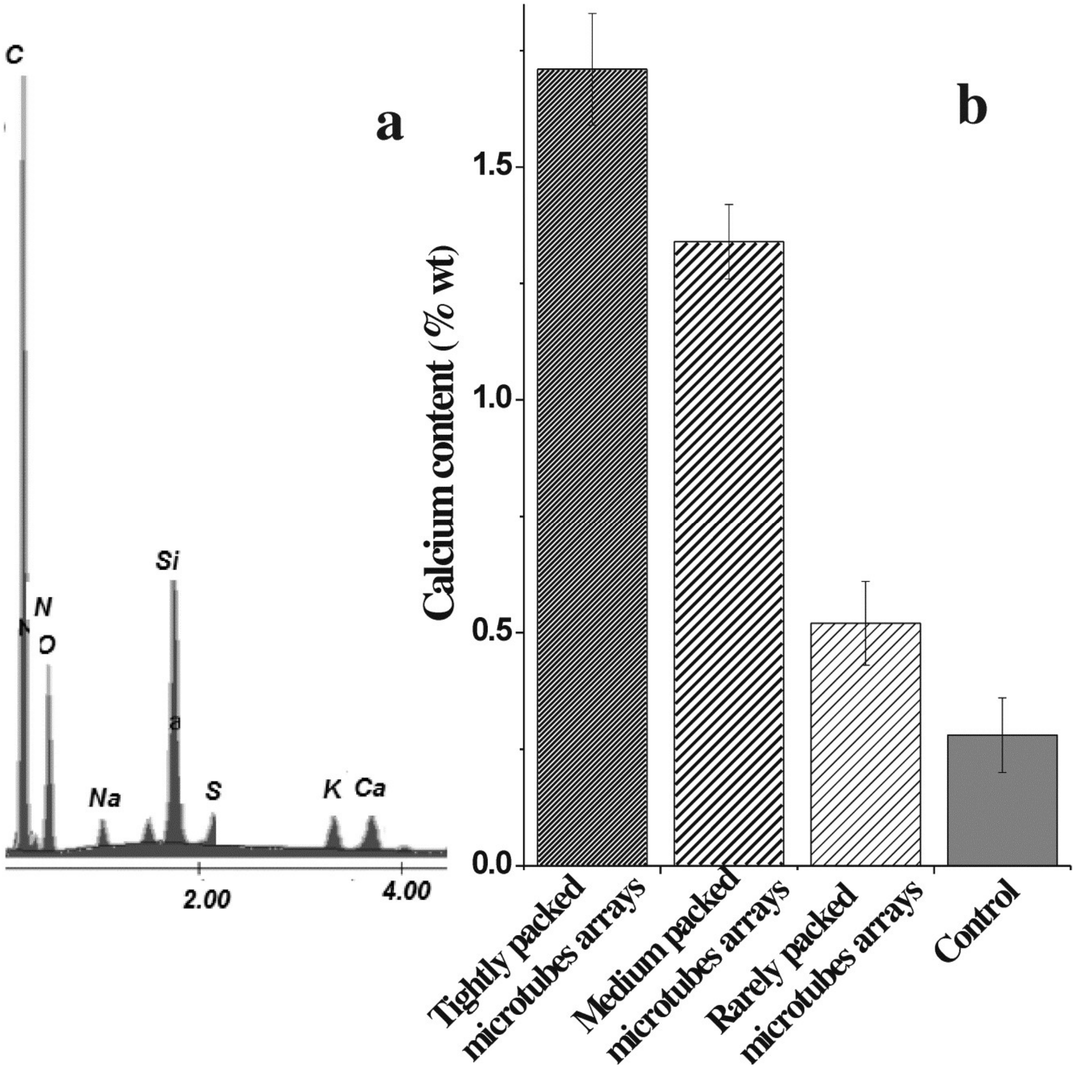

The Ca/P nodules were measured by EDX.

The enhancement of the osteogenesis is attributed to the changes in the cells cytoskeletal arrangement and nucleus shape induced by the microtubes architecture.

M. Mihailescu, I. A. Paun, et al. J Mat Sci (2016)

Applications on LDW by TPP

Electrically-conductive micro-reservoires for controlled delivery of drugs in bone tissue engineering

✓ 2nd step: confer electrical conductivity to the microtubes in view of electrically-controlled delivery of dexamethasone (Dex).

Dex: antiinflammatory drug with osteogenic activity

Applications on LDW by TPP

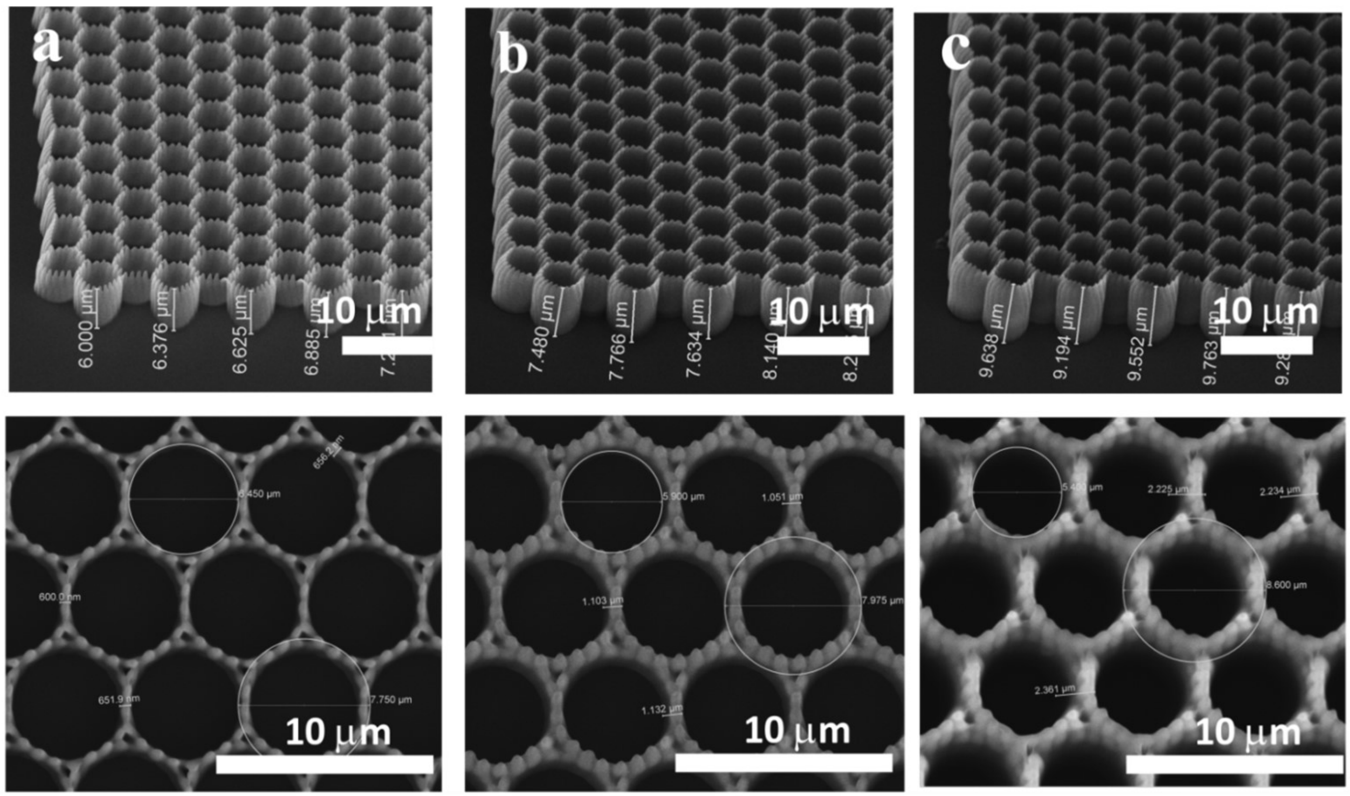

- LDW by TPP was used for producing vertical microtubes arrays; the laser beam was focused through a **100 × microscope objective.**
- From left to right: increasing laser power from 18 mW to 22 mW and up to to 26 mW.

I.A. Paun, et al, APPLIED SURFACE SCIENCE 392 , pp.321-331.

Applications on LDW by TPP

- The microtubes were loaded with **Polypyrrole** **(conductive polymer)** **/ Dexamethasone** **(model drug)** mixture, via a simple immersion process.
- For preventing the passive drug diffusion, the micro-reservoires were sealed with a thin layer of PLGA (using MAPLE)

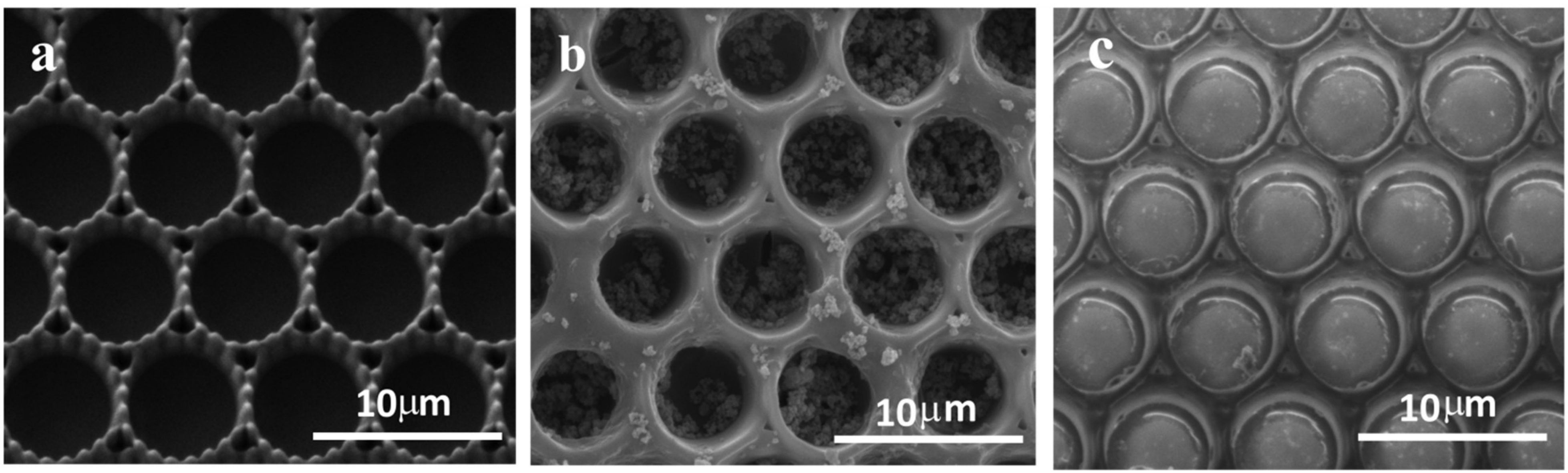

Microtubes arrays → Loading with Polypyrrole/Dexamethasone → Sealing with a thin layer of poly lactide co glycolide (PLGA)

Applications on LDW by TPP

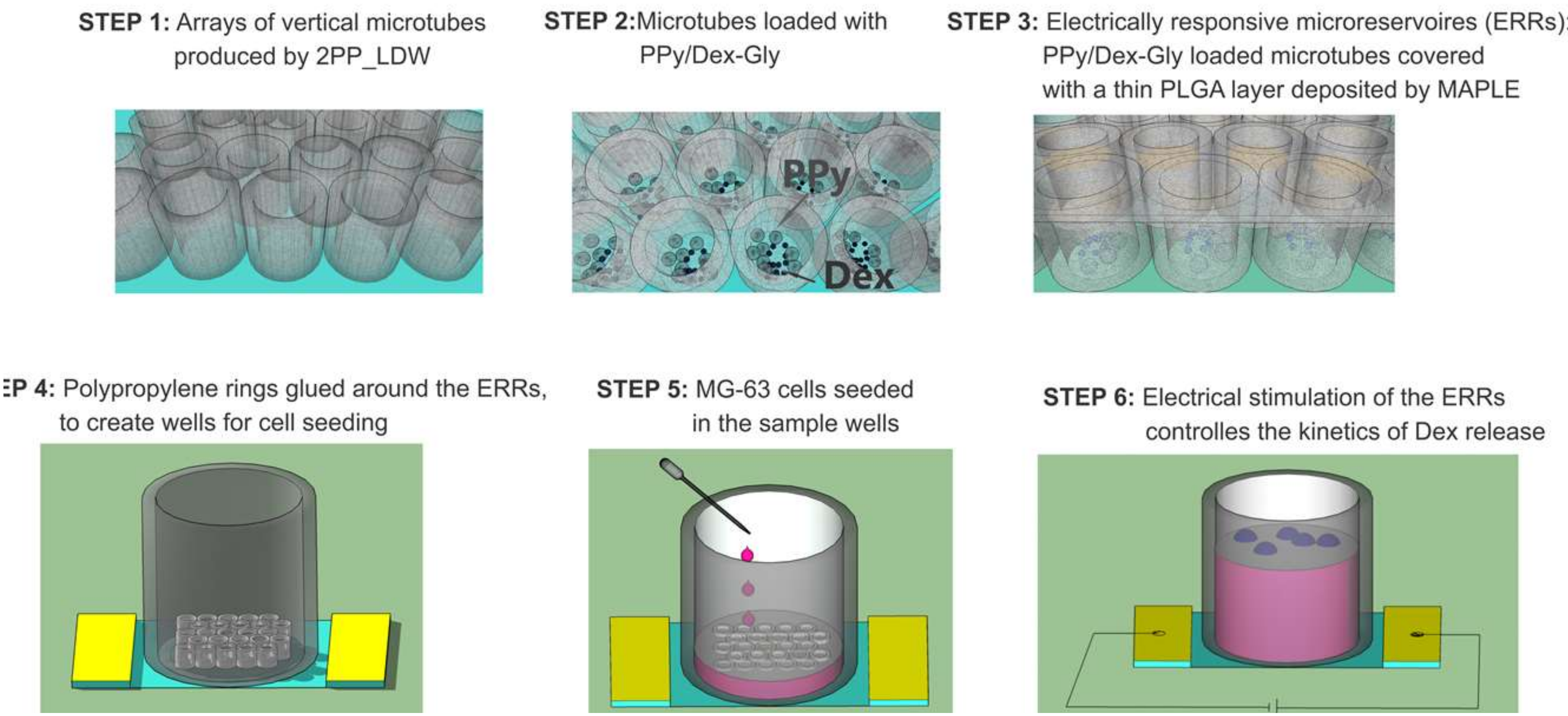

I.A. Paun, et al, APPLIED SURFACE SCIENCE 392 , pp.321-331

Applications on LDW by TPP

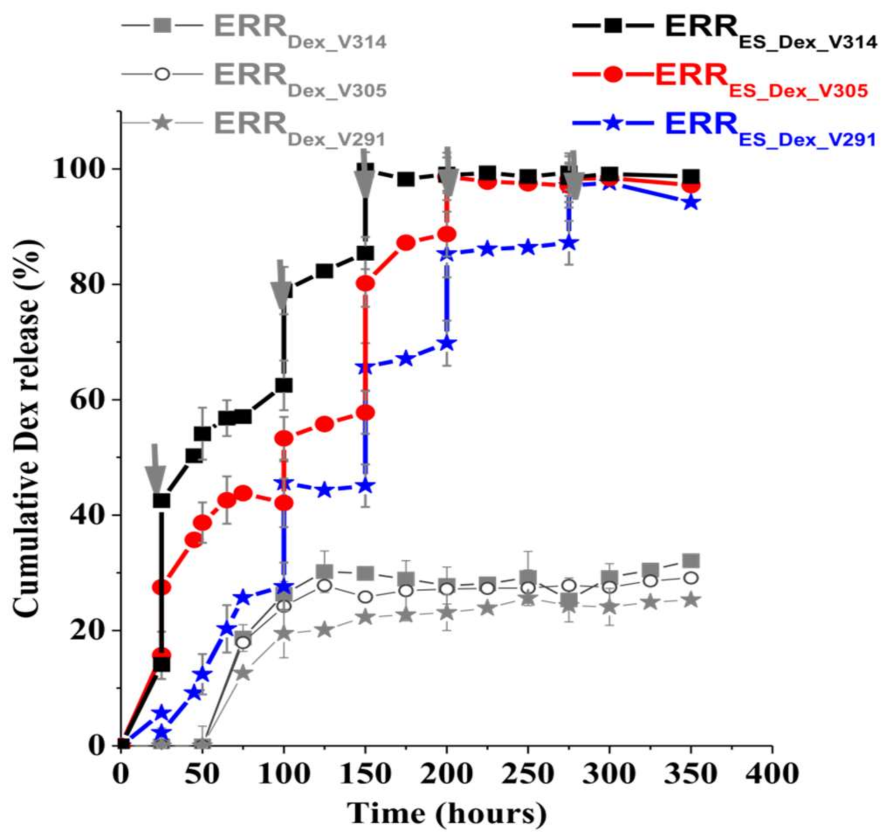

- The kinetics of Dex release can be controlled by electrical stimulation of the microtubes.

I.A. Paun, et al, APPLIED SURFACE SCIENCE 392 , pp.321-331.

Biomedical Implants
Maria Farsari-FORTH

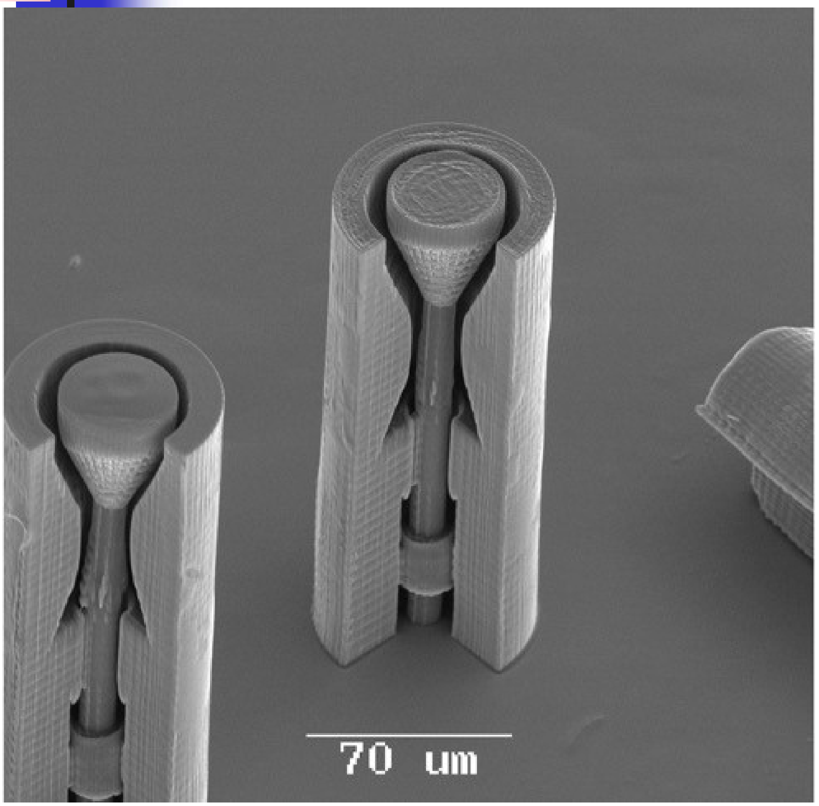

Schizas, J. Adv. Manufact. Technol. 48, 435 (2010).

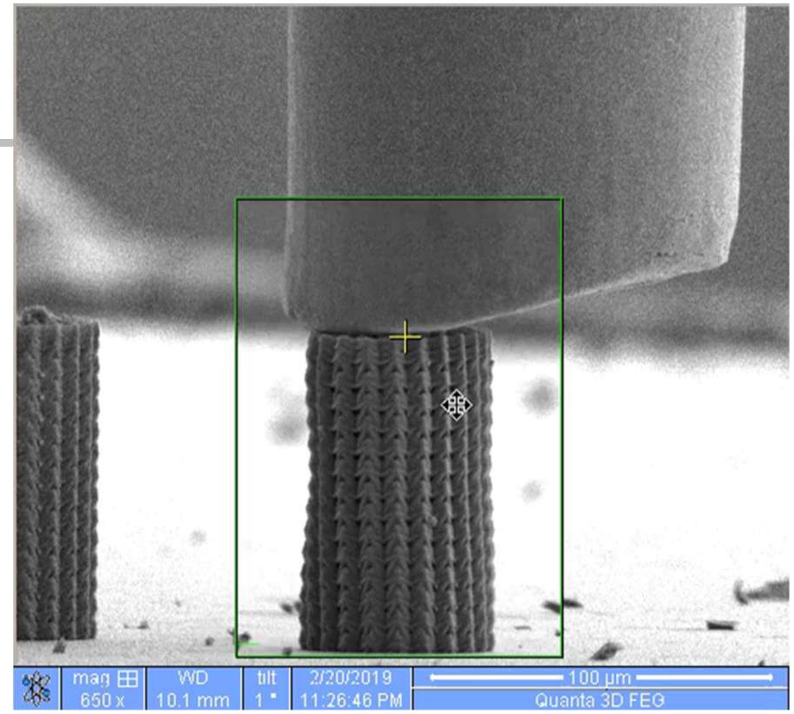

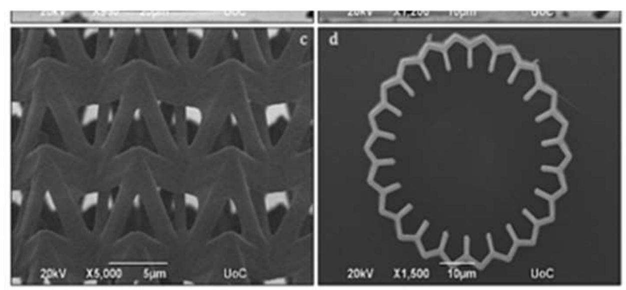

Spanos , Nanomaterials, 11446 (2012)

Hybrid Materials
(Maria Farsari FORTH)

SZ2080

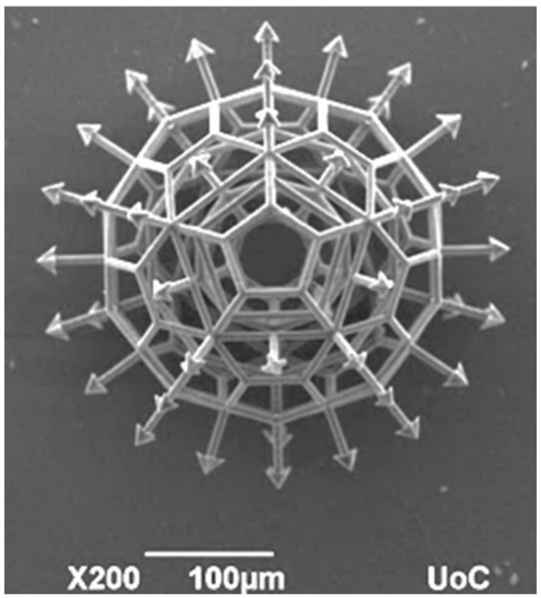

Ovsianikov, , ACS Nano 2, 225 (2008) zirconium propoxide (ZPO)

Thymol-SZ2080

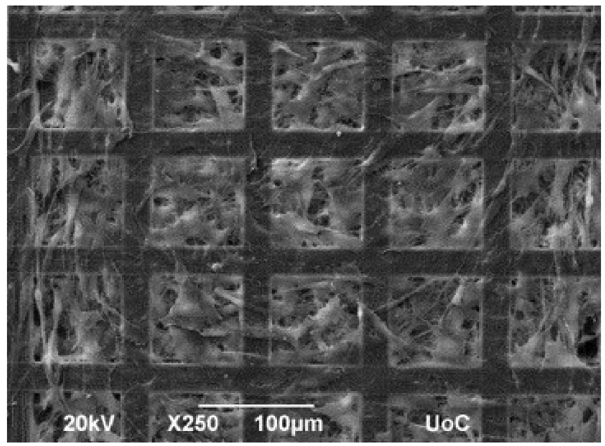

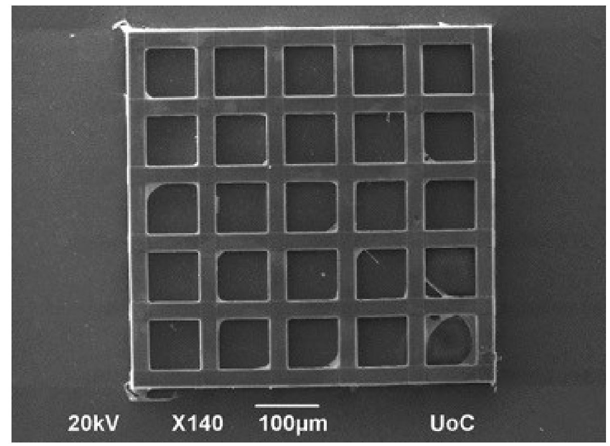

Parkatzidis, Polymer Chemistry 11, 4078 (2020)
THYMA moieties

Collaboration with M. Vamvakaki, U. of Crete

Mechanical Metamaterials
Maria Farsari-FORTH

K. Terzaki, N. Vasilantonakis, A. Gaidukeviciute, C. Reinhardt, C. Fotakis, M. Vamvakaki, M. Farsari, 3D conducting nanostructures fabricated using direct laser writing. *Opt. Mater. Express* **1**, 586–597 (2011)

ENHANCED STRAIN HARDENING AND ENERGY ABSORPTION

PANTOGRAPHS Collaborration with F. dell' Isola, Aquila U

AI-OPTOMIZED MECH. METAMATERIALS

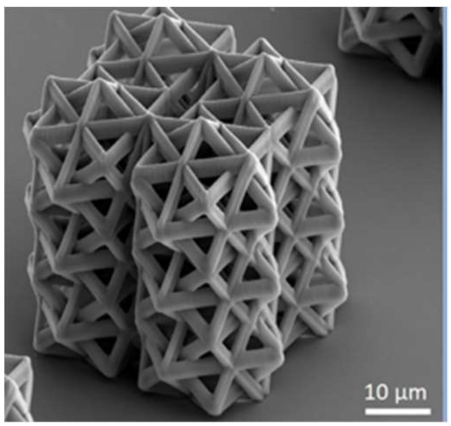

Vangelatos, Int. J. Sol. Struct. 193, 287 (2020).

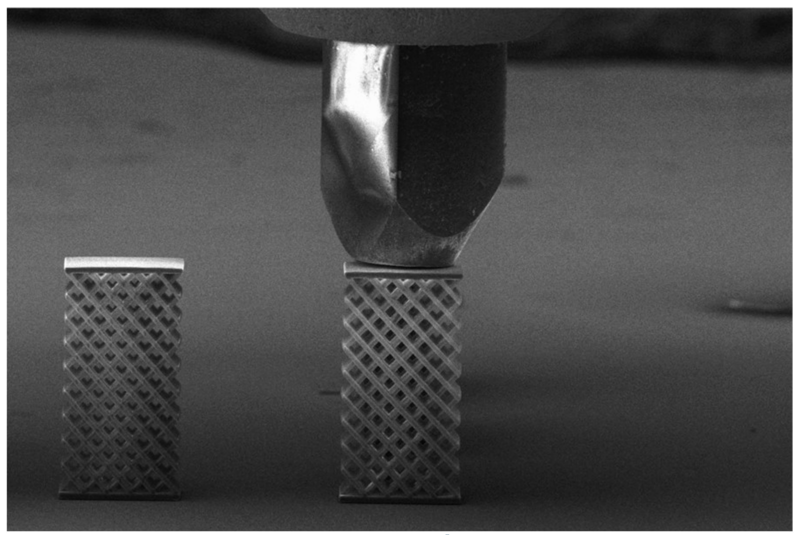

dell' Isola,Comptes Rendus Mécanique, **347**, 397, 2019.

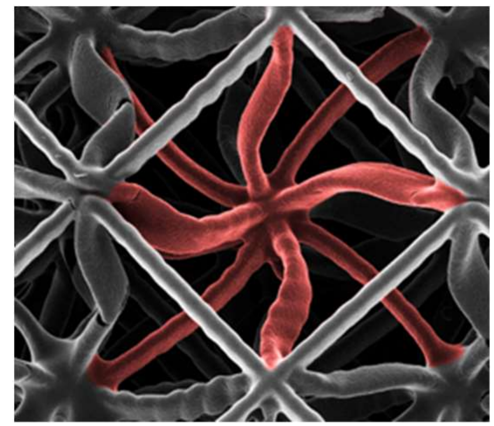

Vangelatos, Science Advances **7**, eabk2218, (2021).

Collaborration with Costas Grigiropoulos, UC Berkeley

Organic-inorganic hybridcomposite, produced by the addition of methacryloxypropyl trimethoxysilane (MAPTMS) tozirconium propoxide (ZPO, 70% in propanol). 2-(dimethylamino)ethyl methacrylate(DMAEMA) was added to provide the metal-binding moieties. MAPTMS and DMAEMA were used as the organic photopolymerizable monomers, while ZPO and the alkoxysilanegroups of MAPTMS served as the inorganic network forming moieties. 4,4-bis(diethylamino)benzophenone (BIS) was used as a photoinitiator.

Horizon 2020: FET Open – Novel ideas for radically new technologies, Grant Agreement: 862016

BioCombs4Nanofibers

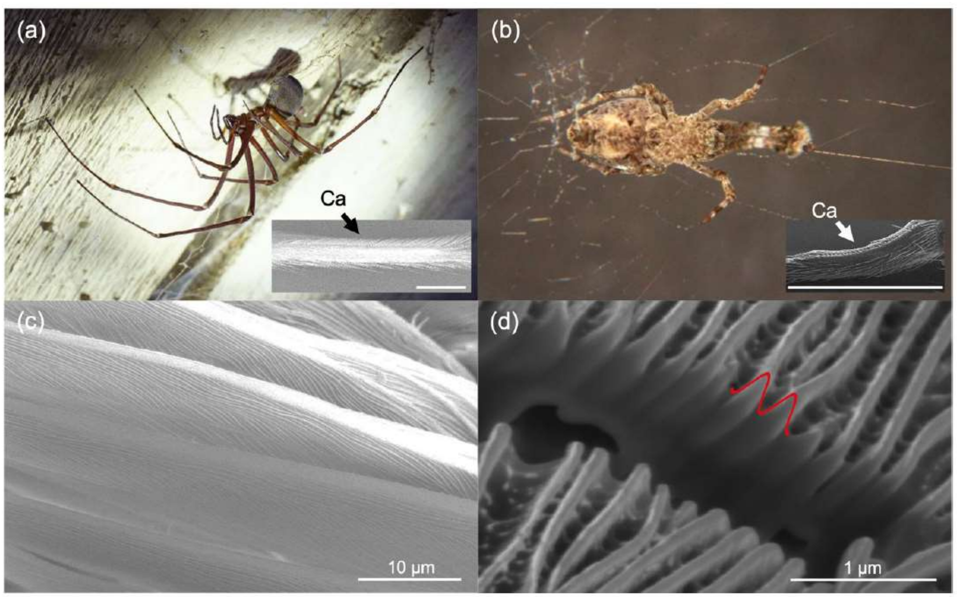

A.-C. Joel, M. Meyer, J. Heitz, A. Heiss, D. Park, H. Adamova, W. Baumgartner*, "Biomimetic Combs as Antiadhesive Tools to Manipulate Nanofibers"*. ACS Appl. Nano Mater. **3** (2020), 3395–3401, https://doi.org/10.1021/acsanm.0c00130 (Open Access, CC-BY-NC-ND)

3D laser lithography system Nanoscribe

- Laser Source: Laser Toptica - 120 fs, 780 nm, 80 MHz, 120mW
- Zeiss inverted microscope
- Piezo stage: PIMars - 300x300x300 um^3
- Translation stages - 100x100 mm^2
- Microscope Camera: 1.4 Mega Pixels
- Microscope Objectives: 100x oil, 100xDiLL, 63x, 20x.

https://cetal.inflpr.ro/newsite/nanoscribe

Performances

•2D lateral resolution: 250 nm
•2D lateral feature size: 90 nm
•3D lateral feature size: 150 nm
•Repeatability (coarse stage) < 1.5 um
•IP-L 780
•IP-DIP

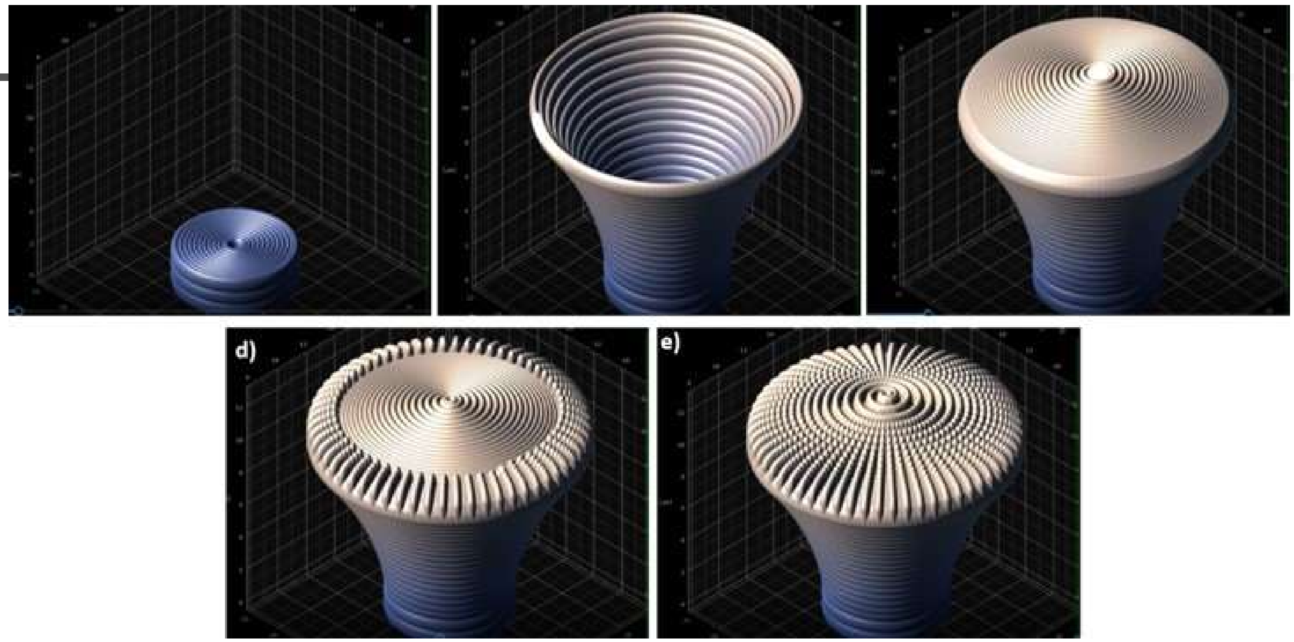

Main steps in the design of mushroom-like nanostructured pillars, showing the trajectory of the laser focused beam through unpolymerized material. Voxel size accounted: a) solid base support; b) mushroom’s leg; c) mushroom’s hat; d) mushroom’s top covered with nanopillars disposed on circular trajectories; e) mushroom-like structures with nanopillars on top.

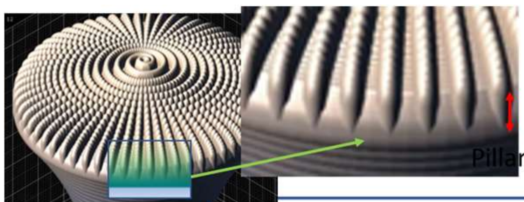

Nanopillars' height set down by design

Design 1: 100 nm

Design 2: 200 nm

Design 3: 300 nm

Design 4: 400 nm

Design 5: 500 nm

Laser writing parameters used for samples fabrication by LDW via TPP

SAMPLE 1
Laser power=12 mW
Scan speed=90 µm/s

SAMPLE 2
Laser power=10.8 mW
Scan speed=90 µm/s

SAMPLE 3
Laser power=9.6 mW
Scan speed=90 µm/s

Optimization of the hierarchic structures

Scope: establish a tradeoff between structures' design, writing parameters and post-processing procedures (developing time, type and combinations of developers) that would get us closer to the scope of BioCombs4Nanofibers: fabrication of periodic nanostructures on ... nd geometry as the calamistrum of cribellate ... ng, having a deviation in periodicity and height

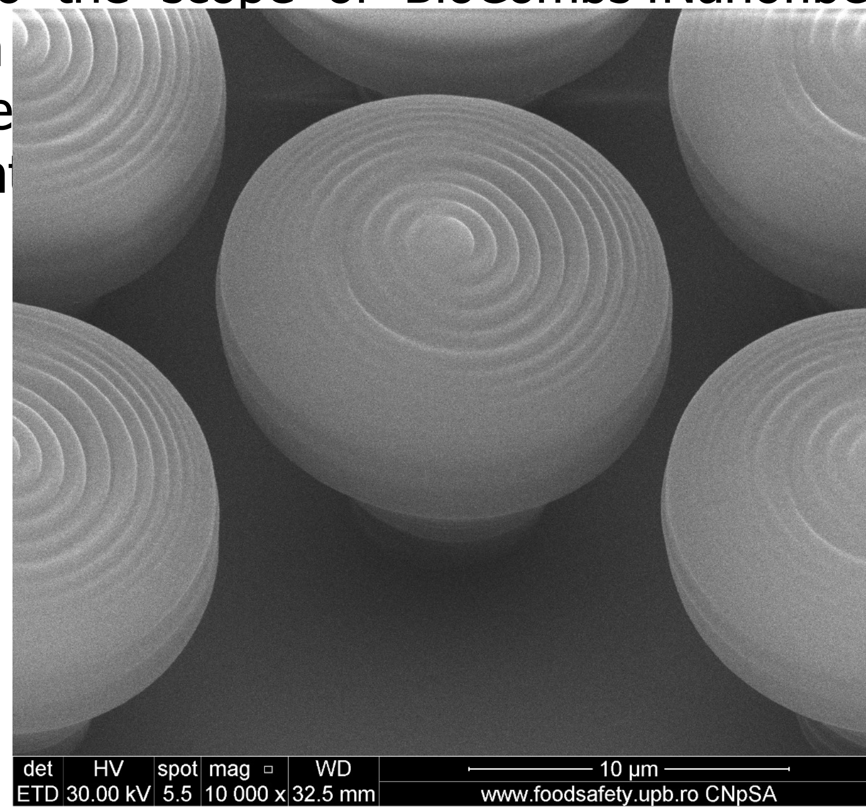

Laser Direct Writing via Two Photons Polymerization (LDW via TPP) of IP-Dip photoresist for the fabrication of hierarchic structures in the shape of mushrooms

-mushrooms' "hats" decorated with n...structures in the shape of r...es

→ **n**anostructured **m**ushroom-like **p**illars (NMP)

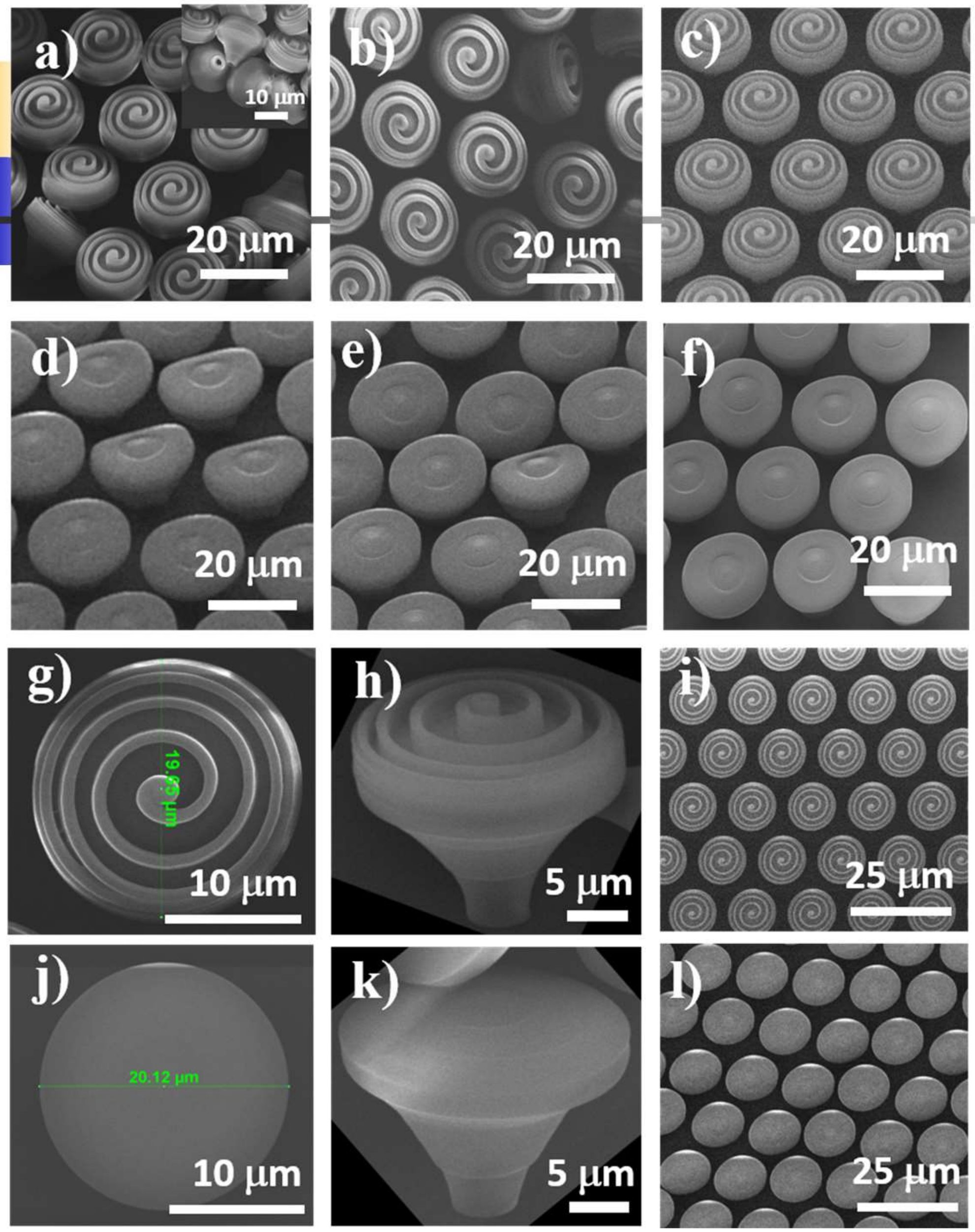

Scanning electron micrographs of nanostructured and micro-structured mushroom-like pillars fabricated by LDW via TPP. Left side - Optimization of laser writing parameters for micro (upper panel) and nanostructured (lower panel) mushroom-like pillars (MMP and NMP respectively) (a,d) laser speed 140 µm/s, laser power 13.8 mW; (b,e) laser speed 120 µm/s, laser power 12.5 mW; (c,f) laser speed 100 µm/s, laser power 12.5 mW.. (g-l) MMP and NMP areas fabricated using laser speed 100 µm/s and laser power 13.8 mW: (g-i) MMP (j-l)NMP; g,j) close, top views of mushrooms' "hats"; h,k) close, tilted view of single MMP and NMP respectively; i,l) large, top views of MMP and MNP areas.

Optimization of the laser power

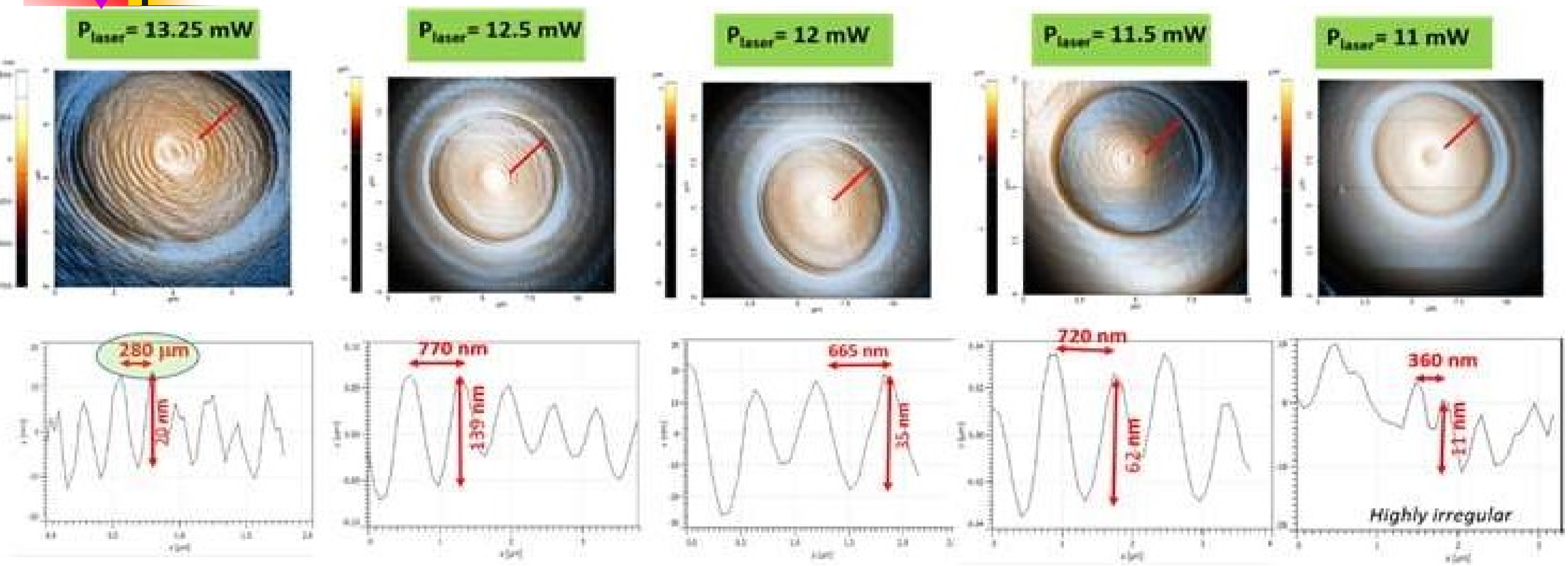

√ Periodicity 280 nm for NMPs structures fabricated with 13.25 mW laser power and scan speed of 100 μm/s (*green oval*)

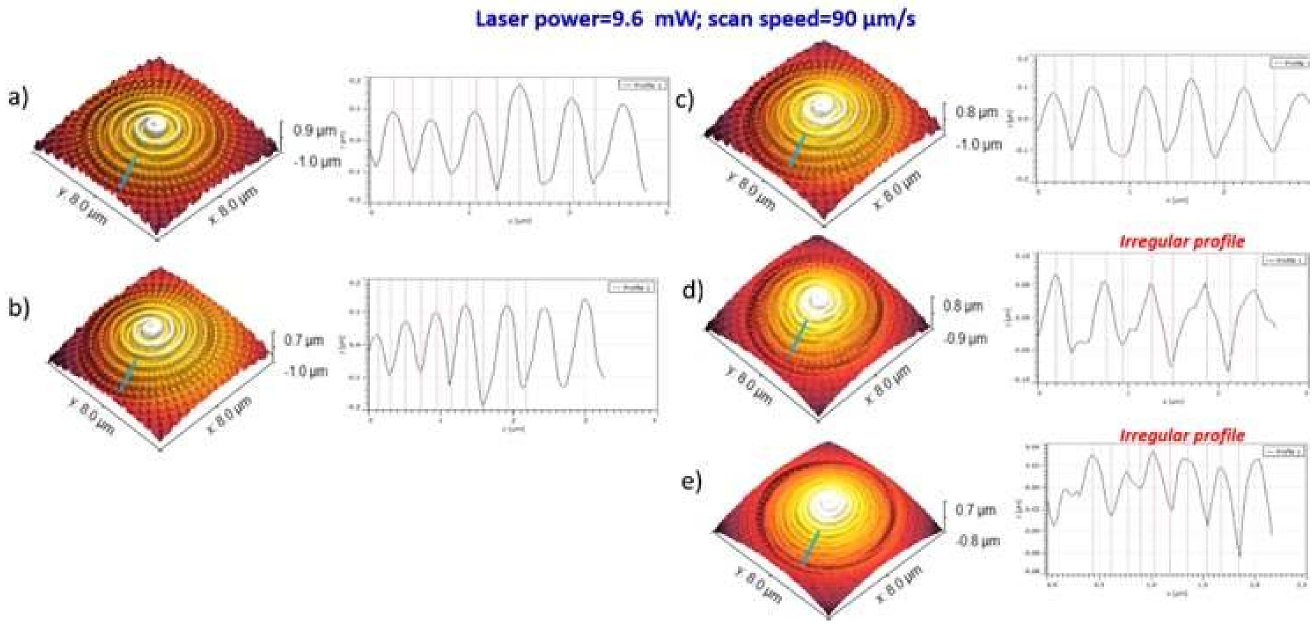

3D images obtained by atomic force microscopy scanning of 8×8 µm^2 areas on top of mushroom-like microstructures. Samples fabricated using scanning speed of 90 µm/s and laser power of 9.6 mW. Pillars' heights settled by design: 500 nm; b) 400 nm; c) 300 nm; d) 200 nm; e) 100 nm.

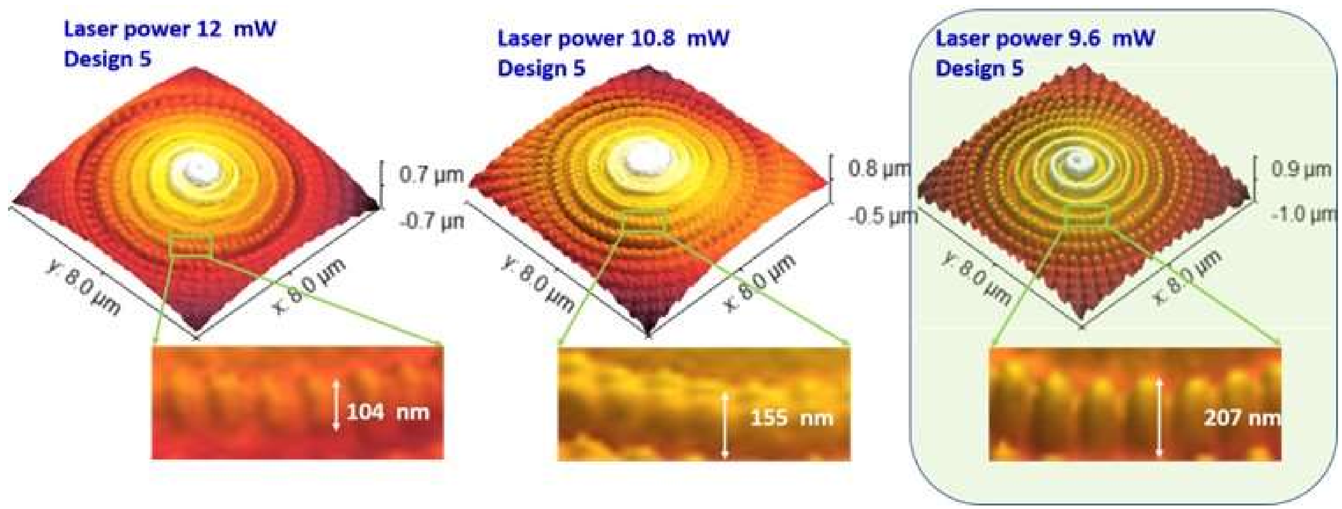

3D images obtained by atomic force microscopy of 8×8 μm^2 areas of nanopillars from the top of mushroom-like structures, fabricated by LDW via TPP using 90 µm/s scan speed and laser powers indicated on each image.

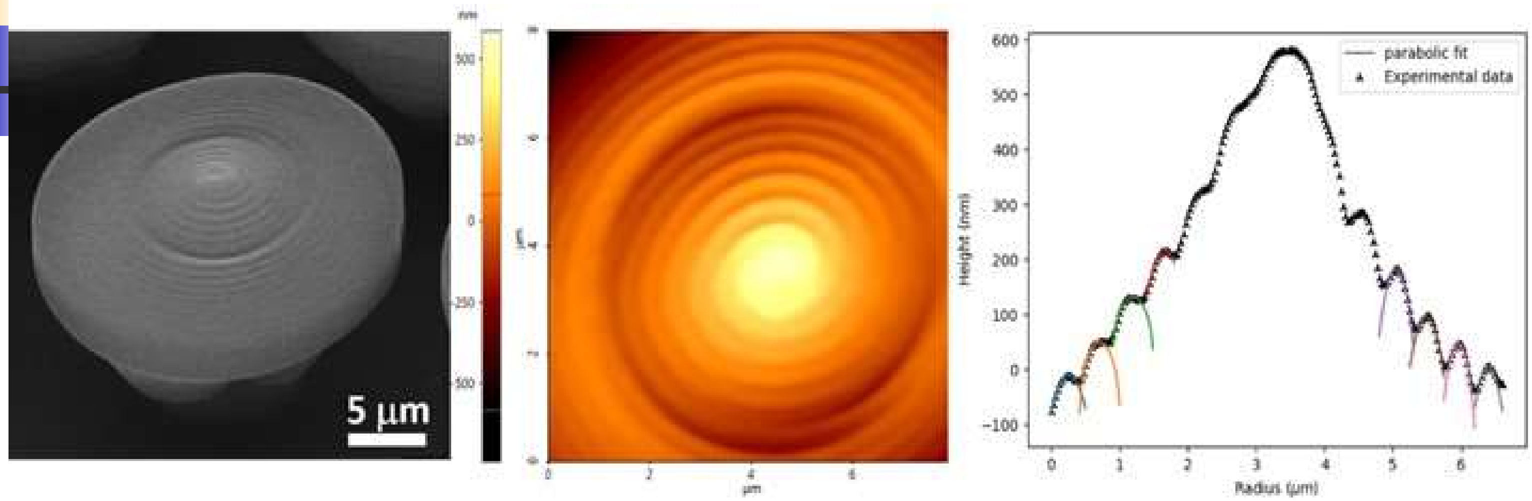

Voxels from the outer edge of the indentation indicate an aspect ratio close to 1:1 height-width

Voxels closer to the center maintain the general 2:1 height-width aspect ratio

This suggests that the voxel is stretched at the point where the indentation is formed

In vitro tests

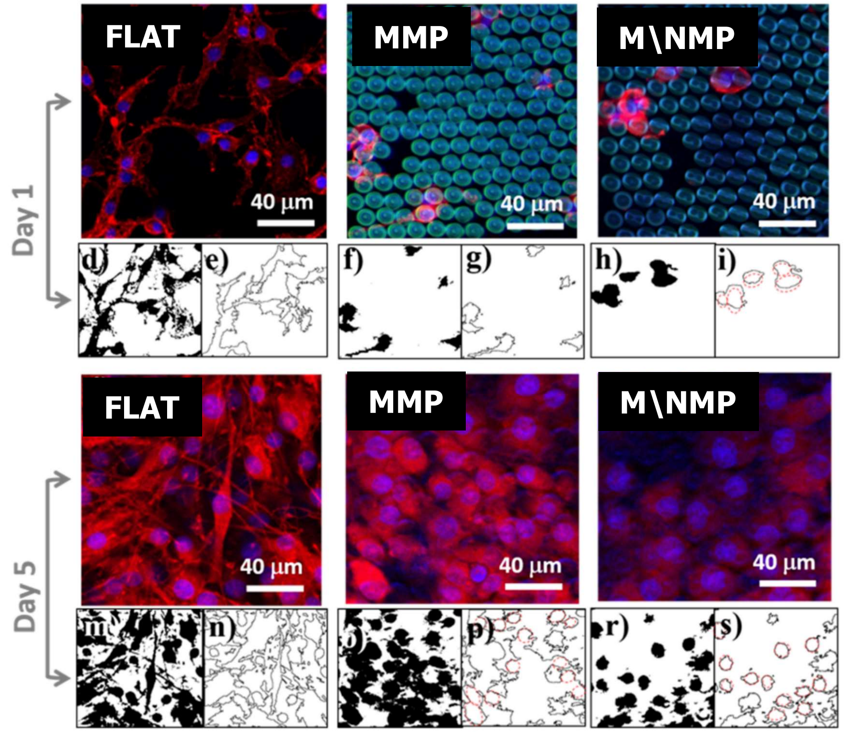

INITIAL TESTS USING LOW CELL DENSITY 50000cells/sample

NMP structures

cell attachment reduced by **55%** as compared to flat surfaces

cells with round shape and no phyllopodia=low adhesion

MMP structures:

cell attachment reduced by **21%** as compared to flat surfaces

preserved the native shape spindle-like with phyllopodia

→ NMP structures are more effective in impeding the cellular attachment

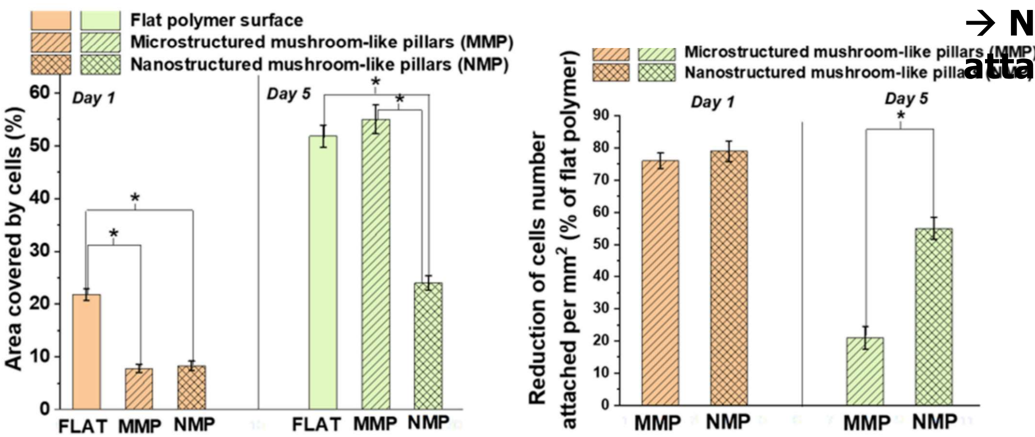

Brief recall on 3D structuers to be teste in vitro

fabrication of periodic nanostructures with same size and geometry as the calamistrum of cribellate spiders, having a deviation in periodicity and height

Optimization of laser power

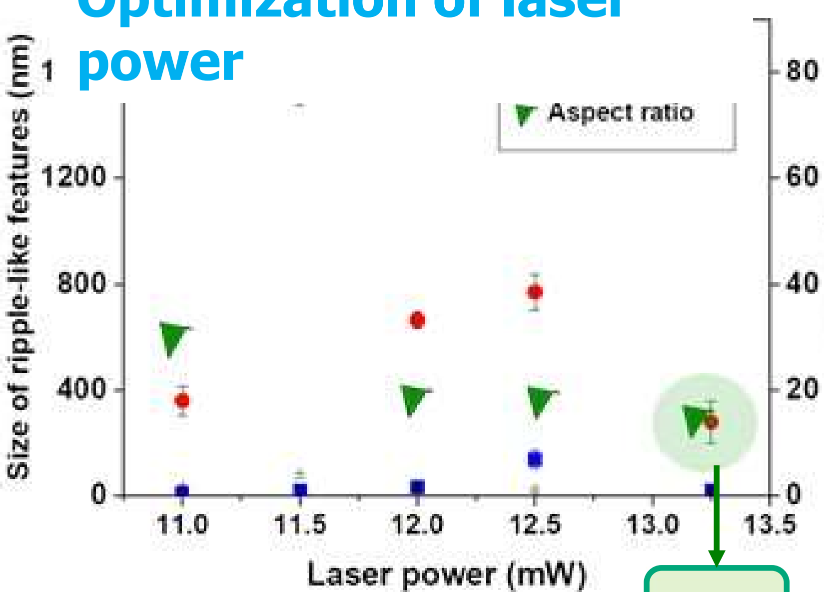

NMP$_{lp}$

LP=optimum Laser Power

Tested in vitro

√ Periodicity ≅ 280 nm (laser power 13.25 mW, scan speed 100 μm/s, *green circle in the plot)*

Optimization of 3D design

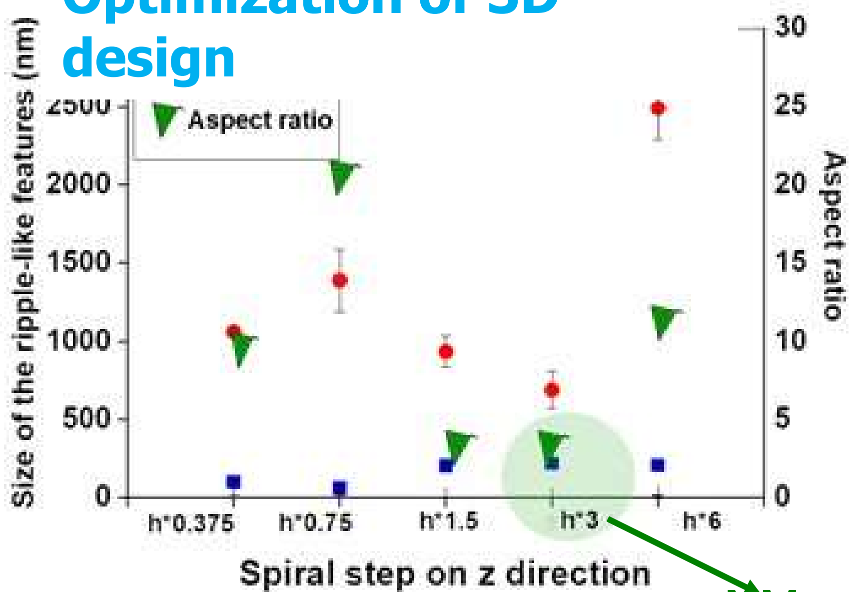

NMP$_D$

D=optimum design

Tested in vitro

√ Height ≅(200-210) nm (laser power 13.25 mW, scan speed 100 μm/s, spiral step scaling on z direction multiplied by 3 *green circle in the plot)*

In vitro tests on optimized structures

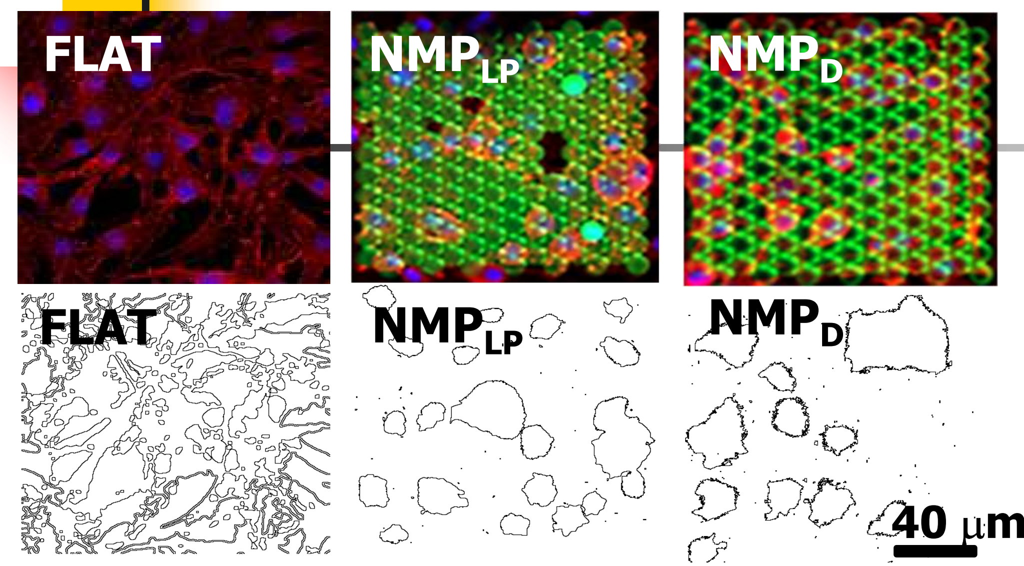

Year 1+2 until May: For 5000 cells/sample, we obtained ≅75% reduction of adherent cells on NMP structures as compared to flat surfaces

Year 2 May-present: HIGH cells density (25 000 cells/sample)

→ **NMP structures preserved their cell-repellent potential**

Tests on optimized design and **laser power for LDW via TPP fabrication of** nanostructured mushroom-like pillars (NMP)
→ both parameters are important for lowering the cell adhesio as compared to flat surfaces- **EVEN AT HIG CELLULAR DENSITIES**

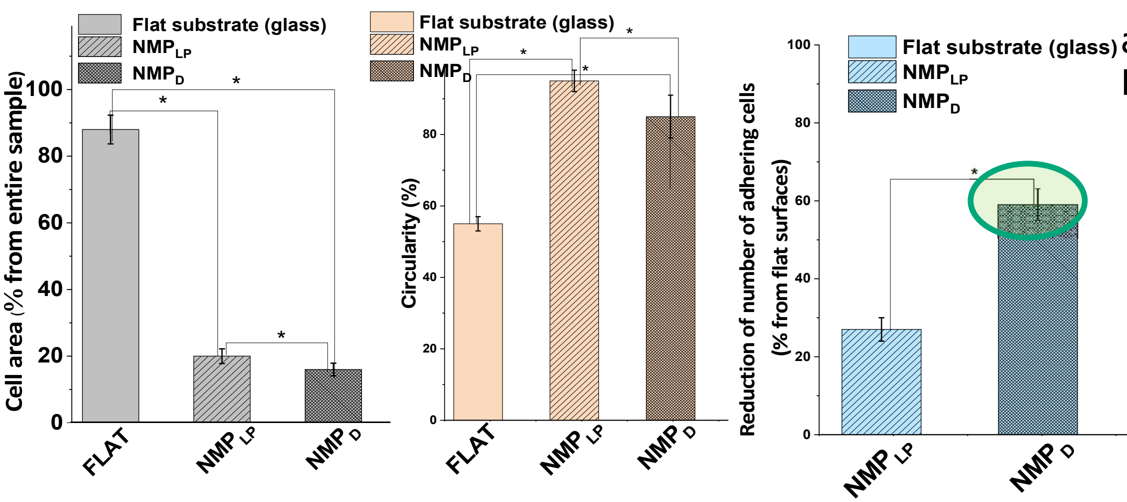

Best results: optimized design (NMP$_D$)
→ ≅60% reduction of adherent cells as compared to flat surfaces
<u>even at HIGH initial cellular densitie</u>

To be tested: synergy between -optimized laser processing parameters (NMP$_{LP}$) *and* -optimized design (NMP$_D$)

Paun, IA ; Calin, BS; Popescu, RC ; Tanasa, E; Moldovan, A. Laser Direct Writing of Dual-Scale 3D Structures for Cell Repelling at High Cellular Density. *Int J Molec Sci* 2022, *23 (6)*, 3247
Https://doi.org/10.3390/ijms23063247

Conclusions

- LDW by TPP is a promising rapid prototyping fabrication method based on two-photon polymerization with ultrashort laser pulses
- The technique allows the fabrication of custom 3D architectures, with a spatial resolution down to 100 nm, by direct laser 'recording' of the desired structure into the volume of a photopolymer.

Conclusions

- LIFT
- 2PP
- MAPLE
- assisted or/+ other techniques ,

appropriate for (soft) material processing

Acknowledgments

- NATO SfP 982671 Project
- e-LIFT Project FP 7 Project
- PNCDI II National Projects
- Horizon 2020: FET Open – Novel ideas for radically new technologies, Grant Agreement: 862016

BioCombs4Nanofibers

A. Palla-Papavlu, I.A. Paun, G. Dinescu, S. Brajnicov, B. Calin , M. Filipescu, A. Moldovan, C. Mustaciosu[1], E. Vasile[2], M. Dinescu
National Institute for Laser, Plasma and Radiation Physics, Magurele, Romania
1. National Institute for Physics and Nuclear Engineering, Magurele, Romania
2. Polytechnical University Bucharest

Maria Dinescu

National Institute for Lasers, Plasma, and Radiation Physics
http://ppam.inflpr.ro